ISSN:2538-516X

Journal of Civil Engineering Researchers

Volume: 5; Number: 1; March 2023

J-Researchers

J-Researchers

JOURNAL OF CIVIL ENGINEERING RESEARCHERS

Volume 5, Number 1, March 2023

Contents

J-Researchers

JOURNAL OF CIVIL ENGINEERING RESEARCHERS

Crack analysis and modeling in concrete beams reinforced with FRP composite sheets

Amir Nazarinejad[a*]

[a]*Ms.c student, Department of Civil Engineering and Surveying, Ramsar Branch, Islamic Azad University*

Article History: : Received date: 2023.02.20; revised date: 2023.03.15; accepted date: 2023.03.20

Abstract

In this article using the principles and relationships governing fracture mechanics and finite elements cracking in the first mode for reinforced concrete beams reinforced with FRP sheets are analyzed and modeled. In this method to simulate the crack in reinforced beams, the relations for determining the stress intensity coefficients with the presence of rebars and reinforcement sheets are developed. Here, it is assumed that a composite sheet is completely bound to the bottom surface of the beam under pure bending moment. In the proposed method beam components are divided into two categories, including components without cracks and components with cracks. In components without cracks, relations, equations, and the conventional stiffness matrix governing the beam are used, taking into account the changes in the moment of inertia caused by the presence of reinforcements and FRP sheets. In the finite component with a crack, the crack profile is simulated by creating a geometric defect in the beam section. So that the reduction in the hardness of the component with a crack is equivalent to the change in the dimensions of the discontinuity. Here, the changes in the hardness of the cracked component are calculated and presented as a function of the modified stress intensity coefficients. To ensure the correctness and accuracy of the presented method, all the analyzes are implemented in Abaqus software. The comparison of the obtained results shows that the presented method is a suitable method for the analysis of reinforced concrete structures resistant to cracking. So that it can be extended and developed for other models with proper accuracy. (DOI:**https//doi.org/10.52547/JCER.5.1.1**)

Keywords: crack; reinforced concrete beams; FRP sheets; stress intensity coefficients; Abaqus software

1. Introduction

Many cracked reinforced concrete structures suffer from basic damage and crack growth due to contact with corrosive factors and cyclic loading until finally the effects of complete failure and exit from access appear in them. This issue causes a lot of costs to repair, rebuild or replace damaged structures all over the world. So that millions of dollars are spent annually to repair and replace these structures. In an official statistic, the cost of repairing damaged rebar corrosion and cracking of reinforced concrete structures in the United States is estimated at 1 to 3 trillion dollars. In different regions of Iran, the destructive effects of crack growth and, as a result, the effect of corrosive factors in the foundations and

* Corresponding author. Tel.: 989111932123; e-mail: amirnazarinejad@gmail.com.

beams of bridges, dams, reinforced concrete channels, etc., cause heavy costs for the restoration and reconstruction of these buildings. Using epoxy coating on steel parts and rebars, injecting polymer into concrete surfaces and cathodic protection of rebars are some effective techniques to prevent the growth of cracks and corrosion of steel in concrete. Research results show that each of these techniques has been only partially successful. Today, researchers have proposed the idea of replacing steel parts and steel bars with new materials that are resistant to stress concentration caused by cracking and erosion of reinforcements. The use of new materials, especially composites instead of steel, has been highly favored by researchers in the last decade. Composites consist of an adhesive material (mostly epoxy) and an appropriate amount of fibers. These fibers may be carbon, glass, aramid, etc., the composite obtained with these fibers is called AFRP, GFRP, CFRP respectively.

1.1. Cracking in concrete structures reinforced with rebar

One of the first studies on the modeling of reinforced concrete structures using the finite element method was done in 1973 by Krishnamoorthy [1] and by presenting a computer program to investigate the behavior of a reinforced concrete frame. Next, Zdenek et al [2] presented an analytical model based on the determination of structural stresses using previous methods to calculate the elasticity of cracked reinforced concrete beams. Since the nonlinear behavior of these structures has a special role in static and dynamic analysis, Hu and William [3] conducted one of the first studies on the nonlinear analysis of cracked reinforced concrete structures in 1989. A suitable and efficient model for modeling these beams is to use the torsion spring model. This method can even be generalized to model cracking in structures with fiber concrete reinforced with FRP sheets, which was presented by Krawczuk [4] in 1995. In this method, by determining the stress intensity coefficients, the stiffness of the torsion spring is determined and corrected. The use of stress intensity coefficients to model the behavior of reinforced concrete structures with cracks was strongly considered by researchers, so studies in this field have continued until now and extensive research has been done on this topic [11-5]. With the progress of science, many numerical methods based on Computer programming have been developed for modeling cracks in reinforced concrete structures and in the field of analyzing the behavior of these structures [12-16].

1.2. Cracking in concrete structures reinforced with FRP sheet

Due to the excellent resistance of FRP composites against corrosion and cracking, these materials have been highly regarded by researchers. So that there have been extensive studies on the modeling and analysis of cracked reinforced concrete beams with the application of FRP sheets [17]. These studies show that the bending strength and fatigue life of the cracked concrete beam increases greatly after strengthening with reinforcement sheets. In their studies, Biokosturik and Hernig [18] theoretically proved that the yield of concrete beams after strengthening by FRP sheets is significantly reduced. Recently, the research conducted by Ardini and Nani [19] prove that by using reinforcement sheets, the final bending capacity and the stiffness of concrete beams with a rectangular cross-section can be significantly increased. Tammy et al. [20] and Zhi and Gerstel [21] investigated and presented cracking propagation in a beam under three-point bending without strengthening methods. They proved that these theoretical predictions cannot be extended to a strengthened beam. Talgestin [22] and Terin Taflo [23] introduced methods to solve stress problems in FRP-reinforced concrete beams. They focused on determining the shear stresses and stresses that lead to the separation of the epoxy material. In these studies, it was found that the modulus of elasticity, thickness, and geometry of the reinforcement sheet affect the maximum shear stress and stress in the area of the glued sheet. In the current studies, if the crack is located in the middle of the beam, a common method for determining the tensile stresses of the sheet has not been provided. Therefore, it is necessary to provide a simple method to determine the stresses on the FRP sheet in order to evaluate the resistance of the sheet to prevent the propagation of cracks. Composites are widely used as a new

advanced material in strengthening cracked concrete structures. While these materials are light in weight, they have high tensile strength and hardness. They also have high fatigue resistance against cyclic loading. Since concrete is a material with low tensile strength (about 1/10 of the ultimate compressive strength), the need for a reinforcing member to overcome this limitation is always felt. In this article, the effects of using FRP reinforcement members on the yield of cracked concrete beams are discussed by presenting a theoretical method. The use of composite reinforcement sheets causes geometrical changes in the beam section and consequently changes in the formulation for determining stress intensity coefficients and correcting the moment of inertia of cracked and uncracked sections. In this method, assuming the existence of a composite sheet on the lower surface of the beam, the relations of stress intensity coefficients are developed for this state. Using these modified stress intensity coefficients, crack modeling is done based on the creation of a geometric defect in the beam section. Finally, using a finite element method, the cracked reinforced concrete beam reinforced with FRP sheets is analyzed in static mode and its results are compared and verified with the simulations performed in Abaqus software.

2. An overview of previous research

One of the accurate and basic methods for analyzing beams with cracks is using the principles of fracture mechanics and determining stress intensity coefficients. In general, this method is based on the changes of strain energy and the changes of the second moment of the surface, before and after the creation of the crack. In this method, first, the geometric characteristics of the crack are simulated by reducing the cross-sectional area of the beam according to Figure (1). Then, the released energy rate is calculated due to the strain energy changes in the complete and cracked section.

In this method, the released energy is related to the values of stress intensity coefficients based on the relationship proposed by Erwin [25-24]. This coefficient for a beam with a rectangular section under pure bending is obtained from equation (1).In this method, the released energy is related to the values of stress intensity coefficients based on the relationship proposed by Erwin [25-24]. This coefficient for a beam with a rectangular section under pure bending is obtained from equation (1).

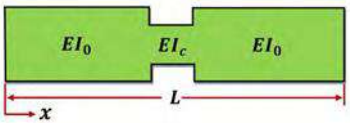

Figure 1- Reducing the cross-section of a cracked beam with changes in the moment of inertia

$$K_{I_M} = M(x)\sqrt{\frac{1}{b}\left(\frac{1}{I_0}-\frac{1}{I_C}\right)} \qquad \text{equation (1)}$$

where K_I is the stress intensity coefficient of the beam under bending moment, M is the bending moment, b is the thickness of the beam, E is the modulus of elasticity, I_0 is the moment of inertia of the cracked section and I_C is the moment of inertia of the cracked section.

By creating a deep link between the principles of fracture mechanics and the finite element method, this model can respond to the static, vibrational, buckling, and dynamic behaviour of composite structures with cracks. Since reinforced concrete structures are among the composite materials, as a result, the present method seems appropriate for the analysis of these structures. The relations presented by Kinzler [26] for calculating stress intensity coefficients were developed by Yokoyama [27-28] and Rice [29] as follows.

$$K_{I_M} = M\sqrt{\frac{1}{bI_0}\left(\frac{I_0}{I_C}-1\right)} \qquad \text{equation (1-2)}$$

$$K_{I_M} = \frac{6M}{bh^2}\sqrt{\pi a}F_M(\xi)\,,0 \le \xi \le 0.6\,,\xi = \frac{a}{h}$$

$$F_M(\xi) = \sqrt{\left(\frac{2}{\pi\xi}\right)tan\frac{\pi\xi}{2}}\frac{0.923+0.199\left[1-\sin\left(\frac{\pi\xi}{2}\right)\right]^4}{\cos\left(\frac{2}{\pi\xi}\right)}$$

equation (2-2)

$$K_{I_M} = \frac{3.99M}{bh\sqrt{h}\sqrt{(1-\xi)^3}}\ ,\ 0.6 < \xi < 1$$

equation (3-2)

where a is the depth of the crack, h is the height of the beam, and is defined as the ratio of the depth of the crack to the height of the beam.
Although extensive studies have been conducted on cracking in unreinforced beams and beams reinforced with steel reinforcements, limited research was done in the field of strengthening cracked beams by external reinforcements. A model for analyzing the problems of fracture mechanics of steel-reinforced concrete beams is the use of the stress intensity coefficients method, which was first presented by Carpentry [30]. In this method, the stress intensity factor in the reinforced concrete beam is determined by two independent factors. The stress intensity coefficient is caused by the external force (KM) and the stress intensity coefficient is caused by the tensile force of closing the rebars (Fs), which is denoted by (KF). As a result, the stress intensity factor for the cracked reinforced concrete beam reinforced with steel bars is presented as follows.

$$K_I = K_M - K_F \qquad \text{equation (3)}$$

3. Crack modeling formulation in reinforced concrete beams reinforced with FRP sheet

In this method, one-dimensional finite elements are used to model cracks in reinforced concrete beams reinforced with FRP sheets. The limited components of the beam are divided into two categories as shown below. The first category is components without cracks, which are simulated with finite elements equivalent to reinforced concrete and FRP sheet. These components are considered once using the transformed section method, integrated with the modulus of elasticity of concrete and by increasing the cross-sectional area at the place of the reinforcements. And once again, the cross-section of FRP sheet is equated with concrete and finally, they are considered as a single cross-section. The second category is the finite component with a crack, which is equated using a geometric defect. Due to the presence of a crack in this limited component, the cross-sectional area of the beam at the place of the crack decreases as much as the depth of the crack. The schematic representation of this category is presented in figure (2).

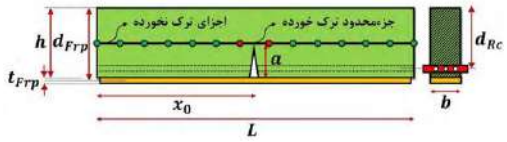

Figure 2- Cracked and uncracked finite elements in reinforced concrete beam reinforced with FRP sheets

3.1. Formulation of finite element method for non-cracked components with FRP sheet

The finite element method for non-cracked elements is investigated according to the Euler-Bernoulli beam theory. So that the basic equations can be defined by ignoring the effects of shear force and rotational inertia in the form of relations (4-1) and (4-2).

$$\varepsilon_x = \frac{\partial u}{\partial x} = \frac{\partial u_0}{\partial x} - z\frac{\partial^2 w}{\partial x^2}, \frac{\partial u_0}{\partial x} = 0 \longrightarrow \varepsilon_x = -z\frac{\partial^2 w}{\partial x^2}$$

equation (4-1)

$$\gamma_{xz} = \frac{\partial u}{\partial z} + \frac{\partial w}{\partial x} = 0 \longrightarrow u = u_0 - z\frac{\partial w}{\partial x}$$

equation (4-2)

where ε_x is the axial strain, u is the axial displacement, w is the vertical displacement and γ_{xz} is the shear strain.
According to equations (4-1), the structural equations for an elastic Euler-Bernoulli beam are defined as equation (5).

$$\sigma_x = E\varepsilon_x \longrightarrow \sigma_x = -E\frac{\partial^2 w}{\partial x^2} \qquad \text{equation (5)}$$

where σ_x is the axial stress and E is the modulus of elasticity of the beam.

In the Euler-Bernoulli beam theory, one-dimensional finite elements are used to analyze the finite elements of beams. The stiffness matrix of the beam without cracking is determined using the potential energy equation according to equations (4) and (6).

$$U = \frac{1}{2}\int {\varepsilon_x}^T \sigma_x dV \longrightarrow U = \frac{1}{2}\int_0^{l_e} EI_0\left(\frac{\partial^2 w}{\partial x^2}\right)^T\left(\frac{\partial^2 w}{\partial x^2}\right)dx, w = [N]u$$

equation (4)

where U is the potential energy, $l_e$is the length of the element and N is the function of the Hermitian shape according to []. By placing relation (5) in relation (4), the stiffness matrix of a limited component of the beam is obtained, which can be generalized for other components.

$$K_0 = EI_0 \int_0^{l_e} [N'']^T [N''] dx$$

equation (6-1)

$$K_0 = \frac{EI_0}{l_e^3} \begin{bmatrix} 12 & 6l_e & -12 & 6l_e \\ 6l_e & 4{l_e}^2 & -6l_e & 2{l_e}^2 \\ -12 & -6l_e & 12 & -6l_e \\ 6l_e & 2{l_e}^2 & -6l_e & 4{l_e}^2 \end{bmatrix}$$

equation (6-2)

where K_0 is the stiffness matrix of a finite component of the beam without cracking.

What is important here is the changes in the moment of inertia caused by the presence of reinforcing armatures and FRP sheets in the structure. whose effects should be considered in relation (2-6). For this purpose, the idea of a transformed cross-section according to Figure (3) is used. In this method, the cross-section of the reinforced concrete beam with a compressive area above the neutral web, and a tensile area below the neutral web, equals n_1- 1 to the cross-sectional area of steel and n_2- 1 to the cross-sectional area of the FRP sheet. As the compressive strength of concrete is known, according to Iran's concrete regulations, the modulus of elasticity of concrete is determined according to equation (1-7).

$$E_c = \left(3300\sqrt{f_c} + 6900\right)\left(\frac{\gamma_c}{23}\right)^{\frac{3}{2}}$$

equation (7-1)

$$n_1 = \frac{E_s}{E_c}$$

equation (7-2)

$$n_2 = \frac{E_{Frp}}{E_c}$$

equation (7-3)

Here, n_1 and n_2 are the ratio of the elasticity coefficient of steel to concrete and the ratio of the elasticity coefficient of composite to concrete, respectively.

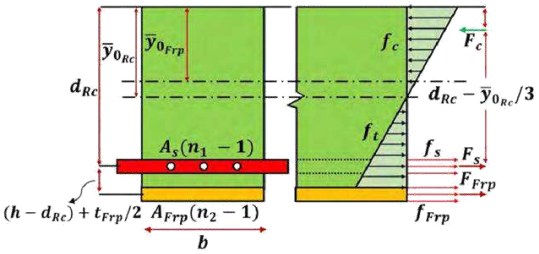

Figure 3- The transformed section of the reinforced concrete beam standard

According to Figure (3), the location of the neutral web and the modified moment of inertia in the beam reinforced with reinforced concrete and FRP sheet in the uncracked state are determined according to relations (1-8) to (3-8):

$$\bar{y}_{0_{Frp}} = \frac{bh\left(\frac{h}{2}\right) + (A_{Frp}(n_2 - 1)d_{Frp})}{bh + A_{Frp}(n_2 - 1)}$$

equation (8-1)

$$\bar{y}_{0_{RC}} = \frac{bh\left(\frac{h}{2}\right) + (A_s(n_1 - 1)d_{RC})}{bh + A_s(n_1 - 1)}$$

equation (8-2)

$$I_{0_{Frp}} = \frac{bh^3}{12} + bh(\frac{h}{2} - \bar{y}_{0_{RC}})^2 + A_s(n_1 - 1)\left(d_{RC} - \bar{y}_{0_{RC}}\right)^2 + bh(\frac{h}{2} - \bar{y}_{0_{Frp}})^2 + A_{Frp}(n_2 - 1)(d_{Frp} - \bar{y}_{0_{Frp}})^2$$

equation (8-3)

where $\bar{y}_{0_{RC}}$is the location of the neutral web in the reinforced concrete beam without cracks, $I_{0_{Frp}}$ is the moment of inertia of the reinforced concrete beam without cracks, A_s is the cross-section of the beams, d_{RC} is the distance between the reinforcements and the upper web of the beam, $\bar{y}_{0_{RC}}$ is the location of the neutral web in the beam reinforced with FRP sheets in the state without Crack, A_{Frp} is the cross-section of the composite sheet and D_{Frp} is the distance between the sheet and the upper web of the beam.

By inserting the equation (3-8) into the equation (2-6), the stiffness matrix of the components of the reinforced concrete beam without cracking is presented according to the equation (9).

$$K_{0_{Frp}}^{st} = \frac{EI_0}{l_e^3}\begin{bmatrix} 12 & 6l_e & -12 & 6l_e \\ 6l_e & 4{l_e}^2 & -6l_e & 2{l_e}^2 \\ -12 & -6l_e & 12 & -6l_e \\ 6l_e & 2{l_e}^2 & -6l_e & 4{l_e}^2 \end{bmatrix}$$

equation (9)

3.2. Formulation of finite element method for the cracked finite element with FRP sheet

The implementation of the finite element method for the cracked (enriched) finite element is done according to the reduced cross-section method according to Figure (4).

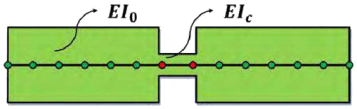

Figure 4- Reducing the cross-section of a reinforced concrete beam with a crack

By reducing the cross-section of the beam, the location of the neutral web and the moment of inertia of the reinforced concrete section at the crack location are shown in figure (5).

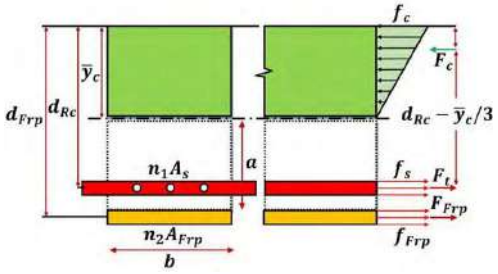

Figure 5- Cracked transformed section

As a result, by rewriting the relations (8-1) to (8-3), the location of the neutral web and the moment of inertia of the cracked reinforced concrete section in the state that they are reinforced with FRP sheet, are determined as relations (10-1) and (10-2).

$$\bar{y}_{C_{Frc}} = \frac{b(h-a)+\frac{h-a}{2}}{b(h-a)}$$

equation (10-1)

$$I_{C_{Frp}} = \frac{b\bar{y}_c^3}{3} + n_1 A_s (d_{RC} - \bar{y}_C)^2 + n_2 A_{Frp}(d_{Frp} - \bar{y}_C)^2$$

equation (10-2)

where $\bar{y}_c$ is the location of the neutral web in the reinforced cracked beam and $I_{C_{Frp}}$ is the moment of inertia of the reinforced cracked reinforced concrete beam.

By placing the moments of inertia extracted for healthy and cracked sections, according to relations (2-10) and (3-8) in relation (1), stress intensity coefficients for cracked reinforced concrete beam with composite reinforcement sheet are determined as relation (11).

$$K_{I_{Frp}} = \frac{M}{b}\frac{1}{\frac{bh^3}{12} + bh(\frac{h}{2} - \bar{y}_{0_{RC}})^2 + A_s(n_1-1)(d_{RC} - \bar{y}_{0_{RC}})^2 + bh(\frac{h}{2} - \bar{y}_{0_{Frp}})^2 + A_{Frp}(n_2-1)(d_{Frp} - \bar{y}_{0_{Frp}})^2} - \frac{M}{b}\frac{1}{\frac{b\bar{y}_c^3}{3} + n_1 A_s(d_{RC} - \bar{y}_c)^2 + n_2 A_{Frp}(d_{Frp} - \bar{y}_c)^2}$$

equation (11)

After determining the modified stress intensity coefficients, the crack-equivalent discontinuity can be replaced by a torsion spring. So that the reduction of the stiffness of the cracked area is equated with the reduction of stiffness and the increase of the torsional moment of the torsion spring. As a result, the degree of softness of the torsion spring is presented as a function of the stress intensity coefficient in the form of equation (12).

$$\lambda_M = \frac{1}{K_S} = \frac{2b(1-v^2)}{E}\int_0^a (\frac{K_{I_{Frp}}}{M})^2 da$$

equation (12)

where λ_M is spring softness, k_S is spring stiffness, v is Poisson's ratio and $K_{I_{Frp}}$ is the corrected stress intensity factor for the reinforced section. By inserting equation (10-2) into equation (6-2), the reinforced stiffness matrix of the cracked component of the reinforced concrete beam is presented according to equation (13).

$$K_{C_{Frp}} = \frac{EI_{Frp}}{l_{e_c}^3}\begin{bmatrix} 12 & 6l_e & -12 & 6l_e \\ 6l_e & 4l_e^2 & -6l_e & 2l_e^2 \\ -12 & -6l_e & 12 & -6l_e \\ 6l_e & 2l_e^2 & -6l_e & 4l_e^2 \end{bmatrix}$$

equation (13)

where l_{e_c} is the length of the cracked area. The stiffness matrix of the standard reinforced concrete components in the reinforced state with the composite sheet is combined with the stiffness matrix of the cracked limited component, which finally forms the final stiffness matrix of the structure.

4. Discussion and results

In this section, to check the accuracy and correctness of the proposed model, the behavior of a reinforced concrete beam with a crack is tested in the form of a practical example. So that the changes in the depth and location of the crack on the elasticity of the elastic beam are investigated and its values are verified with Abaqus software.

4.1. Model specifications

A reinforced concrete beam with a crack and reinforced with a composite sheet with assumed geometric and material specifications according to Table (1) is examined under simple two-end boundary conditions. The crack in the tensile web of the beam is assumed to be constant along the thickness. Crack depth changes from zero to 6.0 height and crack location changes in the area between 0.05 – 0.95 beam length are investigated.

Table 1- Features of the reinforced concrete beam with cracks

$L = 4\ m$	$d_{Frp} = 0.3\ m$	$E_c = 2.5e10\ N/m^2$
$h = 0.35\ m$	$A_S = \pi D^2/4\ m^2$	$E_s = 2.0e11\ N/m^2$
$b = unit$	$A_{Frp} = 0.00113998\ m^2$	$E_{Frp} = 2.6e11\ N/m^2$
$t_{Frp} = 0.0011398\ m$	$\frac{a}{h} = 0.0 - 0.6$	$v_c = 0.25$
$D_{Re} = 3\emptyset 22\ m$	$\frac{x_0}{L} = 0.05 - 0.95$	$v_s = 0.3$
$d_{Re} = 0.27\ m$	$q = w \times L = 4e6\ N/m$	$v_{Frp} = 0.3$

4.2. Verification of crack depth changes

To check the accuracy and efficiency of the proposed model, a reinforced concrete beam reinforced with FRP sheet under the mentioned boundary and geometrical conditions is considered. First, by assuming the location of the crack in the middle of the beam to be fixed ($\frac{x_0}{L} = 0.5$), the deflection changes caused by the increase of the crack depth from zero to 0.6 height of the beam are investigated according to Figure (6) for the reinforced concrete beam under SS-SS boundary conditions.

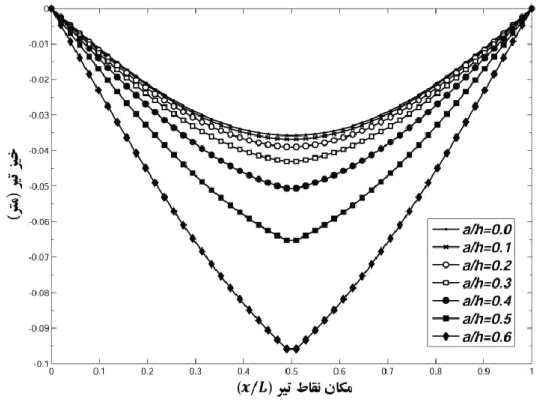

Figure 6- The effect of crack depth on the yield of the reinforced concrete beam (SS-SS)

To ensure the accuracy of the presented model, the obtained results are compared and validated with the simulation results in Abaqus software according to Table (2).

Table 2- Static analysis of reinforced concrete beam with a crack in the middle, under SS-SS boundary conditions with changes in crack depth

a/h	Beam deflection Article method (m)	Beam deflection Abaqus (m)	Error (%)
0	-0.03629	-0.03487	1.49929
0.1	-0.03705	-0.03589	2.329163
0.2	-0.03882	-0.03797	3.327761
0.3	-0.04436	-0.04426	5.115812
0.4	-0.04992	-0.04942	4.58037
0.5	-0.06409	-0.06164	1.581803
0.6	0.093524	-0.09341	5.506505

The results from table (2) show that up to a depth of 0.5 beam height, the modeling error is around 4%. The error growth at depths greater than 0.5 is caused by the nonlinear behavior of concrete and steel, the effects of which are not considered in this research. The validation results show the appropriate accuracy

of the presented method in the static analysis of the elastic-reinforced concrete beam with cracks.

4.3. Checking the changes in the place of crack

In this review, the accuracy of the proposed model is checked by assuming a constant crack depth (a/h=0.3, 0.5) and changing the crack location between -0.05 to 0.95 beam length, according to Figure (7).

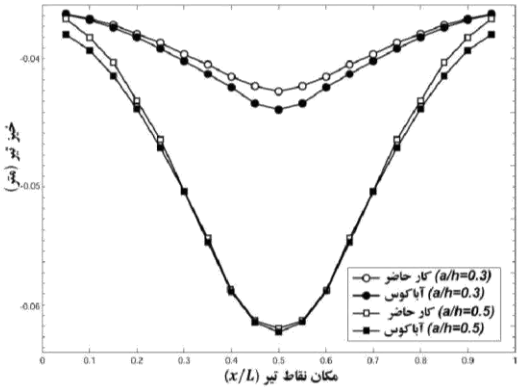

Figure 7- The effect of crack location on the deflection of the reinforced concrete beam (SS-SS)

Examining Figure (7) shows the appropriate accuracy of the presented method, so that it can be seen that the curves related to the results of finite element modeling and abacus completely coincide with each other. In this case, the reason for the error of 5.5% seems to be not considering the effects of the shear force in the assumptions of the Euler-Bernoulli beam theory, which is negligible.

5. Conclusion

In this article, the static behavior of the cracked reinforced concrete beam reinforced with FRP sheet has been analyzed and investigated. The analysis performed is based on the improvement of the finite element method and by dividing the beam components into two categories. The first category is the standard non-cracked components that are modified based on the modification of the moment of inertia caused by the presence of rebars and composite sheet with the converted section method. The other category is the finite element with a crack, which is modeled using the reduced section method. Using the provided relationships, the stiffness matrices of the standard and cracked components are modified and the final stiffness of the cracked structure is determined. In the current study, the effects of the depth and location of the crack on the yield of the beam were investigated and the results were validated. Comparison and analysis of the obtained results show:

A) The changes in rise caused by the depth of the crack in the range of less than 0.1 beam height have not been taken into account due to the lack of influence. Also, due to the non-linear behavior of concrete in a range greater than 0.6 beam height, the changes in creep due to the depth of the crack are not considered in this area.

B) The comparison of the obtained results with changes in crack location and depth showed that the proposed new solution for modeling cracks in reinforced concrete beams using the finite element method is acceptable with appropriate accuracy.

C) As the depth of the crack increases, the amount of deflection of the beam always increases. This increasing process gains more momentum from the depth of 0.4 height so that with small changes in the depth of the crack, the rise increases greatly.

References

[1] Krishnamoorthy, C., Panneerselvam , S. A. (1978). FEP-ACSl-a finite element program for nonlinear analysis of reinforced concrete framed structures, Journal of Computer and Structures, Vol. 9, pp. 451–461J. Newman, Electrochemical Systems, 2nd ed., Prentice-Hall, Englewood Cliffs, NJ, 1991.

[2] Zdenek, P.B., Byung, H. (1984). Deformation of Progressively Cracking Reinforced Concrete Beams, Journal of ACI, Vol. 71, pp. 268–278.B. Miller, Proc. 6th Australian Electrochem. Conf., Geelong, Vic., 19-24 Feb., 1984; J. Electroanal. Chem., 168 (1984) 91.

[3] Hu, H., William, C. (1990). Nonlinear analysis of cracked reinforced concrete, Journal of ACI, Vol. 87, pp. 199–207.

[4] Krawczuk, M., Ostachowicz, W. M. (1995). Modelling and vibration analysis of a cantilever composite beam with a transverse open crack, Journal of Sound and Vibration, Vol. 183, pp. 69–89.

[5] Husnu, M., Alaattin, A. (2000). Analytical and finite element comparisons of stress intensity factors of composite materials, Journal of Composite Structures, Vol. 50, pp. 99–102.

[6] Lau, K., Shi, S. (2001). Estimation of stress intensity factor (KI) for an FRP bonded concrete beam using the superposition method, Journal of Concrete Research, Vol. 53, pp. 31–41.
[7] Yang, Q. G., Chen, Q. (2004). Analysis of the stress intensity factor of vertical cracks in small-size beams bonded with GFRP, Journal of Damage and Fracture Mechanics, Vol. 55, pp. 67–79.
[8] Wang, K., Inman, D., Farrar, C. (2005), Modeling and analysis of a cracked composite cantilever beam vibrating in coupled bending and torsion, Journal of Sound and Vibration, Vol. 284, pp. 23–49.
[9] Ju, S. H., Liu, S. H. (2007), Determining stress intensity factors of composites using crack opening displacement, Journal of Composite Structures, Vol. 81, pp. 614–621.
[10] Mogadpalli, G. P., Parameswaran, V. (2008), Determination of stress intensity factor for cracks in orthotropic composite materials using digital image correlation, Journal of compilation, Vol. 44, pp. 446– 452.
[11] Dotti, F., Cortnez, V., Reguera, F. (2013), Mode I stress intensity factor for cracked thin-walled composite beams, Journal of Theoretical and Applied Fracture Mechanics, Vol. 68, pp. 38–45.
[12] Rogoza, A., Ubysz, A. (2009), Numerical analysis of the crack reainforced concrete beams, 18th International Conference on the Application of Computer Science and Mathematics in Architecture and Civil Engineerings, Germany, 07-09 July.
[13] Benarbia, D., Benguediab, M., Benguediab, S. (2013), Two-dimensional Analysis of Cracks Propagation in Structures of Concrete, Journal of Engineering, Technology & Applied Science Research, Vol. 3, pp. 429– 432.
[14] Subramani, T., Manivannan, R., Kavitha, M. (2014), Crack Identification in Reinforced Concrete Beams Using Ansys Software, Journal of Engineering Research and Applications, Vol. 4, pp. 133–141.
[15] Slowik, M., Smarzewski, P. (2014), Numerical Modeling Of Diagonal Cracks In Concrete Beams, Journal of Archives Of Civil Engineering, Vol. 3, pp. 307–322.
[16] Costa, D., Carmo, R., Costa, R. (2016), Numerical modeling of concrete beams under serviceability conditions with a discrete crack approach and noniterative solution-finding algorithms, Journal of International Federation for Structural Concrete, Vol. 18, pp. 225–236.
[17] Saadatmanesh, H., Ehsani, M. R. (1990), Fibre composite plates can strengthen beam, Journal of the American Concrete Institute, Vol. 12, pp. 65-71.
[18] Buyukozturk, O., Hearing, B. (1998), Failure behaviour of precracked concrete beams retrofitted with FRP, Journal of Composites for Construction, Vol. 3, pp. 138-144.
[19] Arduini, M., Nanni, A. (1997), Behaviour of precracked RC beams strengthened with carbon FRP sheets, Journal of Composites for Construction, Vol. 1, pp. 63-69.
[20] Toumi, A., Bascoul, A., Turatsinze, A. (1998), Crack propagation in concrete subjected to flexural cyclic loading, Journal of Materials and Structures, Vol. 31, pp. 451-458.
[21] Xie, M., Gerstle, W. H., (1995), Energy-based cohesive crack propagation modeling, Journal of Engineering Mechanics, Vol. 121, pp. 1349-1358.
[22] Taljsten, B. (1997), Strengthening of beams by plate bonding, Journal of Materials in Civil Engineering, Vol. 9, pp. 206-212.
[23] Triantafillou, T. C. (1998), Shear strengthening of reinforced concrete beams using epoxy-bonded FRP composites. ACI Structural Journal, Vol. 95, pp. 107-115.
[24] Irwin, G.R., Kies, J.A. (1954), Critical energy rate analysis of fracture strength, Journal of Welding, Vol. 33, pp. 193-198.
[25] Irwin, G.R. (1957), Analysis of stresses and strains near the end of a crack traversing a plate, Journal of Applied Mechanics, Vol. 24, pp. 361-364.
[26] Kienzler, R., Herrmann, G. (1986), An elementary theory of defective beams. Journal ofActa Mechanica,Vol. 62 , pp. 37-46.
[27] Yokoyama, T. (1996), Vibration analysis of Timoshenko beam-columns on two-parameter elastic foundations, Journal of Computers & Structures, Vol. 61, pp. 995-1007.
[28] Yokoyama, T., Chen, M.C. (1998), Vibration analysis of edge-cracked beams using a linespring model, Journal of Engineering Fracture Mechanics, Vol. 59, pp. 403-409.
[29] Ricci, P., Viola, E. (2006), Stress intensity factors for cracked T-sections and dynamic behavior of T-beams, Journal of Engineering Fracture Mechanics, Vol. 73, pp. 91–111.
[30] Carpinteri, A. (1986), Mechanical Damage and Crack Growth in Concrete, Martinus Nijhoff, Dordrecht.

Journal of Civil Engineering Researchers

J-Researchers

JOURNAL OF CIVIL ENGINEERING RESEARCHERS

Investigating the effect of using Multi-Level Yielding Pipe Damper dampers in steel structures under earthquake force in the horizontal direction

Lobat Hosseinzadeh [a,*]

[a]*Ms.c student, Department of Civil Engineering and Surveying, Mahmudabad Branch, Islamic Azad University*

Article History: Received date: 2023.02.19; revised date: 2023.03.15; accepted date: 2023.03.20

Abstract

Multi-level Pipe Damper (MPD) recently proposed by the authors is a passive control device to reduce the seismic vibration. In this research, seismic response of steel structures equipped with MPD is studied. To evaluate the effects of the proposed damper, typical 8 story steel buildings are modeled and their seismic responses under three earthquake excitations are investigated using dynamic nonlinear time-history analyses by ETABS program. Results show the effectiveness of MPD to altering the seismic response of the structures. Moreover, using MPD decreases the structural and nonstructural damages noticeably by limiting the inter story drifts because of the secondary hardening branch of force-displacement respectively proving the effectiveness of the proposed damper as a retrofitting technique for structures at high seismic risk areas. (DOI:**https//doi.org/10.52547/JCER.5.1.10**)

"Keywords: Multi-level pipe damper passive control seismic vibration dynamic analysis structural control"

1. Introduction

Severe earthquakes impose noticeable amount of input energy to structures and cause structural and non-structural damages. Besides, most structural elements show stiffness and strength degradation and low inherent damping ratio during the first cycles of a seismic excitation. So, utilization of new tools and equipment is inevitable to avoid these defects by concentrating on the plastic deformation in some controlled locations in building structures. Using metallic yielding dampers is one of the effective and economical manners to improve the seismic performance of structures by limiting the seismic forces like a fuse and dissipating a major part of input seismic energy. At first Kelly et al. (1972) proposed yielding damper as an effective passive control device. After that many metallic dampers have been suggested by others such as ADAS device (Bergman and Geol 1987), TADAS device (Tsai et al., 1993), and Shear-Panel Damper (Nakashima et al., 1994). The numerical and experimental research proved that the above mentioned devices result in seismic input reduction, increase in the equivalent viscous damping

* Corresponding author. Tel.: +989113927782; e-mail: Lobi_h@yahoo.com.

ratio and damage decrease. Curadelli and Riera (2004) conducted research on steel and concrete frames equipped with metallic dampers. Fragility curves of the structures show that the failure probability of the structures may be decreased to 20% of the initial value by adding external metallic dampers for the cases studied. In another work, Oviedo et al. (2010) studied the seismic response of structure with metallic dampers. Results proved that buildings with low yield story drift ratio show the largest reduction in the inelastic demand. Slit damper is one of the other metallic dampers. Shape optimization of the slit damper has been widely investigated by researchers (Ghabraie et al., 2010; Houng Xu et al., 2011). In addition, Saffari and Hedayat (2013) offered suitable setting relationships to achieve proper behavior using several cyclic testing on 8 samples. In recent years, steel pipes are widely used to improve seismic behavior of Concentrically Braced Frames, CBFs. Kafi (2009) conducted research on the effects of steel pipe to improve seismic behavior of CBFs. The numerical and experimental results showed main influence on the frames ductility and delay in brace buckling. Hollow steel pipes filled with concrete were suggested by Maleki andBagheri (2010a) as hysteresis dampers under shear stresses. According to their results, stiffness and strength of the pipe increased linearly with increasing the length but nonlinearly with increasing the thickness and reducing the diameter. Steel pipes filled with concrete showed no ductile behavior caused by concrete failure while hollow steel pipes had stable hysteresis behavior and high equivalent viscous damping ratios. Also, they used pipe damper to improve the seismic performance of a bridge (Maleki and Bagheri 2010b). Their numerical results presented a proper energy dissipation and reduction in the forces transferred to the foundations of bridges. Another pipe damper proposed by Maleki and Mahjoobi (2013) was Dual Pipe Damper (DPD). This damper consisted of two pipes, welded to the upper part of chevron or diagonal bracing under the lateral loading to increase energy dissipation. The results of the cyclic tests on four samples indicated stable hysteresis curves with a significant increase in ductility and energy dissipation. Besides, seismic performance evaluation and design of steel structures equipped with dual-pipe dampers were investigated (Mahjoubi and Maleki, 2016). Some steel moment frames of 5, 10 and 20 stories were modeled and their seismic responses under seven earthquake excitations were investigated using dynamic nonlinear analyses. The results showed that the DPD is so effective in dissipating a considerable amount of the input seismic energy and reducing the damage. Using two-level control systems is one of the new methods that attracted the researchers in the recent years. The significant idea of these systems is to combine several control systems with various amounts of strength and stiffness resulting desirable energy dissipation in various earthquake intensity levels. Balendra et al. (2001) proposed two-level passive control system consisting of a knee brace and a slotted connection. In service loads, slit connection would create energy dissipation by friction damping, while in severe earthquakes, energy dissipation through plastic behavior of knee member is provided. The concept of multi-level control system was proposed and improved by many researchers during the last decade (Hosseini Hashemi & Alirezai 2010; Zahrai & Rousta 2013). Moreover, Zahrai and Vosoogh (2013) suggested the dual system using a combination of vertical link beam and knee elements. Plastic hinge on the vertical link within low forces, increased energy dissipation while plastic deformation of the knee increased the ductility and energy absorption during extreme forces to improve seismic performance. Cheraghi and Zahrai (2016) recently proposed the innovative Multi-level Pipe Damper (MPD) using two steel pipes. As shown in Fig. 1, the proposed damper consists of a combination of nested pipes that could change dynamic behavior parameters like strength, stiffness and damping ratio for energy absorption at different earthquake levels from moderate to severe conditions. They first investigated numerical study of the innovative damper and then performed experimental quasi-static cyclic tests on two samples showing suitable hysteresis curves up to relatively large displacements and high ductility. Figure 2 displays the deformed shape of a MPD specimen at the end of the cyclic test. Hysteresis diagrams show multi-level behavior with variable strength and stiffness as expected that can dissipate seismic energy in different earthquake levels. In other word, at large deformations, increasing the stiffness was observed

that seems this behavior can prevent large drifts and P-Δ moments in structures subjected to severe earthquakes. Besides, achieving equivalent viscous damping ratio of about 19-38% without use of sophisticated tools is noticeable. In this paper, the seismic responses of 8 story steel buildings equipped with proposed dampers are obtained using nonlinear dynamic time-history analyses by ETABS program. In addition, IDA analyses are performed to evaluate the damper effects on promoting the performance capacity of the frames. Finally, the results are compared with each other to find the new dampers efficacy to alter seismic behavior and energy dissipation.

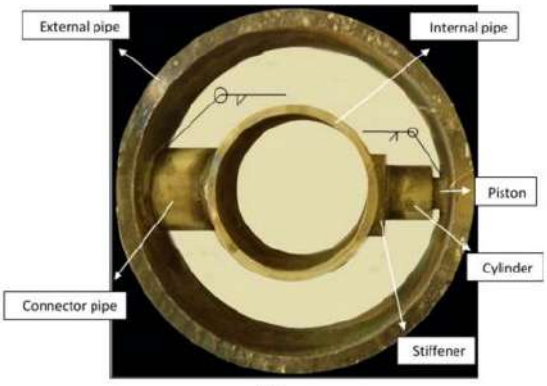

(a)

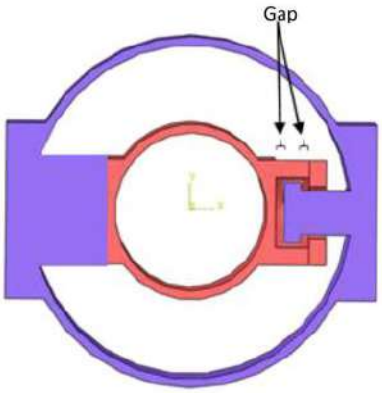

(b)

Figure1 :(a) Assembled damper (b) Cross section of the damper (Cheraghi and Zahrai, 2016).

(a) sample1 (b) sample 2

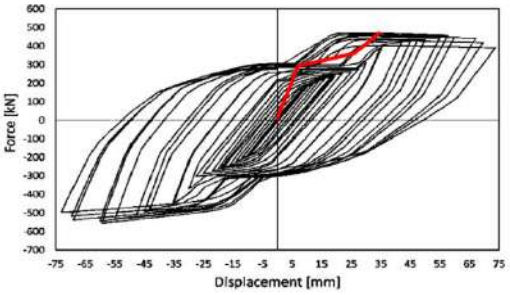

(a) sample 1

Figure 2: Failure details of the test samples (Cheraghi and Zahrai, 2016)

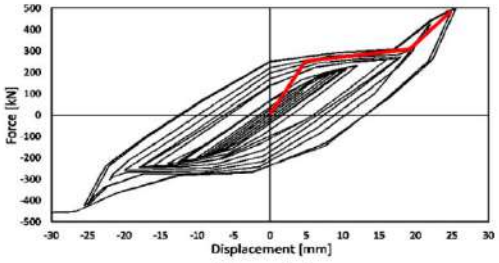

(b) sample 2

Figure3. Simplified tri-linear model representing nonlinear behavior of the MPD according to the experimental hysteresis curves (Cheraghi and Zahrai, 2016)

2.Numerical Modeling and Analysis

In this paper, to obtain the seismic performance of steel structures equipped with proposed dampers, 8 story moment resisting steel building are modeled and their seismic responses under three earthquake excitations are investigated using dynamic nonlinear analyses.

First, In order to evaluate the vulnerability of MDOF structures (multiple degrees of freedom) under the effect of earthquake and aftershock sequences, an 8-story building in Tehran of medium steel bending frame type and type 3 soil by LRFD method based on the 10th topic of the National Building Regulations and the 4th edition 2800 standard was designed. These structures have three 5-meter openings in each direction, and the height of the floors is 3.2 and the height of the parking lot is 2.7. First, the design of this building according to the residential use and located on the area with very high relative risk according to the definition of standard 2800 with the help of software Etabs done. And then in the A and D frames, Multi-Level Yielding Pipe Damper ((a) sample 1) was used.

List of designed column sections

Box180x8
Box200x8
Box200x10
Box200x12
Box240x10
Box240x12
Box240x15
Box240x20
Box300x20

List of designed beam sections:

PG-W180x6-F150x8
PG-W180x6-F150x15
PG-W300x6-F150x10
PG-W300x6-F150x12
PG-W300x6-F150x15
PG-W300x6-F150x20

3D view without damper:

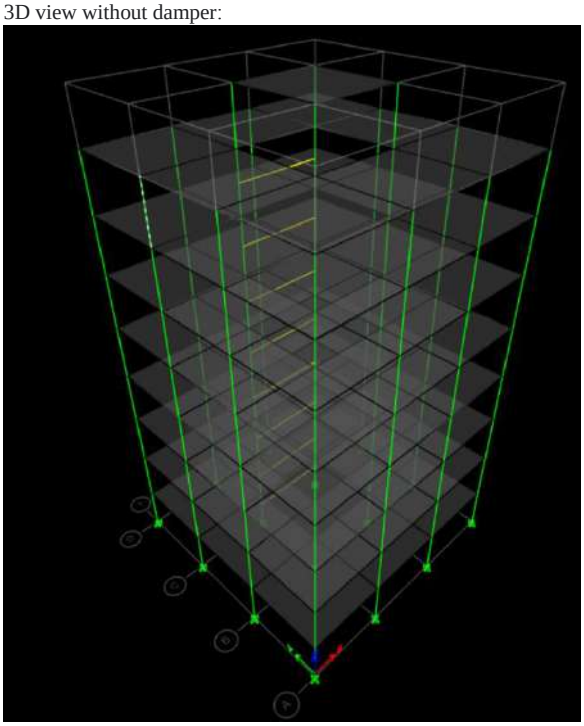

2D view designed with damper:frame A:

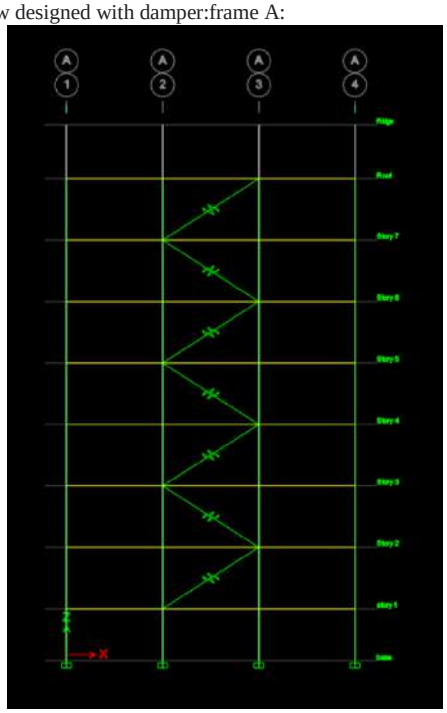

2D view designed with damper:frame D:

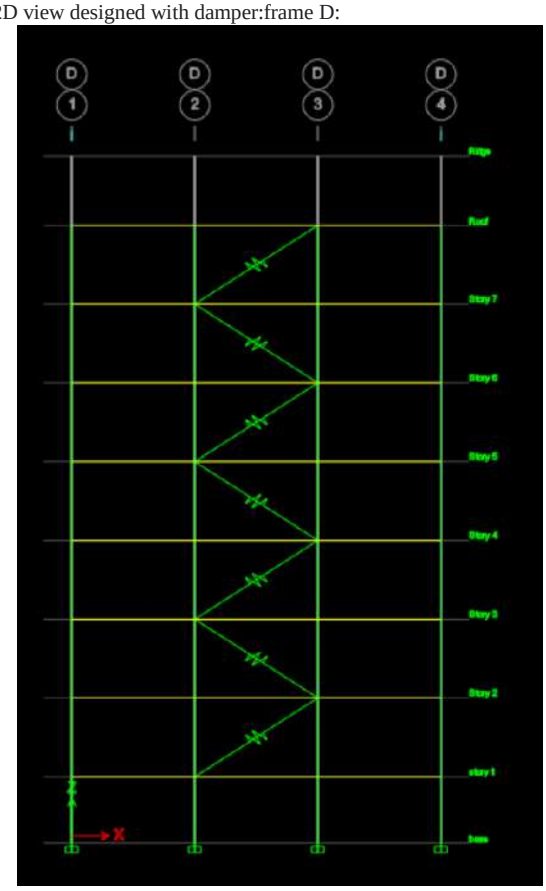

Past studies have shown that in order to achieve a suitable seismic behavior, the records must be scaled to the desired risk level. In this research, from 3 The raw accelerometer that is suitable for the type of soil is extracted from the data of the PEER site and according to the instructions of the fourth edition of the 2800 peer-based standard andscaled and used And comparisons based on HOLISTER earthquake were shown in this article.

In Table 1, the characteristics of each of the earthquake accelerometers and their corresponding aftershocks are given.

Table No. 1 - Characteristics of earthquake and aftershock acceleration maps

The name of the earthquake	Station	Great Earthquake	great aftershocks	spead shear wave
1.HOLISTER	HOLISTER	5.6	5.5	198
2.Imperial Valley	Holtville	6.53	5.01	202
3.Northwest	Jiashi	6.1	5.8	240

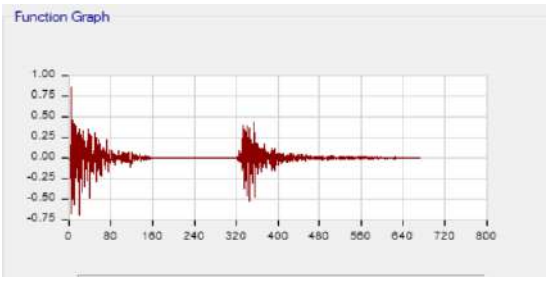

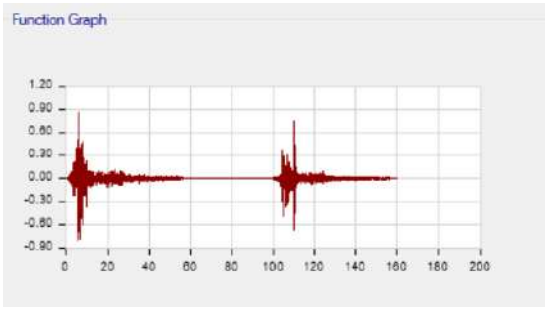

1.Holister earthquake
2.Imperial Vallay earthquake
3.Northwest earthquake

3.Comparison of the drift distribution of floors

The mentioned building has been exposed to the seismic sequences of accelerometers introduced in Table 1 under time history analysis and the changes The drift of floors is shown in tables 2 and 3. As can be seen from the graphs related to the drift of the floors, the use of damper leads to the reduction of the drift of the structure.

Table2. Relative displacement of floors under earthquake 1 without using damper

Story	Output Case	Step Type	Dir.	Drift
Story 7	EQ1	Max	X	0.097923
Story 7	EQ1	Max	Y	0.018276
Story 7	EQ1	Min	X	0.081789
Story 7	EQ1	Min	Y	0.018133
Story 6	EQ1	Max	X	0.123716
Story 6	EQ1	Max	Y	0.032681
Story 6	EQ1	Min	X	0.107888
Story 6	EQ1	Min	Y	0.032492
Story 5	EQ1	Max	X	0.122161
Story 5	EQ1	Max	Y	0.02962
Story 5	EQ1	Min	X	0.108304
Story 5	EQ1	Min	Y	0.029583
Story 4	EQ1	Max	X	0.121894
Story 4	EQ1	Max	Y	0.028441
Story 4	EQ1	Min	X	0.108955
Story 4	EQ1	Min	Y	0.028424
Story 3	EQ1	Max	X	0.119638
Story 3	EQ1	Max	Y	0.028189
Story 3	EQ1	Min	X	0.107224
Story 3	EQ1	Min	Y	0.02817
Story 2	EQ1	Max	X	0.103495
Story 2	EQ1	Max	Y	0.024689
Story 2	EQ1	Min	X	0.091843
Story 2	EQ1	Min	Y	0.024668
story 1	EQ1	Max	X	0.049083
story 1	EQ1	Max	Y	0.011208
story 1	EQ1	Min	X	0.043623
story 1	EQ1	Min	Y	0.011197

4- Comparison of structure periodicity time and frequency in different modes of the structure

The 8-story building has 24 modes, which are shown in tables 4 and 5 of the periodicity and frequencies of the structure in different modes. The comparison of the above tables shows that the use of the damper reduces the period of the structure in different modes.

Table3. Relative displacement of floors under earthquake 1 in the case of using a damper

Story	Output Case	Step Type	Dir.	Drift
Story 7	EQ1	Max	X	0.067256
Story 7	EQ1	Max	Y	0.015419
Story 7	EQ1	Min	X	0.056153
Story 7	EQ1	Min	Y	0.015257
Story 6	EQ1	Max	X	0.080806
Story 6	EQ1	Max	Y	0.02132
Story 6	EQ1	Min	X	0.090603
Story 6	EQ1	Min	Y	0.021276
Story 5	EQ1	Max	X	0.096639
Story 5	EQ1	Max	Y	0.021438
Story 5	EQ1	Min	X	0.085519
Story 5	EQ1	Min	Y	0.021409
Story 4	EQ1	Max	X	0.091282
Story 4	EQ1	Max	Y	0.020917
Story 4	EQ1	Min	X	0.096086
Story 4	EQ1	Min	Y	0.020921
Story 3	EQ1	Max	X	0.099637
Story 3	EQ1	Max	Y	0.022223
Story 3	EQ1	Min	X	0.095368
Story 3	EQ1	Min	Y	0.022305
Story 2	EQ1	Max	X	0.0874
Story 2	EQ1	Max	Y	0.019855
Story 2	EQ1	Min	X	0.09113
Story 2	EQ1	Min	Y	0.019906
story 1	EQ1	Max	X	0.046417
story 1	EQ1	Max	Y	0.011494
story 1	EQ1	Min	X	0.05629
story 1	EQ1	Min	Y	0.011486

Table4.The periodicity of the structure and the frequency due to the earthquake in the state without using a damper in different modes of the structure

TABLE: Modal Periods And Frequencies				
Mode	**Period**	**Frequency**	**CircFreq**	**Eigenvalue**
	sec	cyc/sec	rad/sec	rad²/sec²
1	1.905	0.525	3.2976	10.8742
2	1.753	0.571	3.5852	12.8537
3	1.629	0.614	3.8564	14.8721
4	0.648	1.544	9.6998	94.0859
5	0.627	1.595	10.0201	100.4028
6	0.564	1.774	11.1454	124.2196
7	0.384	2.604	16.3628	267.741
8	0.366	2.729	17.1446	293.9359
9	0.331	3.019	18.9695	359.8415
10	0.278	3.591	22.5627	509.0765
11	0.264	3.789	23.8071	566.777
12	0.247	4.051	25.4509	647.75
13	0.227	4.407	27.6876	766.6035
14	0.217	4.617	29.0126	841.7308
15	0.214	4.67	29.3405	860.8638
16	0.184	5.423	34.074	1161.0359
17	0.182	5.498	34.5476	1193.535
18	0.173	5.786	36.3535	1321.5794
19	0.139	7.18	45.1137	2035.2478
20	0.138	7.225	45.3936	2060.5804
21	0.133	7.533	47.3312	2240.2443
22	0.109	9.205	57.8366	3345.0668
23	0.107	9.306	58.4685	3418.5632
24	0.104	9.597	60.2992	3635.994

Table 5. Period of the structure and frequency due to earthquake in the mode of using the damper in different modes of the structure

Mode	**Period**	**Frequency**	**CircFreq**	**Eigenvalue**
1	1.752	0.571	3.5853	12.8546
2	1.377	0.726	4.5617	20.8088
3	1.219	0.82	5.1552	26.5761
4	0.627	1.595	10.0215	100.4305
5	0.459	2.177	13.6805	187.1571
6	0.411	2.434	15.2937	233.8976
7	0.366	2.731	17.1568	294.3571
8	0.278	3.596	22.5955	510.5558
9	0.264	3.789	23.807	566.7731
10	0.248	4.035	25.3553	642.8924
11	0.228	4.382	27.535	758.1781
12	0.223	4.492	28.2254	796.6725
13	0.214	4.669	29.3386	860.753
14	0.182	5.486	34.4688	1188.0975
15	0.182	5.506	34.5934	1196.7002
16	0.172	5.821	36.5722	1337.529
17	0.145	6.893	43.3101	1875.7675
18	0.138	7.224	45.3922	2060.456
19	0.134	7.447	46.7885	2189.1634
20	0.114	8.744	54.9376	3018.1452
21	0.109	9.193	57.7599	3336.208
22	0.107	9.306	58.4687	3418.5889
23	0.094	10.671	67.046	4495.1643
24	0.089	11.178	70.2352	4932.9782

5. Comparison of the shear force of floors under the effect of earthquake 1 in the horizontal direction in the state without dampers

Tables 6 and 7 show that the use of this type of damper increases the shear force of floors.

6.Conclusions

Results show that the proposed Multi-Level Yielding Pipe Damper damper is so effective to improve the seismic behavior of the structures under all three selected earthquakes. It seems that having a specific secondary hardening portion in force displacement shows multi-level behavior with variable strength and stiffness that can dissipate seismic energy in different acting as a two-level damping system.

In this article, two-frame attenuators were used in the horizontal direction of an 8-story steel building, and the shear force of the floors, rotation time, and relative displacement of the floors under the earthquake were studied in the horizontal direction, and the results showed that the use of this type of damper increases the shear force of the floors and

reduces the relative displacement of the floors and reduces the period of the structure in different modes.

Table 6. story force due to earthquake in horizontal direction without using damper.

Story	Output Case	Step Type	Location	VX
				tonf
Story 7	EQ1	Max	Top	917.1827
Story 7	EQ1	Max	Bottom	917.1827
Story 7	EQ1	Min	Top	-1081.3662
Story 7	EQ1	Min	Bottom	-1081.3662
Story 6	EQ1	Max	Top	1247.8159
Story 6	EQ1	Max	Bottom	1247.8159
Story 6	EQ1	Min	Top	-1358.3237
Story 6	EQ1	Min	Bottom	-1358.3237
Story 5	EQ1	Max	Top	1511.0533
Story 5	EQ1	Max	Bottom	1511.0533
Story 5	EQ1	Min	Top	-1498.0265
Story 5	EQ1	Min	Bottom	-1498.0265
Story 4	EQ1	Max	Top	1707.3772
Story 4	EQ1	Max	Bottom	1707.3772
Story 4	EQ1	Min	Top	-1664.4234
Story 4	EQ1	Min	Bottom	-1664.4234
Story 3	EQ1	Max	Top	1855.3592
Story 3	EQ1	Max	Bottom	1855.3592
Story 3	EQ1	Min	Top	-1804.9272
Story 3	EQ1	Min	Bottom	-1804.9272
Story 2	EQ1	Max	Top	1916.6557
Story 2	EQ1	Max	Bottom	1916.6557
Story 2	EQ1	Min	Top	-1904.1255
Story 2	EQ1	Min	Bottom	-1904.1255
story 1	EQ1	Max	Top	1937.1745
story 1	EQ1	Max	Bottom	1937.1745
story 1	EQ1	Min	Top	-1940.1856
story 1	EQ1	Min	Bottom	-1940.1856

Table 7. story force due to type 1 earthquake in the horizontal direction in the case of using the damper

Story	Output Case	Step Type	Location	VX
				tonf
Story 7	EQ1	Max	Top	1079.8332
Story 7	EQ1	Max	Bottom	1079.8332
Story 7	EQ1	Min	Top	-1133.6256
Story 7	EQ1	Min	Bottom	-1133.6256
Story 6	EQ1	Max	Top	1473.0102
Story 6	EQ1	Max	Bottom	1473.0102
Story 6	EQ1	Min	Top	-1616.3961
Story 6	EQ1	Min	Bottom	-1616.3961
Story 5	EQ1	Max	Top	1955.2678
Story 5	EQ1	Max	Bottom	1955.2678
Story 5	EQ1	Min	Top	-1973.892
Story 5	EQ1	Min	Bottom	-1973.892
Story 4	EQ1	Max	Top	2040.8156
Story 4	EQ1	Max	Bottom	2040.8156
Story 4	EQ1	Min	Top	-2369.3402
Story 4	EQ1	Min	Bottom	-2369.3402
Story 3	EQ1	Max	Top	2762.5299
Story 3	EQ1	Max	Bottom	2762.5299
Story 3	EQ1	Min	Top	-2374.2996
Story 3	EQ1	Min	Bottom	-2374.2996
Story 2	EQ1	Max	Top	2092.6127
Story 2	EQ1	Max	Bottom	2092.6127
Story 2	EQ1	Min	Top	-2816.1085
Story 2	EQ1	Min	Bottom	-2816.1085
story 1	EQ1	Max	Top	3277.1995
story 1	EQ1	Max	Bottom	3277.1995
story 1	EQ1	Min	Top	-2387.5161
story 1	EQ1	Min	Bottom	-2387.5161

7.Refrences

[1] Seyed Mehdi Zahrai and Abdullah Cheraghi (2017) "Reducing Seismic Vibrations of Typical Steel Buildings Using New Multi-Level Yielding Pipe Damper" International Journal of Steel Structures 17(3): 1-16

[2] Ehsan Omranian,Gholamreza Abdullahzadeh and Javadpour Ali(2018) "Evaluation of aftershock effects on steel bending frame

structures in different types of soil" 11th international congress on civil engineering
[3] Code of Design of Buildings Against Earthquake, Standard 2800, Edition 4, Building and Housing Research Center, Publication No. Z-253, First Edition 1

J-Researchers

JOURNAL OF CIVIL ENGINEERING RESEARCHERS

Investigating the implementation and performance of architecture in zero energy buildings in order to producing passive energy

Ghasem Azizi Daronkolaie[a,*] Fatemeh Azizi Daronkolaee[b]

[a]*Ms.c student, department of civil engineering, islamic azad university of Yazd, Islamic Republic of Iran*
[b]*Education Department, Babol, Islamic Republic of Iran*

Article History: Received date: 2023.02.03; revised date: 2023.03.16; accepted date: 2023.03.20

Abstract

Challenges in recent decades for humans and the rapidly changing planet. The increase in pollution and difficult access to energy despite the problems of war and political and economic disputes between countries and the rapid decrease in the amount of energy in the world, which with this growth rate, is a tangible danger for the whole world. It prompted scientists to look for new methods of energy production and consumption. In this article, we are looking for a topic of such projects, which are called zero energy buildings. As it is understood from the name of this project, the result of all energy consumption and production in these buildings must be zero or the energy production of the building should be more than its consumption, which is the concept of energy related to all the energy in the building such as thermal, electrical and ... which should be considered in the initial calculations and construction. For this purpose, this research, which is a descriptive analytical research, was conducted using library resources and electronic books and articles. We will review the execution and performance of architecture in zero energy building and concepts related to passive energy and building orientation for energy production, architectural components and materials of zero energy building, review the economic approach and leading challenges, construction and operation in connection with zero energy building. The results obtained from this research, zero energy buildings are faced with upcoming challenges such as technical knowledge, efficient and trained staff, and existing laws and regulations. Accordingly, the need to reduce energy consumption and optimize it is felt more and more. Zero energy buildings are the best solution to moderate energy consumption in housing. But reaching this goal has basic and fundamental needs that must be met. (DOI:**https//doi.org/10.52547/JCER.5.1.19**)

Keywords: Architecture; zero energy building; energy

1. Introduction

Today, the correct way of using the available energies in the world has been affected for various reasons, including the relationship between energy security and the economy of governments and societies, and the national and transnational environment of countries. In these few years, with the tangible changes in weather and climates in different parts of the earth, its importance has become concretely clear for the people of different societies,

* Corresponding author. e-mail: ghasem.azizi.d@gmail.com

it is necessary to pay more attention than in the past and to take immediate measures. [1]

One of the points of intersection of all sciences in the world is the field of electrical energy from production to consumption, every step of which needs to be reviewed. Maybe from the construction phase, for example; A power plant that has a direct impact on the regional climate of the construction site and the many losses it has for us due to the high inefficiency of the systems, than the transmission of energy by traveling very long distances and incurring a lot of costs during implementation and operation, as well as The stage of distribution of this energy can lead to many problems for us and should be considered. By using new and low-error methods in the stages of production, transfer and consumption, we can face the lowest cost and increase productivity. [2]

Keeping these things in mind, as well as other considerations and necessities related to optimization in energy production, transmission and consumption, one of the ways to increase productivity is to bring these steps closer to the point of consumption, such as designing and building a zero-emission building. By applying modern engineering sciences in fields related to the goal, such as civil engineering, architecture, electricity, etc., we can lead to increasing energy security and reducing losses in the stages of production, transmission and consumption. In the present research, the method of passive energy production with the implementation and performance of the architectural type in the zero energy building is investigated with the aim of optimizing energy and increasing productivity and production under the title of creating zero energy in buildings. [3]

2. Statement of the problem and necessity of research

Old buildings consume 40% of the total fossil fuel energy in the country and are important producers of greenhouse gases. The principle of net zero energy consumption is considered as a tool to reduce carbon emissions and dependence on fossil fuels. Although zero energy buildings are uncommon even in developed countries, they are gaining importance and popularity day by day. Before producing clean energy, the zero energy building optimizes the energy consumption in different parts of the building and balances energy production and consumption with the smart use of renewable technology. The importance of the research and use of such buildings can be the protection of the owners of these buildings from the increase in energy prices, greater comfort due to the design and regulation of the environment temperature in a uniform and isothermal manner, the need for less energy, and lower maintenance costs due to high energy efficiency. , reduction of net monthly living costs, high reliability, for example, photovoltaic systems have a 25-year warranty and rarely suffer from problems caused by climate changes, reduction of costs due to the reconstruction of the building if you decide to convert it He called the zero energy building in the future, increasing the value of zero energy buildings compared to traditional buildings with the increase in the cost of fossil fuels.

3. Research purposes

The idea of these zero energy buildings is to reduce the consumption of a building that actually offers zero energy living and working facilities in a space without fossil fuels, without a doubt, the construction of zero energy buildings will be a need for future thinking. For the future success of these buildings, creativity, precise timing and collective cooperation between different groups are required. In fact, zero energy offers the possibility of living and working in a space without fossil fuels. These buildings produce energy throughout the year based on their energy consumption needs. Proper physics and structure and the use of renewable resources in these buildings make it possible to achieve the above goal to a great extent, which can be attractive to engineers and designers.

4. research background

Esadi and his colleagues [4]. In an article titled design, construction supervision of buildings with net zero energy with the aim of sustainability in energy sources were investigated. In part of their article, they

have investigated passive energy and have come to the conclusion that such buildings can be used in addition to integrating optimization of passive-active strategies in the initial phase of a building's life cycle, timely monitoring of energy consumption in The time of use of the building during its lifetime also did. At the end of their work, they have mentioned the general implementation strategies for the realization of zero net energy buildings. Abbasi and his colleagues [5]. In an article entitled "A step towards the implementation of the principles of sustainable architecture" (ZEB), they gave solutions for realizing the idea of zero energy buildings. In their article, they presented the solutions to realize this idea of zero energy buildings in two parts: 1) theoretical discussions of the design of these buildings and 2) implementation and construction methods. Based on the results of their research, it is possible to help realize the idea of these buildings with active and passive design methods.

5. Definition of the general concept of zero energy building

A zero energy building is generally referred to as a building whose energy consumption can be reduced to a large extent by using different methods and its energy production is compensated by the use of clean sources and renewable energies. At the heart of the concept and general idea of zero energy building is the idea that buildings can meet all their energy needs in a low-cost way, with local access, without pollution and with renewable resources. It is very difficult to find a building that can be called the first zero energy building. Because zero energy is just a new name for the progress of reducing energy consumption in buildings [6].

In a zero energy building, no fossil fuel is consumed and its annual energy consumption is equal to its annual production. A zero energy building may or may not be connected to existing city networks. A zero energy building that is not connected to the grid has equipment for storing large amounts of energy, which is usually of the battery type. In a zero energy building that is not connected to the grid, due to the shape and type of battery storage, a part of the circuit may remain unused, while in a zero energy building connected to the grid, no circuit is unused and is not isolated. A zero energy building connected to the grid may generate more electricity than it needs. During the period when the building does not need production energy, i.e. when we are using the energy stored in the batteries, a zero energy building produces the energy it needs, as well as providing the owner with reassurance about the security of the storage. Surplus energy gives off its own needs [7].

6. Passive energies

The use of latent energies has been the focus of mankind since the distant past, and even today it is considered as one of the facilities to be considered in choosing a good building. Now, with these interpretations, we can point to the vital role of latent energies in building construction [8].

The term buildings facing the sun or wind has always represented the quality of the property, which had special uses in different hot and dry, cold and humid, mountainous or desert areas.

Architectural engineering has a fundamental role in using hidden energy mechanisms, such as:

- Selection and optimal use of sunlight in the building according to the geographical location and seasons
- Use of daylight concepts
- Using the prevailing wind direction continuously and seasonally
- Separation of building spaces and zoning based on usage (bedroom, kitchen, etc.) and different cooling, heating and lighting needs.
- Using underground spaces and returning cold air in summer and hot air in winter

7. Elongation and orientation of the building and placement of internal spaces

The length of the building as well as its orientation has a significant impact on the acquisition of thermal energy from the sun and also the use of natural lighting of the building. In zero energy buildings, they try to build the building in one or at most two floors, and on the other hand, they spread the building on the ground. In addition to making more

space available on the roof for the implementation of facilities, this causes more spaces to be placed on the south side of the building and increases the possibility of using the sun's energy during the day [9]. The location of these spaces on the south side makes it possible to make maximum use of the light and heat of the sun in these spaces. In addition, due to the higher traffic that takes place in these spaces, their placement on the ground floor makes it easier to access these spaces and prevent energy loss in other low-traffic spaces. Spaces with less use are also considered on the north side of the building and on the first floor. Considering that these spaces require less energy, their location on the north side allows them to access the energy they need only through the utility system of the building and when in use, as well as their location on the first floor of the building and Staying away from high traffic places makes them waste less energy.4- Review and compare the results

8. How to place spaces in the building

Placement of spaces with high heat demand on the south side of the building

Placement of spaces with low thermal requirements on the north side of the building

Placement of spaces with high traffic on the ground floor and near the entrance of the building

Placement of spaces with low traffic in parts far from the entrance door or the first floor of the building

Due to the fact that the angle of the sun's radiation in different parts of the globe is different depending on the geographical coordinates of that point, therefore the orientation of the building in each part of the globe is also different to absorb the maximum solar energy [10] . Then, according to the conditions of the building and the priorities considered for it, the best orientation for the building is chosen.

9. Use of shade on the facade of the building

The use of shade in tropical regions reduces the cooling load of the building during its cooling period. But in areas with a colder climate, this can have a negative effect on the heating process of the building in the cold seasons of the year. Therefore, it is necessary to optimize the size of the shades that are chosen for the building, according to their effect on the amount of solar energy received during the heating period of the building [11]. Types of shades may have different effects such as direct sunlight control, light control, landscape and natural ventilation. The importance of these effects depends on the location and type of building. Figure 1 shows the effect of using sunshades with different positions on the amount of solar energy absorption.

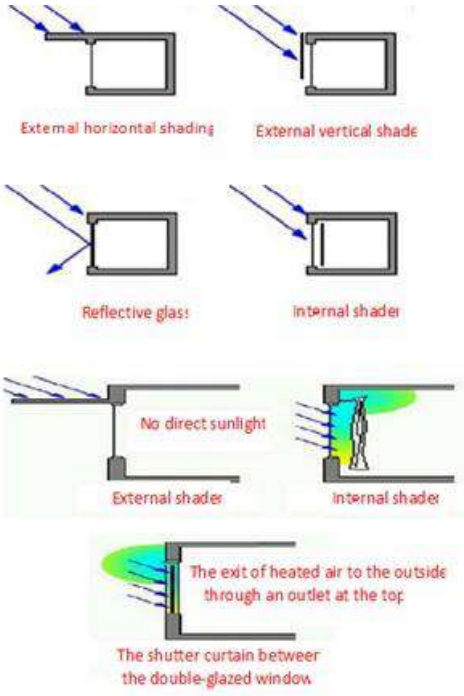

Fig 1: Comparison of the types of shades according to the installation positions

10. Use of wind deflector in zero energy building

The use of wind turbines has been common in Iran since ancient times. Wind deflectors with different shapes have been built in the central and southern cities of Iran, each of which has been designed and implemented according to the desired height and direction of the wind. He observed the hot and humid south in cities such as Bandar Abbas, Bandarlange, Qeshm, Bushehr and the hot and dry climate of the

central regions such as Kerman, Nayin, Yazd, Tabas, Kashan, Semnan, Isfahan and even the southern areas of Tehran city [12] .

Since in the building, one wind deflector is used as an inlet and another as an air outlet, therefore, for its design, the winds of the area are examined and the inlet tower openings are open towards the prevailing wind and the outlet tower openings are closed in this direction. Also, the height of the towers and the opening level of the openings are designed according to the amount of air flow required.

11. Isolation

It is necessary to isolate the external walls, floors, ceilings, etc. in such a way that the exchange of energy with the outside space is as minimal as possible and practically the whole building is considered as an isolated component. For this purpose, it is necessary to comply with building insulation optimization standards both in terms of applied materials and the way of implementation for different geographical areas. Also, the use of 2- or 3-paned windows with or without gas also prevents

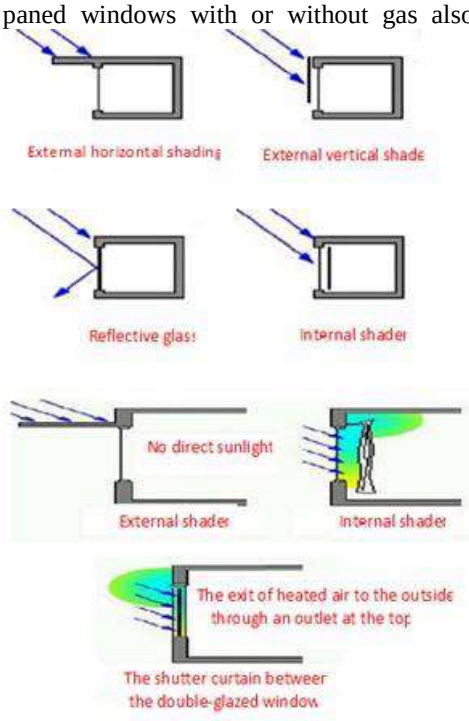

uilding
ng to

he project
ıe energy
necessary
ısumption
crease the
inding an
on in the
ın energy
vest initial
ed amount
it can be
ı process.
ducing the

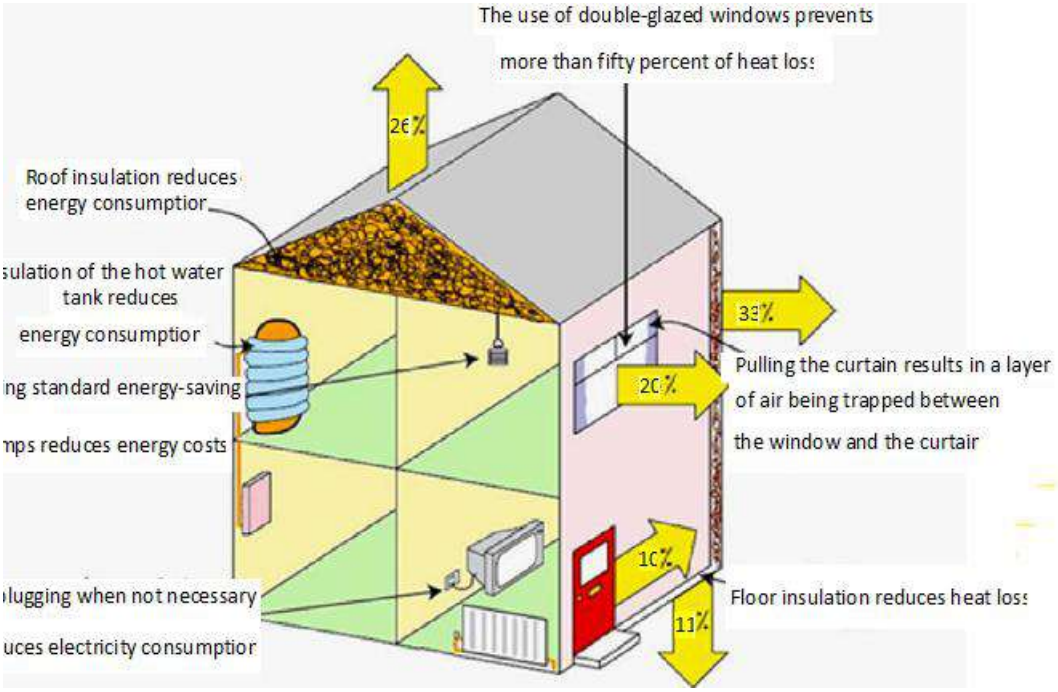

Fig 2: The role of insulation in reducing thermal load

13. Static approach in architecture

With the large expansion of air conditioning systems and available sources of cheap energy in the 20th century, architecture no longer had to respond to climatic limitations. By using artificial facilities to control environmental conditions, the interior space of any building can be adapted to environmental comfort standards. Therefore, the use of emerging architectural materials and forms became possible. This argument also led to the forgetting of knowledge and skills in the field of energy and static design in the architectural profession. In addition, with the increasing expectations of the audience in the field of controlling the conditions of the indoor environment, people are used to constant temperature and light conditions throughout the year.

The most general definition of a passive solar heating and cooling system is that thermal energy flows in it in natural ways such as radiation, conduction and natural displacement. Basically, the structure of the building itself or some of its elements constitute the system itself. Static design is defined as the use of architecture and climate to provide heating, cooling, ventilation and light. It is also possible to change the static design by using architecture in order to harvest the free energy of the environment. Utilizing static design in parallel with equipment with low energy consumption will lead to the creation of an interior space with optimal quality.

Static design is not only an opportunity in the field of energy but also an opportunity in the field of architecture. In static design, the relationship between energy and space is defined in a beautiful, functional and meaningful way. The most successful buildings today are the buildings that have correctly followed static strategies, and the most progressive architectural offices are those that have invested in advancing these methods. It can be said that the history of architecture is closely related to static design because static design techniques for dams (if not millennia) have been very common in the history of architecture.

14. Static strategies

The ease of designing 100% active buildings is definitely one of the most important obstacles to the expansion of static or double buildings. But by passing these obstacles, there is a valuable opportunity to improve the quality and productivity of buildings. Static strategies usually do not completely replace active building systems, but in most times of the year they come to the aid of active systems or replace them. This double combination of active and passive solutions leads to the present combined buildings. In fact, a successful zero energy building benefits from an integral combination of active Vista systems. Static solutions are usually used to provide one or several of the 4 basic building services, namely heating, cooling, ventilation and lighting. The techniques related to static cooling and heating are given below.

14.1. Construction shell

The shell of the building is the front line of the building's exposure to the outside environment and climate. Therefore, it plays a key role in the application of static systems and should be investigated along with the issues related to orientation and building mass, as well as the design of electrical-mechanical systems. The building shell is a key element in the energy performance of any building, but it plays a vital role in the performance of zero-energy buildings. Orientation, building mass and proper design of the city make it easier to overcome thermal loads. These issues, along with a building shell with appropriate design and details, are considered the key to successful neutralization of the shell. The concept of neutralizing the building shell means neutralizing the thermal loads of the shell. The neutralization of the shell leads to the reduction of the surrounding cooling and heating loads. Shell parts should be designed with a minimum thermal transfer coefficient and insulating materials with a maximum thermal resistance coefficient.

14.2. Duplex view

The use of two skins is a solution for neutralizing large glass surfaces. The ease of controlling the heat of the sun and the improvement of thermal resistance

due to the cavity between the two transparent layers are known as the advantages of this method. With the advancement of surfaces with glasses with a reflective coefficient, the possibility of controlling the energy received from the sun increases. Figure 3 The function of these glasses is that they limit the transmission of ultraviolet and infrared waves in the sunlight spectrum and at the same time they absorb the waves of the visible light spectrum. Also, the solar heat transfer coefficient and the glass resistance coefficient have been optimized.

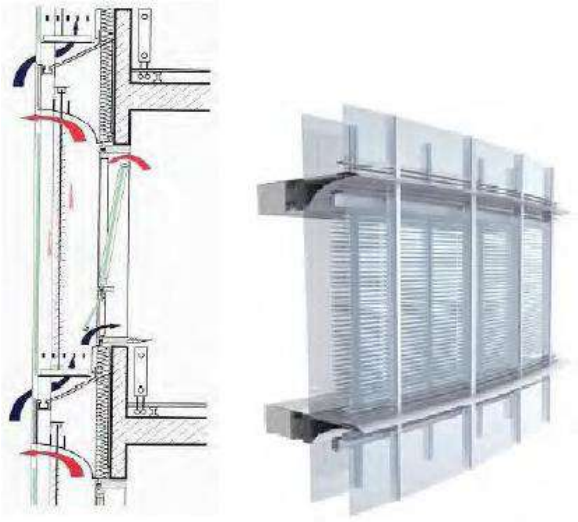

Fig 3: double-glazed facade - controlling the heat received from the sun's rays due to the use of glasses with a low diffusion coefficient - creating air flow with appropriate details

14.3. The ratio of the opening to the walls

This ratio is a critical factor in creating a balance between thermal capabilities and performance benefits such as daylight and visibility. However, window design is influenced by the orientation, climate and functional program of the building. The ratio of the opening to the low window is suitable for climates with many cold or hot days and for climates with a lot of sunlight. It also moderates the weak thermal performance of the window. In addition, a lower opening-to-wall ratio is synonymous with a lower glass surface and, as a result, a lower cost. This saved cost can be used to improve the thermal performance of the window.

14.4. Advanced technologies of transparent surfaces

Chromogenic glass or smart glass can change its characteristics based on environmental stimuli. Chromogenic glass includes gas-reactive, electricity-reactive, light-reactive, and heat-reactive types.
Airgel: Airgel is a new generation of insulating materials that creates a high thermal resistance while allowing light to pass through. Airgel is used in the air chamber between the glasses and as a result the transparency of the glass piece is maintained.
Thermal mass: transparent phase change materials are added to glass parts to play the role of thermal mass.
Movable shading: self-made or manual shading is installed inside the glass parts, their internal or external facades, and they provide the possibility of complete shading or unobstructed vision (when shading is not needed).
Prism glasses: Glass or plastic glasses are used to direct sunlight. The use of this type of transparent material in order to direct light to the depth of space has a historical background. Its other use is the reflection of wide-angle rays and at the same time the passage of low-angle rays, which improves the control of solar absorption during summer.
Built-in photovoltaics: Some photovoltaic technologies are embedded inside transparent glass parts and generate electricity. Depending on the need for shade or visibility, variable values of glass transparency or opacity can be achieved.

14.5. Thermal mass

Heavy thermal mass materials have high density and thermal capacity. Materials such as concrete, stone, masonry and water have the ability to store heat and return it to the environment when the ambient temperature drops. This short-term thermal storage has many cooling and static heating applications. One of the benefits of the thermal mass is the adjustment of daily temperature fluctuations in the indoor space. It is better for the thermal mass to be exposed in the inner space to be more effective in regulating the temperature.

14.6. Insulation

The outer shell design has a great effect on reducing heat exchange through the building shell. The main

approach in insulation is to use parts with high thermal resistance coefficient. The integrity of the external shell forming elements is a factor that causes the integrity of the building shell, the reduction of thermal bridges is another very important factor, insulation of the shell is very necessary in cold climates that require considerable energy. In more moderate climates, insulation is important to control the heat exchange with the environment and to reach the equilibrium temperature point.

14.7. Connection with the earth

The ground is a mass thermal mass that can be used as a tool to achieve an almost constant internal temperature throughout the year. In fact, the temperature of the earth is cooler in summer and warmer in winter than the surrounding air. In some places, the temperature of the depth of the earth is constant throughout the year and is almost equivalent to the average temperature of the air in the region. At critical times of the year, the outside temperature affects the temperature of the earth. Also, the characteristics of the soil and the surface of the earth's crust are also effective on this temperature. This solution has been manifested in traditional architecture in an element called "Shavadan". Figure 4 shows the relationship between the air and the internal temperature of the earth.

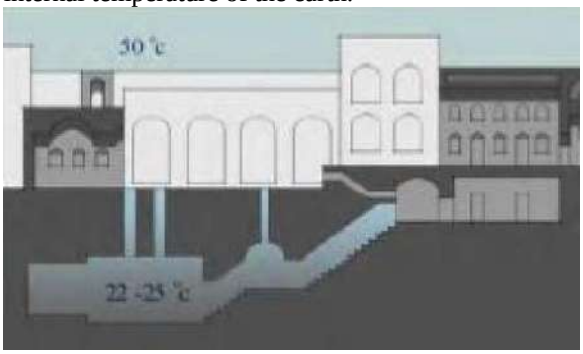

Fig 4: Connection with the ground

Connecting with the ground or sheltering in the heart of the ground by digging and penetrating into the ground causes the temperature outside and inside the building to have more balanced differences. This reduces the heat exchange inside the building. Connecting with the earth from a distance by drilling long pipes in the heart of the earth is a method to provide cool air and transfer it to the interior space. be viewed with caution.

14.8. Shading

Shading is one of the primary cooling strategies that has been tested over time. Avoiding heat should always be the first priority for cooling. Shading is highly dependent on climate and building characteristics. This means that the design of the shade should meet the needs of seasonal cooling, the orientation of the building and the path of the sun throughout the building. Since glass surfaces are the main way of receiving the sun's rays, shades are usually designed in relation to glass surfaces. But the shading should be in such a way that it does not interfere with the lighting due to daylight.

14.9. air conditioning

Natural ventilation is a simple and effective tool that provides cooling and fresh outside air for the residents of the building. Opening windows used to be used in commercial buildings, but nowadays they are very rare. Today, commercial buildings usually have a highly engineered environment, and opening windows interfere with the proper functioning of many common air conditioning systems. However, natural ventilation can be used along with many low-energy air conditioning systems such as evaporative cooling and radiant cooling.
Whenever the building needs cooling and the outside air is cool enough, natural ventilation will be an effective cooling strategy. The movement of air in the building and the resulting cooling phenomenon make the residents comfortable and absorb the excess heat of the building during the night. For this purpose, suitable ventilation paths for lateral ventilation and chimney ventilation should be carefully considered in the design of the building. These techniques rely on the differences in air temperature and wind pressure to move the air. Opening windows are the most common method, but other solutions such as ventilators, wind towers and solar fireplaces can also be used.

14.10. The solar collector protrudes

Protruding solar collectors are an economical technique for static heating of outside air for use in ventilation or heating systems. Figure 5. The protruding solar collector consists of a corrugated metal panel with a dark color that has tiny holes.

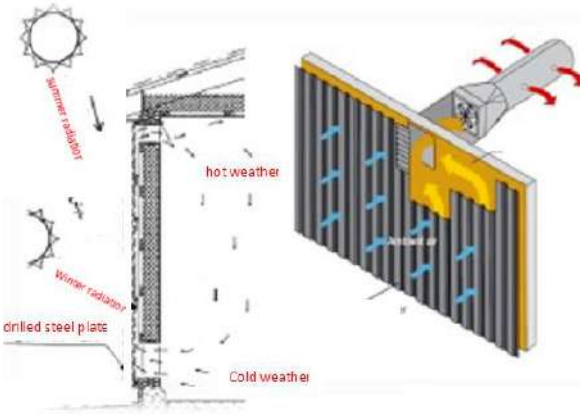

Fig 5: Protruding solar collector

In order to receive optimal solar energy, the panels are installed on the south face with a distance from the wall so that air flows in this gap. The air enters through the small holes on the sheet and is heated by receiving the sun's rays. Then the preheated air can be used for heating the ventilation air. Since the warm air rises under the collector, usually the air is collected at the top of the building. It is also common to use an electric fan to direct the air inside the collector. During the cooling periods, the air inside the collector is discharged from the top.

14.11. Receiving internal heat

Every building absorbs internal heat from people, lighting equipment and other equipment. When the building is in heating mode, receiving internal heat is a useful static solution, especially when it is done in parallel with complete insulation and air sealing of the building openings. This technique is more efficient by recovering heat from the exhaust air of the ventilation system.

14.12. Evaporative cooling

Evaporative cooling is widely used in hot and dry climates. In this system, water is placed in the vicinity of hot air, then the heat of the air is absorbed by the water and the resulting steam is absorbed in the air. With the continuation of this process, the air temperature decreases and its humidity increases. Evaporative cooling may be done with an electromechanical device with low energy consumption. This technique can also be used statically by using a tool such as wind tower.

14.13. Static dehumidification

In climates with high humidity, high humidity reduces thermal comfort and requires a lot of energy to overcome it. Just as hot dry air can be statically cooled by evaporating water and adding to the amount of air humidity, it is also possible to statically dehumidify the air using a dehumidifier. By removing moisture from the air and changing its phase to liquid, the heat of the air is added. Silica gel is a common dehumidifier that is used in many dehumidifiers. After each dehumidification cycle, the dehumidifier must be dried. Static dehumidification is still not very popular.

15. Economic approach

The construction of buildings that can provide all of their energy needs around the clock with renewable energy sources requires a detailed economic evaluation, therefore, depending on the area where such buildings are constructed, the economic efficiency of these buildings is very important, because the return of capital costs Construction in the shortest possible time is of particular importance, there are many differences of opinion regarding the issue of how the investment return should be, whether the said building can be called economic or not, which is considered a research vacuum. The use of energy in the world is growing rapidly, and there is concern about the supply, exhaustion and loss of fossil energy sources, as well as their environmental effects (ozone layer hole, global warming, climate change, etc.) and the global share. Residential and commercial buildings in energy consumption have continuously increased, and for this reason, energy efficiency is the main goal in today's buildings, and therefore, the construction of zero energy buildings is a necessity.

15.1. Effective conditions in economic analysis

In designing on a specific piece of land, the following factors are recommended to prevent heat and cold waste:

- Choosing the land, the land that has good access to the winter sun is the right land.
- The orientation of the shape of the building, the optimal orientation of a building to collect heat from the sun in winter is considered. Studies show that the optimal economic state is the highest level in the direction of 5 to 15 degrees southeast.
- The use of solar systems, solar windows, solar wall, solar roofs, horizontal and vertical canopies, shade trees, wind deflectors, ground heat, underground and...
- It is possible to reduce the ratio of the surface of the outer shell of the building to the useful volume, the ratio of the roof surface to the useful surface of the building, and the ratio of the surface of the openings in the outer shell (doors and windows) to the useful surface of the building.

16. Challenges of zero energy architecture in I.R Iran

Iran, as a part of the world, is not exempt from international crises. Including the increase in earth's heat and greenhouse gases, and in some directions, even more severe effects can be observed. Including air pollution in big cities, which is caused by the production of gases caused by the improper burning of energy in the housing and transportation industries. Iran, as one of the largest producers of fossil energy, may not have to worry about its shortage in the future, but considering that oil and natural gas account for about 31% of Iran's total energy consumption.The slightest problem in energy supply puts the country in irreversible crises.

The intensity of energy consumption in Iran has increased by an average of 1 percent annually in the last decade, which has reached 5 percent. The reasons for the increase in energy can be considered the increase in population, urbanization, the lack of comprehensive environmental laws, the wrong consumption pattern and allocation of government subsidies. The share of the housing sector in the country's energy consumption is 15% and it is the largest producer of greenhouse gases, and due to the growth of the construction industry, it is increasing day by day.

Another problem in contemporary Iranian architecture is moving away from traditional architectural methods and principles, which unknowingly caused many problems in terms of energy consumption due to being influenced by modern architectural methods and technology that are used in large numbers. For example, we can mention the problems of new buildings in hot and humid and hot and dry areas. For this reason, achieving principles in the direction of sustainable architecture can be a bit useful to return to architecture compatible with nature in the style of the past.

Accordingly, the need to reduce energy consumption and optimize it is felt more and more. Zero energy buildings are the best solution to moderate energy consumption in housing. But reaching this goal has basic and basic needs that must be met. A review of contemporary architecture in Iran and contemporary architecture of developing countries shows that these countries, like many developed countries, move towards the concept of sustainability and sustainable architecture on the agenda. have placed The challenges facing the design and implementation of zero energy buildings in Iran's contemporary architecture can be analyzed in the following three axes, which are:

- Technical knowledge: the necessity of reproducing local technical knowledge in the field of contemporary architecture, especially the design and

implementation of zero energy buildings.

- Efficient trained force: Efficient trained force is the basis of achieving optimal patterns in the field of design and implementation of zero energy buildings, which is why they have mentioned it as the basic pillar of realizing the concept of sustainability and sustainable architecture.
- Laws and regulations: Laws, regulations and regulations derived from the principles of the concept of sustainability and sustainable architecture are considered an important and essential step in this field. Laws, regulations and ordinances that directly or indirectly interact constructively with the construction industry and housing production.

17. conclusion

In this research, choosing the type of architectural system that fits the climatic, economic and technical conditions of Iran in order to achieve the concept of zero energy buildings in a practical and practical way is of particular importance. For this purpose, the use of modern equipment and efficient technology

Above should be in such a way that it meets the needs of energy, economy, repairs and maintenance in this type of buildings, and in this research, common static solutions in the field of cooling and heating of zero energy buildings such as insulation, ground connection, air sealing, shade Endai, building shell, thermal mass, natural ventilation, protruding solar collector, receiving internal heat, evaporative cooling and dehumidification have been discussed. The economic approach and existing architectural challenges in zero energy buildings are stated.

The idea of these zero energy buildings is to reduce the energy consumption of the building, which actually offers zero energy living and working facilities in a space without fossil fuels. Without a doubt, the construction of zero energy buildings is the need of the next century for the future success of these buildings, creativity, Accurate timing and collective cooperation between different groups. In fact, "zero energy" offers the possibilities of living and working in a space without fossil fuels. These buildings produce energy throughout the year based on their energy consumption needs. Proper physics and structure and the use of architecture in these buildings make it possible to achieve the above goal to a great extent. Zero energy buildings face challenges such as technical knowledge, efficient and trained staff, and existing laws and regulations. Accordingly, the need to reduce energy consumption and optimize it is felt more and more. Zero energy buildings are the best solution to moderate energy consumption in housing. But reaching this goal has basic and fundamental needs that must be met.

References

[1] M.Aladdini, Optimizing energy consumption by introducing and presenting examples of zero energy buildings, 17th National Conference on Modern Researches in Science and Technology, in electronic form, Elm Mohoran Asman Company, 2018.

[2] M.Rezaei, static cooling and heating solutions in zero energy buildings, the second international conference on civil engineering, architecture and urban development management in Iran, Tehran, Maragheh University of Technology,2018.

[3] N.Dehghan Manshadi, and M.Sashorpour, Safar Energy Buildings, First International Conference on Civil Engineering, Architecture and Urban Regeneration, Tehran - Shahid Beheshti University of Medical Sciences - Imam Khomeini (RA) International Conference Center, Conference Permanent Secretariat,2018.

[4] A.Esadi Zarch, and Seyed M.Khanqaei Zarch, design, construction monitoring of zero net energy buildings with the aim of sustainability in energy resources, 15th International Industrial Engineering Conference, Yazd, Yazd University, 2017.

[5] S.Abbasi, and D.Rezaei, review of the solutions for the realization of the idea of zero energy buildings (ZEB), a step to implement the principles of sustainable architecture, National Conference on Architectural Engineering, Civil Engineering and Physical Development, Kohdasht, Kohdasht Municipality, Panam Khat Novin Company, 2014.

[6] A.Tadjad, and S.Arab, Review of science and technology parks with the perspective of zero energy buildings, Payashehr Monthly 1, 2017.

[7] A.Ghaffari, Z.Abbaszadeh and M.H.Islampour, 2017, investigation and recognition of effective factors in the design of buildings with zero energy, civil conference, architecture and urban planning of the countries of the Islamic world, Tabriz, Tabriz University - Shahid Madani University of Azerbaijan - Tabriz Municipal Applied Science University

[8] A.Asghari, and M.Seyyedal Masi, the level of social awareness towards zero energy buildings, Civil, Architecture and Urban Planning Conference of Islamic World Countries, Tabriz, Tabriz University - Martyr Madani University of Azerbaijan - Tabriz Municipal Applied Science University, 2017.

[9] K.Shirazizadeh; I. Kazemi; K.Shirazizadeh and K.Shirazizadeh, sustainable and zero energy buildings for hot and dry climate region, the second conference on energy infrastructure, electrical engineering and nanotechnology, Tehran, Iran Energy Association, 2017.

[10] A.Raif Panah, and M.Sarmi Tehrani, energy optimization for low-consumption and near-zero buildings in Tehran, international conference on the role of mechanical engineering in urban construction, Tehran, Tehran Province Building Engineering System Organization - Central Council of the Organization Building engineering system, 2017.

[11] M.Sabouni, and M.Hedayati Marzbali, a review of the factors of zero energy buildings effective in locating, the second national conference on civil engineering, architecture with an emphasis on job creation in the construction industry, Tehran, the conference's permanent secretariat. 2017.

[12] A.Tadjd, and S.Arab, factors affecting building physics in order to optimize energy consumption with the approach of zero-emission buildings. Energy, Payashehr Monthly 1 (10), page 11-18, 2017.

J-Researchers

JOURNAL OF CIVIL ENGINEERING RESEARCHERS

Geometric optimization of stepped spillways using genetic algorithm

Pouria Nik Nafs[a*]

[a]*Ms.c student, Department of Civil Engineering, Centeral Tehran Branch, Islamic Azad University*

Article History: Received date: 2023.02.06; revised date: 2023.03.08; accepted date: 2023.03.25

Abstract

Recent advances in technology have created wide possibilities for building large dams, reservoirs and canals. These advances require the development of design and construction methods, especially for systems that can discharge sufficient flood. Shots and overflows are designed in such a way that no major damage is caused to the structure itself or to the surrounding environment to pass large flows through a hydraulic structure. During the flow of water over the spillway, it is necessary to consume some energy in order to prevent damage to the toe of the dam and its surroundings and finally to the dam itself. In this research, a method was presented to optimize the geometric parameters of the stepped overflow. For this purpose, using laboratory model data (275 tests in total). And the use of strong statistical software WEKA and MATLAB software obtained a formula to predict the amount of energy consumption. This formula was given to the genetic algorithm as an objective function. Entering the Yc/Hdam parameter, which includes both the flow rate and the total height of the dam, and the desired energy consumption value, this program is optimized by genetic algorithm and obtains the optimal number, length and width of steps. The results of this research show that: with the increase in flow rate, the amount of maximum energy consumption decreases, and with the increase of the head slope at a constant flow rate, the number of optimal steps for equal energy consumption increases. (DOI:https//**doi.org/10.52547/JCER.5.1.31**)

Keywords: Genetic algorithm, optimization of geometric, energy dissipation, stepped spillways

1. *Introduction*

Recent advances in technology have created wide possibilities for the construction of large dams, reservoirs and canals. These advances require the development of: design and construction methods, especially for systems that can discharge sufficient flood. Shots and overflows are designed in such a way that no major damage is caused to the structure itself or to the surrounding environment to pass large flows through a hydraulic structure. With free fall, it flows at a considerable speed, and it is necessary that some of its energy be consumed in order to prevent damage to the dam's toe and its surroundings, and finally the dam itself. The energy resulting from the overflow flow is usually consumed by the following methods:

1. By reducing the speed of the water flow through the throwing cup (or from the crown of the dam) and throwing it into a pool full of water at the bottom, which acts like a water cushion.

* Corresponding author. Tel.: +989123123545; fax: +981154632245; e-mail: pourianiknafs@gmail.com.

2. Construction of a standard relaxation pond downstream of the overflow in such a way that the hydraulic jump created in it can consume a significant amount of energy.

3. Installing a number of steps on the overflow to help energy consumption.

In the first two methods, a major part of the energy at the lower end of the hand is consumed in the middle of the pool filled with water and in the relaxation pool, respectively. The stairs in the stair overflow can significantly increase the intensity of energy consumption resulting from the shot and need. To build a system to eliminate energy consumption in the downstream or reduce it to a considerable extent.

The flow of water on an uneven or stepped floor is very turbulent and this type of flow can consume a large part of its energy.

During the last three decades, a large number of earthen dams have been designed using a concrete body and in the form of a step. In recent years, the tendency towards stair overflows is growing and the main reason is that they are economical. Compared to smooth weirs, the discharge of flood unit will be smaller and limited to At the same time, the possibility of cavitation is also less. In general, the stepped shot of an overflow can consume more energy than the smooth shot, and as a result, the amount of remaining energy at the end that must be consumed by the depleting structures will be much less than normal.

A stair overflow consists of steps that start from near the crown of the overflow and continue to the bottom heel. The use of stair overflows has been common since ancient times (3500 years or more) and their design method was abandoned in the 1920s. But in recent years, attention to this type of overflows has increased due to the significant effect of stairs on the energy consumption of the flow. This will reduce the implementation costs of this type of overflow. Also, the recognition of the new technology of using rolled concrete materials and the compatibility of this construction method with the aforementioned overflow has led to the use of stair overflows in a large number of projects. The large amount of energy loss created by the stairs causes the excavation depth of the downstream relaxation basin, the length of the relaxation basin and the height of its side walls to be reduced, and in this sense, great economic savings are created in the construction of the dam (Chanson 2002). At the end, the amount of energy not consumed and remaining at the end of the overflow should be fully consumed by other energy consumers. The aim of this study is to find a combination of the number and width of stairs that minimizes the total cost of constructing a stair spillway and a depreciating structure downstream.

2. Research objectives

1) Determining an equation with a very small error to calculate the maximum consumption of energy according to the height of the overflow and the flow rate entering the stepped overflow.

2) Obtaining a program using the genetic algorithm, which calculates the geometric parameters of the overflow with any amount of optimal energy consumption that is given to the system by the expert and presents it as an output.

In this research, a method for optimizing the geometric parameters of the stepped overflow is presented. This method includes two separate steps:

1) Identifying the best formula for predicting the amount of energy consumption (ΔH/Ht)

2) Optimizing the formula by genetic algorithm.

3. Extraction of laboratory results

In this step, we want to use the data that has been measured through the laboratory model to determine the amount of energy consumption. All the steps of the test were carried out in the hydraulic laboratory of Shahid Chamran University of Ahvaz by Mr. Siavash Heydari, who is in the following specifications. The flume used in the mentioned research is given.

4. Specifications of hydraulic laboratory flume

The length of the flume is 7 meters and its height is variable (1.4 meters in the initial 2.3 meters of the flume and 0.6 meters in the final 4.7 meters of the flume). According to the thickness of the flume wall, the useful width of the flume is 56 cm. This flume is designed in such a way that it has a closed system of water flow, so that water enters the flume from the

beginning of the flume through a pipe from the top of the flume, and after passing through the length of the flume, it flows from its end into a final tank. At the end of this tank, a triangular overflow is installed in order to measure the flow rate. After passing through this overflow, the water is directed into the underground tank of the laboratory, from where it is returned to the flume by a centrifugal pump.

A vertical sliding valve is located at the end of the flume to control the depth of the downstream water and the place where the hydraulic jump is formed. Also, in order to measure the water depth in the flume, a graduated indicator equipped with a vernier with an accuracy of 0.1 mm was used. There is a flow control valve at the inlet of the flume feeding pipe, and two porous metal boxes are used to slow down the water flow at the beginning of the flume. A number of 54 models of stair overflows were made with 6 mm plexiglass sheet and experiments with 5 discharges (10-20-30-40-50 liters per second per unit width) and 3 slopes (h/l) (30, 56/ 26, 21.8 degrees) were performed (275 tests in total). In physical models with the same slope, the variable parameter was the number of stairs (or the height of the stairs). In Fig.1, the schematic of the flume in the hydraulic laboratory is presented.

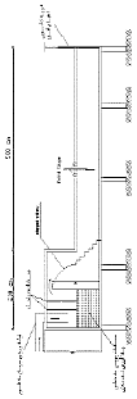

Fig. 1. schematic of the flume in the hydraulic laboratory

5. Determining the effective parameters in the flow through stepped overflows

According to the type of overflow and the studies done, the important and effective factors and parameters on the flow over the stepped overflows are as described in Table 1:

Table 1

Dimensional analysis table and unit of required parameters of this research

Dimensions based on mass system	unit	symbol	Variable	Row
$M.L^{-1}.T^{-1}$	$Kg/m.s$	μ	Dynamic viscosity	**1**
$M.L^{-3}$	Kg/m^3	ρ	Specific gravity of the fluid	**2**
$L.T^{-2}$	m/s^2	g	acceleration of gravity	**3**
L	m	y	depth of flow	**4**
$L.T^{-1}$	m/s	v	flow rate	**5**
L	m	H_{dam}	overflow height	**6**
L	m	l	Step progress	**7**
L	m	h	step height	**8**
---	---	**N**	number of steps	**9**

6. Evaluation of the information obtained from the laboratory model

6.1. First step assessment

In the first step, among the mentioned parameters, we selected six parameters N, L, H, q, Hdam and ΔH/Ht, four dimensionless parameters Yc/h, Yc/Hdam, h/L and N as input and ΔH/Ht is considered as output. Fig. 2 shows the frequency of all five input and output parameters.

In the following, the two-by-two diagram (1 to 4) of the input parameters compared to the output parameter ΔH/Ht is shown. The following graphs show the values of parameters Yc/h, Yc/Hdam, h/L and N in comparison with the output parameter ΔH/Ht.

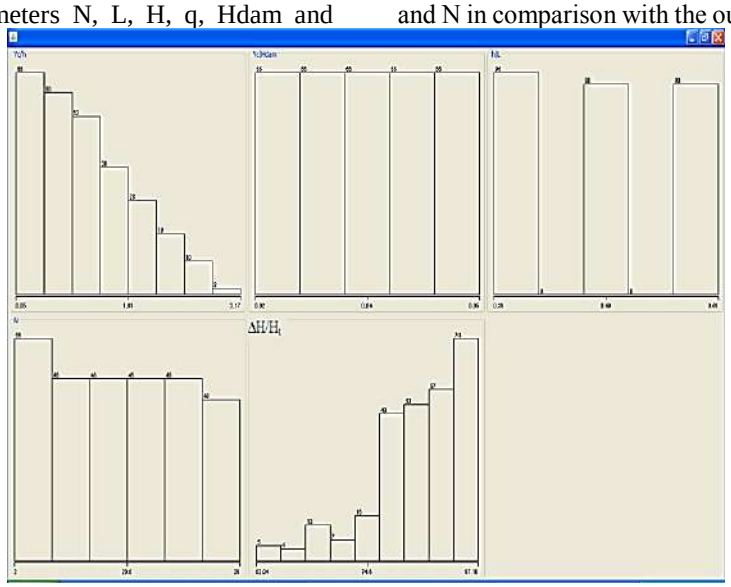

Fig. 2. frequency of five parameters Yc/h, Yc/Hdam, h/L and N and ΔH/Ht used

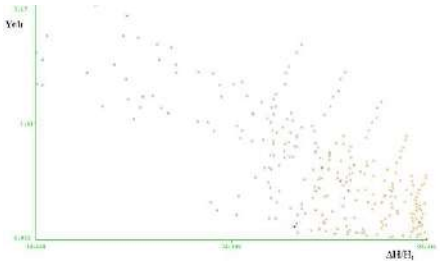

Diagram 1. Two-by-two diagram of input parameter Yc/h and output parameter ΔH/Ht

Diagram 2. Two-by-two diagram of input parameter Yc/Hdam and output parameter ΔH/Ht

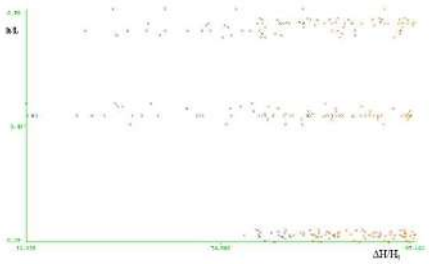

Diagrams 3. Two-by-two diagram of input parameter h/L and output parameter ΔH/H

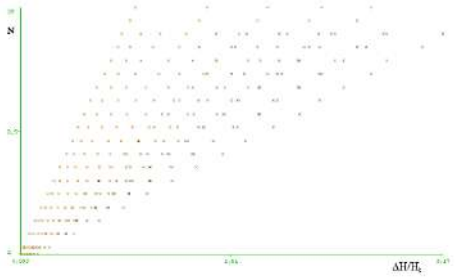

Diagram 4. Two-by-two diagram of input parameter N and output parameter ΔH/Ht

6.2. Evaluation of the second step

In this section, we use the IG method for feature selection due to its high accuracy and efficiency. As

can be seen in Fig. 3, the parameters Yc/Hdam, Yc/h, h/L and N are effective on the output parameter ΔH/Ht, respectively. As can be seen in the mentioned figure, the parameter Yc/Hdam has the most influence on the output parameter ΔH/Ht.

6.3. Third step evaluation

In this section, we present the results of linear, tree, SVM-based and combined tree and linear regression methods for estimating ΔH/Ht.

Linear regression: Fig. 4, shows the results of linear regression to estimate ΔH/Ht based on Yc/Hdam, Yc/h, h/L and N parameters.

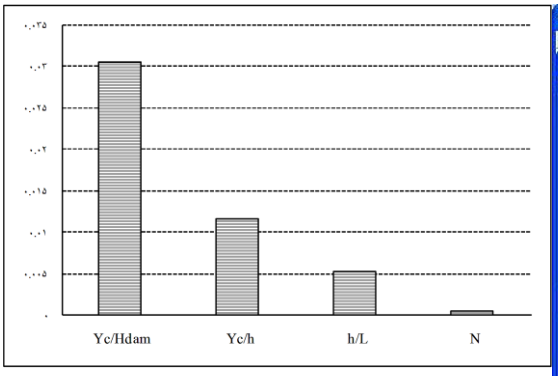

Fig. 3. Ranking the impact of input parameters on output

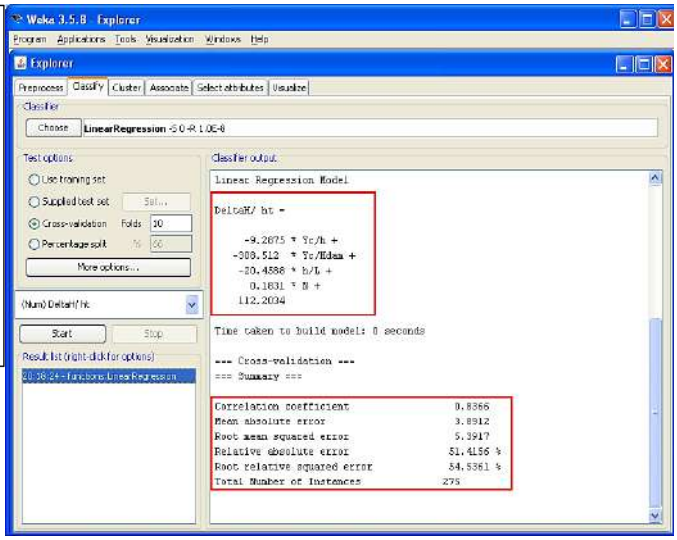

Fig. 4. Linear regression results on ΔH/Ht estimation

Tree regression: In Fig. 5, the ΔH/Ht prediction tree is shown based on Yc/Hdam, Yc/h, h/L and N parameters.

Regression based on SVM: In Fig. 6, the prediction function of ΔH/Ht based on SVM is displayed on the parameters Yc/Hdam, Yc/h, h/L and N.

Combined tree and linear regression:

In the following, the rules extracted by combined tree and linear regression to predict ΔH/Hta are presented.

If equation 1 is true:

$$\frac{\Delta h}{H_t} = -0.639\left(\frac{Y_c}{h}\right) - 443.746\left(\frac{Y_c}{H_{dam}}\right) - 14.217\left(\frac{h}{l}\right) - 0.1056\,(N$$

If equation 2 holds true:

$$\frac{\Delta h}{H_t} = -814.28\left(\frac{Y_c}{H_{dam}}\right) + 55.5\left(\frac{h}{l}\right) - 1.119\,(N) + 108.198$$

If the above two conditions are not met, equation 3 is met.

$$\frac{\Delta h}{H_t} = -814.28\left(\frac{Y_c}{H_{dam}}\right) + 55.5\left(\frac{h}{l}\right) - 1.119\,(N) + 108.19$$

```
REPTree
============

Yc/h < 1.62
|   Yc/Hdam < 0.03
|   |   Yc/h < 0.88
|   |   |   Yc/Hdam < 0.02 : 95.32
|   |   |   Yc/Hdam >= 0.02 : 92.24
|   |   Yc/h >= 0.88
|   |   |   h/L < 0.45 : 94.06
|   |   |   h/L >= 0.45 : 86.03
|   Yc/Hdam >= 0.03
|   |   Yc/Hdam < 0.04
|   |   |   Yc/h < 1.13 : 87.94
|   |   |   Yc/h >= 1.13 : 82.51
|   |   Yc/Hdam >= 0.04 : 82.03
Yc/h >= 1.62
|   h/L < 0.45
|   |   Yc/Hdam < 0.05
|   |   |   Yc/Hdam < 0.04 : 91.53
|   |   |   Yc/Hdam >= 0.04 : 86.47
|   |   Yc/Hdam >= 0.05 : 80.77
|   h/L >= 0.45
|   |   h/L < 0.54
|   |   |   Yc/h < 2.03 : 64.88
|   |   |   Yc/h >= 2.03 : 55.54
|   |   h/L >= 0.54
|   |   |   Yc/h < 2.26 : 77.46
|   |   |   Yc/h >= 2.26 : 65.55
```

Fig. 5. prediction tree ΔH/Ht

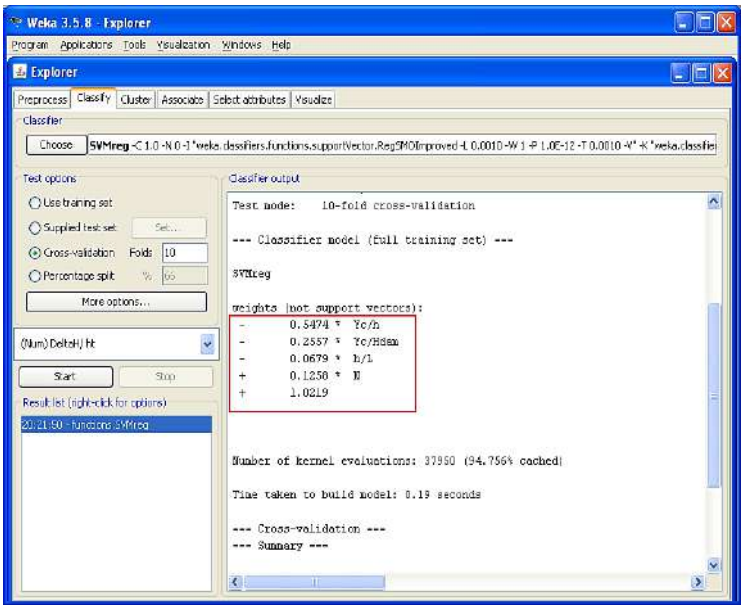

Fig. 6. prediction function based on SVM to predict ΔH/Ht

7. Evaluation of the second stage of the proposed method

In this section, we want to optimize the prediction function obtained in the previous section. Our goal is to identify the optimal value of other geometrical parameters such as Yc/h, h/L and N by giving the desired value of ΔH/Ht and Yc/Hdam. As seen in the previous section, the proposed estimation function of the linear and tree regression method obtained the best correlation coefficient and the least error, so at this stage we use this function as a fitness or target function. In the following table (3), the parameters of the genetic algorithm used are described.

Table 3
parameters used in the proposed genetic algorithm

The value of the parameter used in the evaluation of the proposed method of genetic	algorithm parameters
100	people in the audience
real number	real number data type of genes
Roulette cycle	Roulette cycle selection method
Gossin	Gaussian mutation function
single point	Single point intersection function
After producing 1000 generations	final conditions

8. Operators

In the evaluation of the proposed method, two Gaussian jump operators and one-point intersection operator have been used. In fig. 7 & Fig. 8 shown An example of applying a mutation and single point intersection operator in the proposed method.

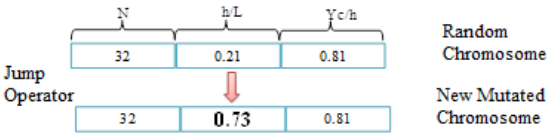

Fig. 7. An example of applying a mutation operator in the proposed method

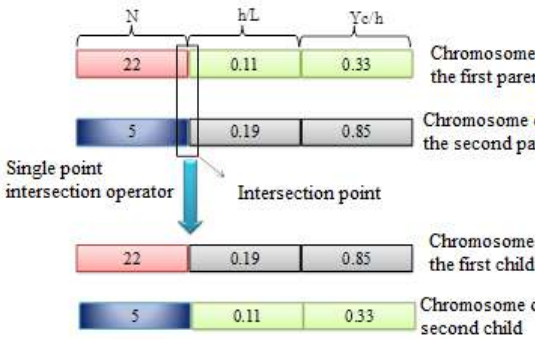

Fig. 8. An example of applying a single point intersection operator in the proposed method

9. Fitness function

In the following, the code of the fitness function, which is actually the same as the linear combined regression, is displayed. It should be noted that the chromosome in this code (shown in fig .9) is displayed using the vector x and the fitness function is also called nestedfun. As you can see, for the x1 variable (N parameter), we have used the Int32 command to convert this variable into an integer. As can be seen, our proposed fitness function is in the form ((regression formula Y=ABS (ΔH/Ht -)). Because our goal is that by giving the desired value of ΔH/Ht, the difference between the regression output and ΔH/ Ht reaches its lowest state. In this case, the regression parameters that cause the minimization of this fitness function are considered as optimal parameters.

Evaluations: To evaluate and validate the proposed method, we determine the value of Yc by using different flow rates (q) and by giving the desired value of Hdam and ΔH/Ht, from the proposed genetic algorithm, the optimal geometric parameters of Yc/h, h We request /L and N. After identifying these three parameters from them and given Yc, we extract three parameters h, L and N. In this section, as the first evaluation, we use the flow parameter equal to 0.01, the Hdam parameter equal to 1.2, and the ΔH/Ht parameter equal to 90%.

Given parameters:

q	H_{dam}	Yc	Yc/H_{dam}	$\Delta H/H_t$
0.01	1.2	0.0215	0.0181	**90**

By implementing the proposed genetic algorithm, a random population is first generated and minimizes the fitness function in each generation. In fig .10, the trend of movement of the best chromosome (Best Fitness) and the average value of the fitness function of all members of the population are shown. As can be seen in the fig. 10, the individuals of the population gradually move towards the best chromosome in each generation until in

```
function [x, fval, exitflag, output, population] =  runga(DeltaH_ht,Yc_Hdam,NVARS)

[x, fval, exitflag, output, population] = ga(@nestedfun,NVARS);

    function y = nestedfun(x)
        if (x(3) <= 1.456)
            y = abs ( DeltaH_ht + 0.639 * x(3) + 443.746 * Yc_Hdam + 14.2174 * x(2)+ 0.1056 * int32(x(1)) - 112.399);
        else if (x(2) > 0.449)
            y = abs ( DeltaH_ht + 814.2825 * x(3) - 55.5584 * x(2) + 1.1196 * int32(x(1)) - 108.1981);
        else
        y = abs ( DeltaH_ht -3.3914 * x(3) + 782.8367 * Yc_Hdam - 115.0264);

        end
    end
end
```

Fig. 9. Fitness function code

the 1000th generation, all chromosomes converge to an optimal point. In the diagram (6), the distance between the members of the population in the generation is also shown, as can be seen, at the beginning of the evolution of the proposed genetic algorithm, the chromosomes have a significant distance from each other, but gradually when they tend to the optimal point, the distance between the chromosomes of the population decreases a lot and becomes close to zero.

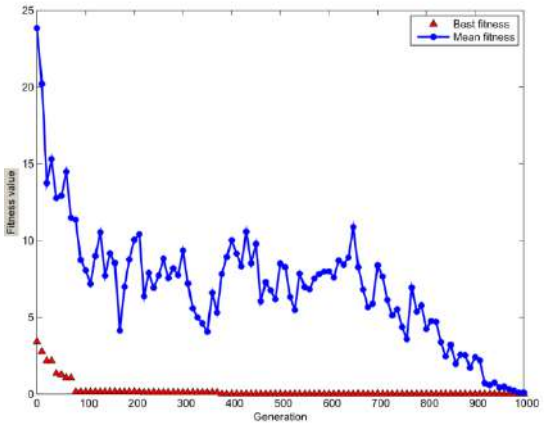

Diagram (5): The evolution diagram of population individuals in the generations of the proposed genetic algorithm

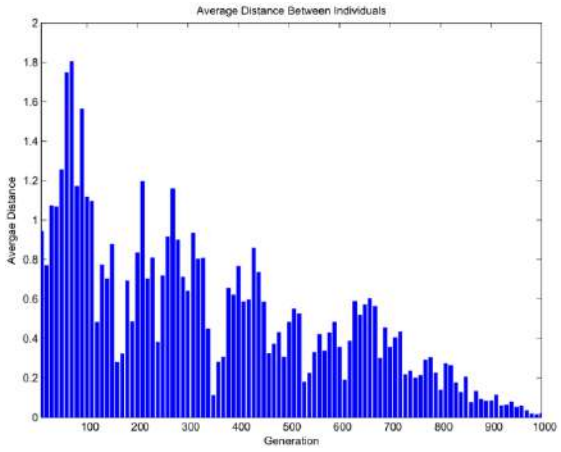

Diagram (6): The diagram of the distance between the individuals of the population in the proposed genetic algorithm

When the proposed genetic algorithm moves to an optimal point for the given parameters Yc/Hdam equal to 0.0181 and ΔH/Ht equal to 90 and stops there, our algorithm ends. The output of the proposed genetic algorithm can be seen in the table below.

As seen in table number (4), the difference between the given ΔH/Ht and the regression formula used at the optimal point found is very very small (0.00008). The chromosome that obtained this optimal value is shown in the table below. In the following, we have calculated the amount of two parameters h and L separately using the given value of Yc:

H	L
0.0388651704176774	0.04288690411356

To evaluate the proposed method, because we have laboratory results for Yc/Hdam equal to 0.0181 and ΔH/Ht equal to 90, we have done this evaluation so that we can compare the results obtained by the proposed method with the results obtained in the laboratory. Let's make a comparison. In table (5), the laboratory results for flow rate equal to 0.01 and Hdam equal to 1.2 are displayed and in that parameters N, Yc/h, h/L and ΔH/Ht are measured in four different modes. In this table, based on the regression formula used (linear and tree combination), the goodness-of-fit function has been calculated on each of these four laboratory data.

As can be seen in table (5), none of the laboratory data could bring the value of the fitness function below 1. Here, the importance and accuracy of the proposed method is more revealed, which has been able to minimize the fitness function and, as a result, be more optimal.

10. Results and discussion

As can be seen from the evaluation of the previous two sections, first we extracted the best among the regression methods that had the highest correlation coefficient. The more accurate regression method in this thesis is the combined linear and tree regression method, which has been able to increase the correlation coefficient to more than 0.94. In the second step of the proposed method, we proposed a genetic algorithm to optimize the selected regression function. The evaluations show that our proposed

Table 4
Output of the proposed genetic algorithm for data parameters

N	h/L	Yc/h	Fitness function value
17	0.912113709472540	0.557967359617298	**0.0000831841496591323**

Table 5
measured laboratory data

	N	h/L	Yc/h	Yc/H_{dam}	$\Delta H/H_t$	Fitness function value
1	33	0.567568	1.032643	0.0181	90	2.1665
2	35	0.571429	1.084275	0.0181	90	1.8674
3	25	0.507692	0.657136	0.0181	90	4.1025
4	27	0.5	0.72285	0.0181	90	3.9587

Table 6

Output of the proposed genetic algorithm for geometric parameters for q=0.01 m2/s

	N	h/L	Yc/h	Delta	h	NH	Fitness
0.01	89	0.58	2.765366	85	0.007956	0.708044	0.000010961
0.01	57	0.58	1.793144	88	0.012269	0.69933	0.993787164
0.01	50	0.58	1.385675	90	0.015877	0.793837	0.000033413
0.01	9	0.58	0.282789	95	0.077797	0.700169	0.034377889
0.01	2	0.58	0.05	97	0.44	0.88	1.077670000

It is meaningless for more than 95%

Table 7

Output of the proposed genetic algorithm for geometric parameters for q=0.01 m2/s

q	N	h/L	Yc/h	Delta	h	NH	Fitness
0.01	98	0.5	3.057975	85	0.007194	0.705042	0.000026267
0.01	77	0.5	1.833574	88	0.011998	0.923879	0.000018074
0.01	61	0.5	1.347859	90	0.016322	0.995653	0.000009803
0.01	19	0.5	0.463957	95	0.047418	0.900946	0.000003498
0.01	11	0.5	0.242019	96	0.090902	0.999922	0.003378014
0.01	3	0.5	0.066043	97	0.333116	0.999348	0.056129527

It's meaningless to more than 96% ---

method, we proposed a genetic algorithm to optimize the selected regression function. The evaluations show that our proposed method works much more accurately than the laboratory results and can identify the optimal geometrical parameters N, h and L by giving the desired Yc/Hdam and ΔH/Ht. In the following, by placing the depreciation of different energies in the proposed program, the number of steps corresponding to each energy depreciation has been obtained according to the tables and diagrams below.

According to table (6), for q=0.01 m2/s and a small slope, energy consumption is possible up to 95%. And bigger than that is meaningless because of the high fitness number that the program gives.

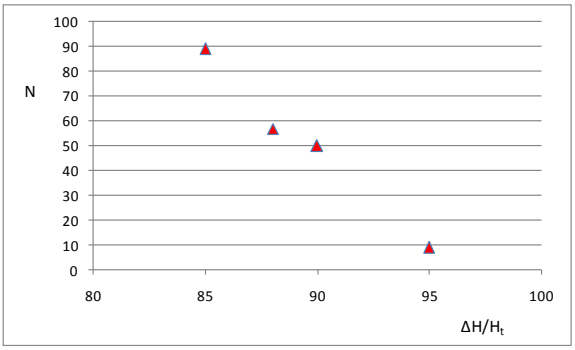

Diagram 7. The output of the proposed genetic algorithm for q=0.01 m2/s

Table 8

Output of the proposed genetic algorithm for geometric parameters for q=0.01 m2/s

q	N	h/L	Yc/h	Delta	h	NH	Fitness
0.01	110	0.4	3.299916	85	0.006667	0.733352	0.000034515
0.01	86	0.4	2.571196	88	0.008556	0.735844	0.000017533
0.01	70	0.4	2.085514	90	0.010549	0.738427	0.000031551
0.01	30	0.4	0.871012	95	0.025258	0.757739	0.000035290
0.01	14	0.4	0.385312	97	0.057097	0.799351	0.000002683

It made sense for 97% but not 98%

Table 9

Output of the proposed genetic algorithm for geometric parameters for q=0.02 m2/s

q	N	h/L	Yc/h	Delta	h	NH	Fitness
0.02	114	0.58	3.514654	77	0.00626	0.713584	0.0000102732
0.02	90	0.58	2.786091	80	0.007896	0.710673	0.0000384104
0.02	50	0.58	1.571404	85	0.014	0.700011	0.0001469038
0.02	10	0.58	0.314225	39	0.070013	0.700135	0.0274841438
0.02	2	0.58	0.050017	94	0.439849	0.879699	2.9588869448

It is meaningless for more than 93%

Table 10

Output of the proposed genetic algorithm for geometric parameters for q=0.02 m2/s

q	N	h/L	Yc/h	Delta	h	NH	Fitness
0.02	123	0.5	3.807243	77	0.005778	0.710751	0.000038009
0.02	99	0.5	3.078614	80	0.007146	0.707461	0.000031776
0.02	59	0.5	1.854165	85	0.011865	0.700046	0.006454728
0.02	20	0.5	0.484665	90	0.045392	0.907843	0.000034964
0.02	12	0.5	0.264106	91	0.0833	0.9996	0.014297569
0.02	2	0.5	0.05	94	0.44	0.88	1.821484000

It is meaningless for more than 91%.

Table 11

Output of the proposed genetic algorithm for geometric parameters for q=0.02 m2/s

q	N	h/L	Yc/h	Delta	h	NH	Fitness
0.02	134	0.4	4.211308	77	0.005224	0.70002	0.001980163
0.02	110	0.4	3.457143	80	0.006364	0.7	0.00182917156
0.02	74	0.4	1.628032	85	0.013513	0.99998	0.00113064290
0.02	32	0.4	0.726438	90	0.030285	0.969113	0.00001237970
0.02	7	0.4	0.163114	89	0.134875	0.944126	0.00002374533
0.02	2	0.4	0.050122	94	0.438932	0.877864	0.39982172718

It is meaningless for more than 93%.

Table 12

Output of the proposed genetic algorithm for geometric parameters for q=0.02 m2/s)

q	N	h/L	Yc/h	Delta	h	NH	Fitness
0.03	172	0.58	4.894208	66	0.004495	0.773159	0.000038716
0.03	97	0.58	3.048506	75	0.007217	0.700015	0.009936478
0.03	58	0.58	1.822828	85	0.012069	0.700011	0.000973029
0.03	19	0.58	0.444708	90	0.049471	0.939943	0.000008329
0.03	2	0.58	0.05	91	0.44	0.88	3.952590000

For more than 90% it was meaningless.

Table 13

Output of the proposed genetic algorithm for geometric parameters for q=0.03 m2/s

q	N	h/L	Yc/h	Delta	h	NH	Fitness
0.03	182	0.5	4.999964	66	0.0044	0.800806	0.013774911
0.03	107	0.5	3.331363	75	0.006604	0.706618	0.000010846
0.03	68	0.5	1.951718	85	0.011272	0.766504	0.000004189
0.03	28	0.5	0.7373	90	0.029839	0.835481	0.000017425
0.03	2	0.5	0.05	91	0.44	0.88	1.815198000

For more than 90% it was meaningless.

Table 14

Output of the proposed genetic algorithm for geometric parameters for q=0.03 m2/s

q	N	h/L	Yc/h	Delta	h	NH	Fitness
0.03	158	0.4	4.952886	66	0.004442	0.701813	0.000002449
0.03	118	0.4	3.708515	75	0.005932	0.700011	0.001951064
0.03	79	0.4	2.358792	85	0.009327	0.736818	0.000023628
0.03	40	0.4	0.979155	90	0.022468	0.898734	0.000011975
0.03	2	0.4	0.05	91	0.44	0.88	0.393458000

For more than 90% it was meaningless.

In this amount of energy consumption, the number of 9 steps is the answer.

And the graph (7) of proportional values of the number of steps with the corresponding energy consumption is given for table (5-22).

According to table (8), for q=0.01 m2/s and a small slope, energy consumption is possible up to 97%. And bigger than that is meaningless because of the high fitness number that the program gives. In this amount of energy consumption, the number of 14 stairs is the answer, and the graph (9) of the proportional values of the number of stairs and the corresponding energy consumption is given for table (5-24).

According to table (9), for q=0.02 m2/s and a small slope, energy consumption is possible up to 93%. And bigger than that is meaningless because of the high fitness number that the program gives. In this amount of energy consumption, the number of 14 stairs is the answer, and the graph (10) of the proportional values of the number of stairs and the corresponding energy consumption is given for table (5-25).

According to table (10) for q=0.02 m2/s) and a small slope, energy consumption is possible up to 91%. And bigger than that is meaningless because of the high fitness number that the program gives. In this amount of energy consumption, the number of 12 steps is the answer.

And the graph (11) of the proportional values of the number of steps with the corresponding energy consumption is given for the table (5-26).

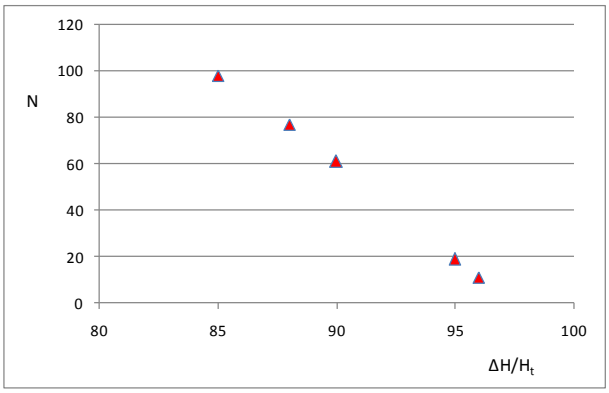

Diagram (8): The output of the proposed genetic algorithm for q=0.01 m2/s

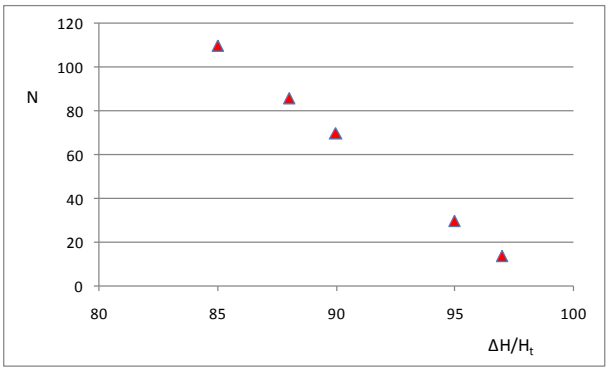

Diagram (9): The output of the proposed genetic algorithm for q=0.01 m2/s

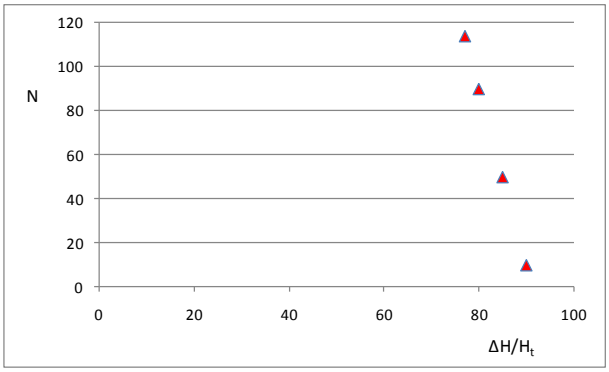

Diagram (10): The output of the proposed genetic algorithm for q=0.02 m2/s

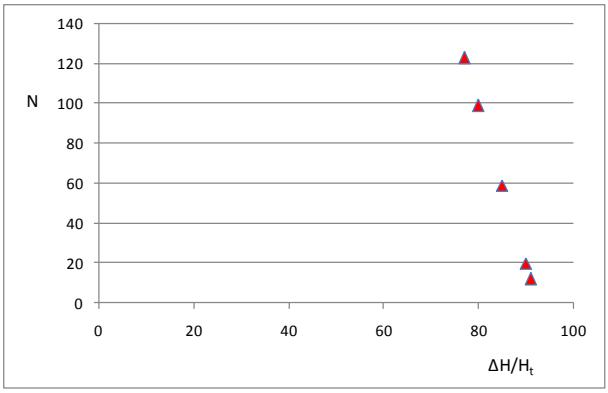

Diagram (11): The output of the proposed genetic algorithm for q=0.02 m2/s

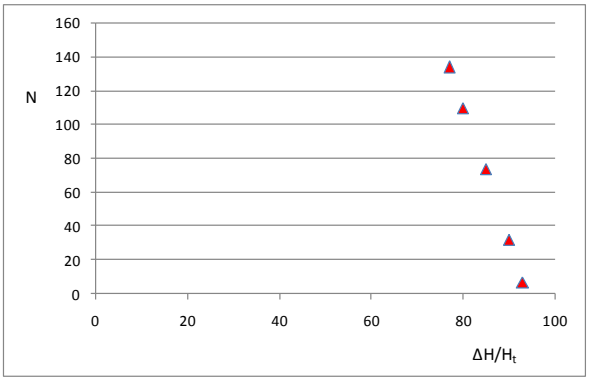

Diagram (12): The output of the proposed genetic algorithm for q=0.02 m2/s)

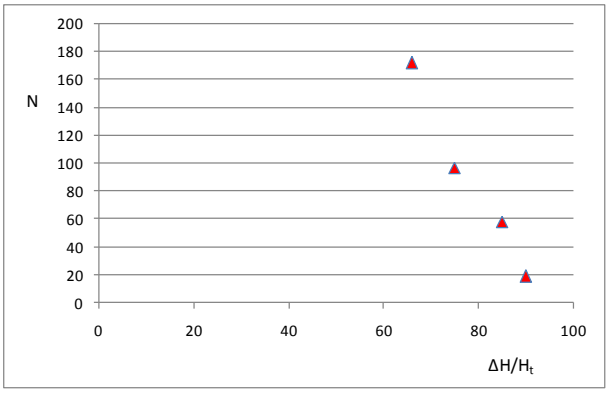

Diagram (13): The output of the proposed genetic algorithm for q=0.03 m2/s)

According to table (11), for q=0.02 m2/s) and a small slope, energy consumption is possible up to 89%. And bigger than that is meaningless because of the high fitness number that the program gives.

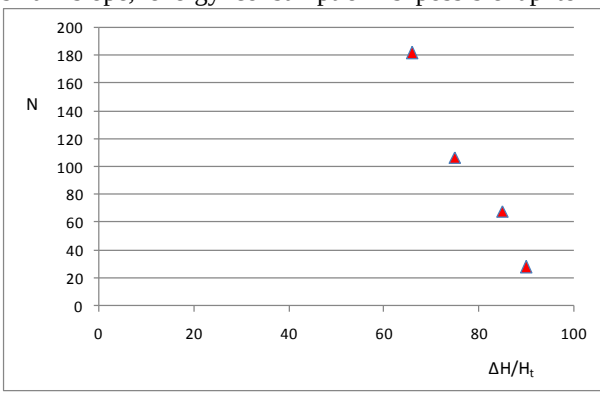

Diagram (14): The output of the proposed genetic algorithm for q=0.03 m2/s)

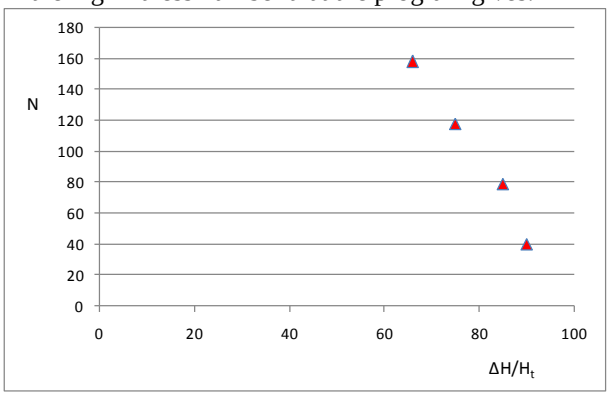

Diagram (15): The output of the proposed genetic algorithm for q=0.03 m2/s)

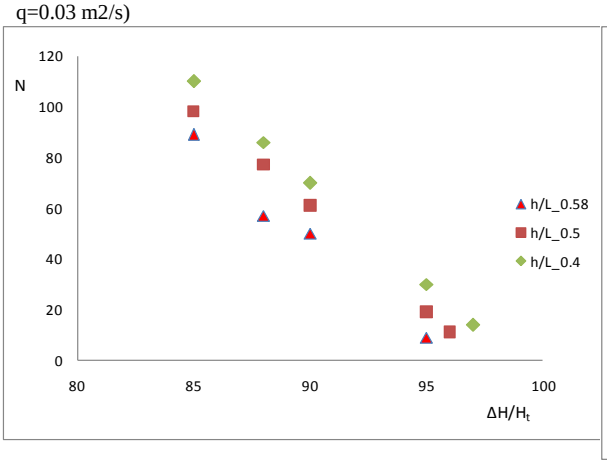

Diagram (16): Output of the proposed genetic algorithm for q=0.01 m2/s)

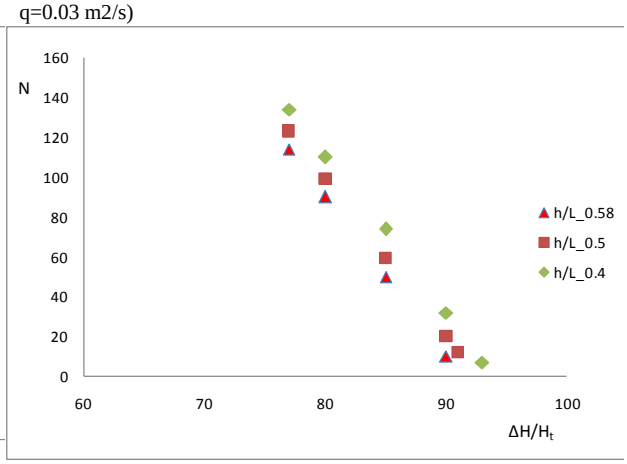

Diagram (17): Output of the proposed genetic algorithm for q=0.02 m2/s; For q equal to 0.03

In this amount of energy consumption, the number of 7 stairs is the answer, and the graph (12) of the corresponding values of the number of stairs and the corresponding energy consumption is given for table (5-27).

According to table (12), for q=0.03 m2/s) and a small slope, energy consumption is possible up to 90%. And bigger than that is meaningless because of the high fitness number that the program gives. In this amount of energy consumption, the number of 19 stairs is the answer, and the graph (13) of the proportional values of the number of stairs and the corresponding energy consumption is given for table (5-28).

According to table (13), for q=0.03 m2/s) and a small slope, energy consumption is possible up to 90%. And bigger than that is meaningless because of the high fitness number that the program gives. In this amount of energy consumption, the number of 28 stairs is the answer, and the graph (14) of the proportional values of the number of stairs with the corresponding energy consumption is given for table (5-29).

According to table (14), for q=0.03 m2/s) and a small slope, energy consumption is possible up to

90%. And bigger than that is meaningless because of the high fitness number that the program gives. In this amount of energy consumption, the number of 40 stairs is the answer, and the graph (5-15) of the proportional values of the number of stairs with the corresponding energy consumption is given for table (5-30).

In diagrams 16, 17 and 18, the amount of energy consumption according to the number of steps corresponding to it for each constant flow rate and in 3 different slopes in each of the graphs is given for their comparison.

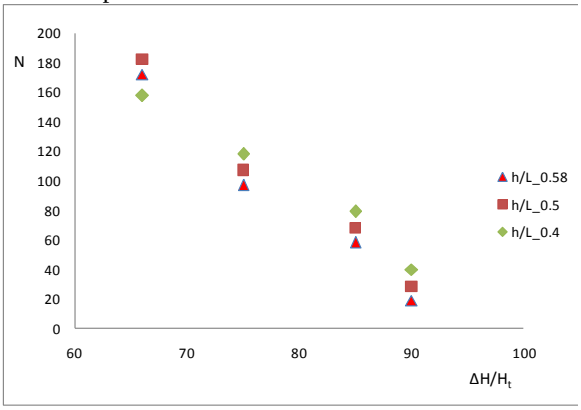

Diagram (18): Output of the proposed genetic algorithm for q=0.03 m2/s)

11. Conclusions

The results obtained from the analyzes performed in this study are as follows:

1) With the increase in flow rate, the amount of maximum energy consumption decreases.

2) By increasing the slope of the small head at a constant flow rate, the number of optimal steps for equal energy consumption increases.

3) From the very high number of steps that results in low energy consumption, we come to the conclusion that the effect of the existence of the step is reduced in the high step and the small head is inclined towards the smooth bottom head, which makes the percentage Reduce its energy loss.

References

[1] Barani ,G,A.(2005)."Optimization of stepped spillway Dimensions and investigation of flow Energy Dissipation over a Physical Model". Journal of Applied Science 5.878-882.

[2] Chanson, H. (2001) . "The hydraulics of stepped chutes and spillways". Balkema, Lisse, The Netherlands, 418 pages.

[3] Chanson, H. and Gonzalez, C.A. (2004). "Stepped Spillways for Embankment Dams: Review, Progress and Development in Overflow Hydraulics". Proceedings of the International Conference on Hydraulics of Dams and River Structures, Tehran, Iran, Balkema Publ., The Netherlands,287–294.

Journal of Civil Engineering Researchers

J-Researchers

JOURNAL OF CIVIL ENGINEERING RESEARCHERS

Seismic Assessment of Combined Effects of Knee Bracing and Dog-bone Connections in Dual Moment Frame Systems for Tall Steel Structures

Ali Zahmatkesh[a,*], Kazem Seyyedan[a], Seyed Mojtaba Mosavi Nezhad[b]

[a]*Department of Civil Engineering, Ferdows Branch, Islamic Azad University, Ferdows, Iran*

[b]*Assistant Professor, Department of Civil Engineering, Ferdows Faculty of Engineering, University of Birjand, Birjand, Iran*

Article History: Received date: 2023.02.27; revised date: 2023.03.10; accepted date: 2023.03.22

Abstract

The growing population and urbanization have led to an increasing interest in constructing tall buildings, particularly in large cities. However, the frequent occurrence of earthquakes worldwide has necessitated the development of systems with high ductility and sufficient lateral stiffness. The special dual system of moment frame with bone connections and knee bracing systems are two examples of such systems. In this study, the seismic behavior of these two systems in combination with tall structures was investigated. Ten, thirteen, and sixteen-story frames with four different combinations of bone joints and knee bracing were analyzed using ETABS software. Linear and nonlinear static (pushover) analyses, as well as linear and nonlinear dynamic (time history) analyses, were conducted. Seismic parameters were then calculated for each case and compared. The results emphasized the importance of considering multiple factors and coefficients when evaluating the seismic performance of structures. (DOI:https//doi.org/10.52547/JCER.5.1.46)

Keywords: Behavior coefficient; Special dual system of moment frame; Dog-bone connections; Knee bracing; Tall steel structures, Seismic behavior

1. Introduction

The concept of using behavior factor to calculate earthquake forces was first introduced in 1957, and since then, it has become widely used in seismic design codes. Researchers from different nationalities have proposed various methods to calculate the behavior factor, which can be broadly divided into two groups: American and European methods. While American methods are simpler and more practical, European methods are more complex and difficult to use in practice [1].

Bone joints are an innovative design solution for improving the flexibility and seismic resistance of frames exposed to severe vibrational loads. The

* Corresponding author. Tel.: +0-000-000-0000 ; e-mail: zahmatkesh@ferdowsiau.ac.ir.

concept of weak arrow-strong column was the driving force behind the development of these joints. Essentially, a reduced section along a limited length of the arrow near the connection site is used, similar to a bone muscle. This reduction is applied at the top width of the arrow, hence the name "Reduced Beam Sections" (RBS) [2].

The use of bone connections offers several advantages, including preventing stress concentration at the node, redistributing stress around the connection of the arrow to the column, and limiting the amount of stress redistributed and made uniform at the top width of the arrow. These connections also increase the flexibility of the joint, forming a hardened post-plastic joint, which can warn the residents before damage occurs due to excessive flexibility. Additionally, bone connections increase the frequency period and behavior coefficient of the special bending frame system, and the bone fuse prevents unwanted forces from passing through the hardened joint, thereby ensuring the connection of the arrow to the column is not threatened. Moreover, bone connections change the type of failure from sudden and brittle to flexible and adaptable. They also reduce the costs of connection and structure implementation, reduce implementation time, and increase the reliability of the structure. Overall, bone joints are a promising solution for enhancing the seismic performance of structures.

Fig1. shows a Dog-bone connection. Based on Engelhardt et al [2], the following ranges and values are suggested for selecting dimensions a, b, and c in knee braced frames:

$$a \cong (0.5\sim0.75)b_f \quad (1)$$

$$\mathrm{b} \cong (0.65\sim0.85)d \quad (2)$$

$$c = 0.25b_f \quad (3)$$

$$\mathrm{R} = \frac{4\mathrm{c}^2 + \mathrm{b}^2}{8\mathrm{c}} \quad (4)$$

A knee braced frame system uses the knee member as a secondary structural member, acting like a "fuse" that creates suitable ductility. In addition, the diagonal bracing member provides excellent lateral stiffness to the frame. This combination results in a system that has both sufficient ductility and lateral stiffness, with the knee member acting as a structural fuse during severe earthquakes to prevent damage to the main structural members.

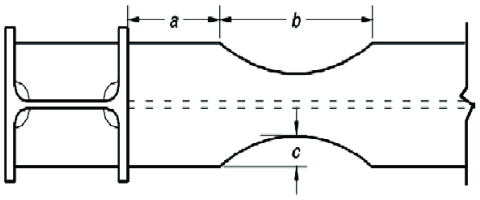

Fig1. Dog-bone connection

The advantages of knee braced frames include their ability to create suitable ductility and lateral stiffness, prevent damage to main structural members during earthquakes, and allow for simple and economical repair and reconstruction of knee members as structural fuses. Strengthening the diagonal bracing member does not affect the lateral performance of the frame and increasing the cross-sectional area of beams and columns can improve the lateral performance, with the effect of increasing the cross-sectional area of the column being greater than that of the beam. However, architectural limitations may restrict changes to beam length or column height, making knee members a valuable option for improving lateral performance by adjusting their own cross-sectional area and length. [3].

Various researchers have investigated the behavior factor Knee bracing and Dog-bone [4-11]. The objective of this study is to evaluate the behavior of steel structures under earthquake loads. Specifically, the effect of factors such as building height (low-rise, mid-rise, and high-rise), the use of dual systems of moment-resisting frames with bone joints and knee braces on the static response of the structure under earthquake loads is investigated. The results of these analyses are compared to provide useful information about the behavior factor of structures, from its fundamental definition to determining it for different types of structures.

2. Modelling

Frames have been designed with three different heights: 30 meters (10-story frame), 39 meters (13-story frame), and 48 meters (16-story frame), all with an equal floor height of 3 meters. The distribution of

bone joints in these structures at different heights is presented in the table 1.

Table1. Position of plastic joints in diffrent frame

	Tape af frame	Stories in which plastic joints are used
1	Brace	Without plastic joints
2	Fail	5, 6, 7
3	Middle	3, 4, 5, 6, 7
4	All	All Stories

Previous studies have indicated that "most damages in tall structures occur between half to two-thirds of their height." Therefore, four different conditions were considered for the distribution of bone joints in height. The first condition involved no bone joints. The second condition placed bone joints between half to two-thirds of the height of the structure. The third condition placed bone joints between one-third to two-thirds of the height of the structure. Finally, in the fourth condition, bone joints were distributed throughout the entire height of the structure. The fourth condition was added based on the author's engineering sense, which stated that in braced structures, the effect of bone joints would be less due to the bracing system's presence and power in controlling lateral deformation compared to non-braced structures. Therefore, adding bone joints would have a better effect.

It should be noted that there are several differences in the structural models, which will be discussed shortly. For example, in the 10-story buildings, a 5-meter span is placed between the span containing the bone joints and the span containing the knee braces. This is done to prevent the knee members and bone joints from being located near each other and around a connection (beam to column) that could potentially impact their performance. In contrast to the 10-story buildings, in 13-story structures, the 5-meter span is placed next to the 6-meter span containing the bone joints. The 4-meter span containing the knee braces is placed next to the 5-meter span to examine the effects of knee members, bone joints, and braced frame on the behavior coefficient of the structures. In 10-story buildings, the 6-meter span is used as the side span, and in 13-story buildings, it is used as the middle span. However, since the placement of bone joints in the side span may affect their performance, in 16-story structures, another 4-meter span is added to the right side of the frame to examine the frame stiffness simultaneously and to study the new distance from the braced frame. The earthquake motions used are summarized in Table 2.

Table2. Earthquake motions used

Motion	Time(Sec)	a_{max}	Predominant period (sec)
Bam	50	0.799g	0.70
El Centro	16	0.463g	0.74
Tabas	25	0.852g	0.20
Northridge	10	0.843g	0.34
Naghan	10	0.730g	0.08
Mexico City	12	0.621g	0.22

3. Results and Discussion

According to research conducted by scholars from Berkeley University, the behavior factor of a structure is composed of four coefficients, as mentioned in equation (5) [12]:

$$R_U = R_S \times R_\mu \times R_R \times R_\zeta \quad (5)$$

where RS is the Overstrength factor, Rμ is the ductility factor, RR is the uncertainty coefficient, and R_ζ is the damping coefficient. While RR is significant for analyzing structures against wind loads, and R_ζ is important when dampers are employed in the structure, they are not considered in this study.

The first step in this study was to conduct linear and nonlinear dynamic analyses (Time History) on sample frames subjected to scaled seismic excitations

Table3. Ductility factor (R_μ) in different system

Number of storis	Braced	Fail	Middle	All
10	4.4403	4.4379	4.4335	4.4409
13	4.4299	4.4306	4.4307	4.4407
16	4.0115	4.0138	4.0145	4.0169
average	4.2939	4.2941	4.2926	4.2995

Table 4. Overstrength factor in different system

Number of storis	Braced	Fail	Middle	All
10	2.1892	2.1877	2.2053	2.2087
13	2.1892	2.1877	2.2053	2.2087
16	1.7678	1.7655	1.7668	1.7851
average	2.0487	2.0469	2.0591	2.0675

Table 5. behavior coefficient in different system

Number of storis	Braced	Fail	Middle	All
R_μ	4.2939	4.2941	4.2929	4.2995
R_S	2.0084	2.0071	2.0165	2.0282
R_U	8.6239	8.6187	8.6566	8.7202

using the graphical software ETABS v2018. The ductility factor (R_μ) was then calculated by dividing the linear base shear to the nonlinear base shear. Table 3 illustrates ductility factors in diffrent frames.The results of the study showed that the rate of increase in the ductility factor is higher in the All type frames compared to other types. This finding indicates that braced frames should maintain a better distribution of skeletal joints throughout the structure's height, and concentrating these joints within the lower half or two-thirds of the height will not be significantly effective.

The overstrength factor is defined as the ratio of the maximum base shear to the base shear at the first plastic hinge formation. The values of base shear at the first plastic hinge formation and during structural damage with cracking, as well as the calculated values of overstrength factor for each frame, can be found in columns 2, 3, and 4 of tables 6 to 8, respectively. Table 4 shows the overstrength factors in lateral-resistant systems for frames.

The reduction coefficient due to ductility was also assessed, and it was found that as the number of stories in the frames increased, this coefficient improved relatively in Fail and Middle systems. However, as seen in Table4, the Fail and Middle systems decrease with an increase in the number of stories and become equal or lower in comparison to the Brace system. This is consistent with the inverse relationship between the reduction coefficients due to ductility and increased resistance, which was mentioned earlier. Despite the superiority of the All system in the reduction coefficient due to ductility, this system also showed superiority in the increase resistance coefficient, which is noteworthy. This indicates that the combination of knee braces and distributed bone joints throughout the structure's height is superior to other configurations.

Comparing similar peripheral systems at levels 15 to 18, it was observed that the added resistance coefficient decreases with height, consistent with the

results obtained by other researchers. This trend can be predicted for different numbers of stories. The final values of these coefficients were calculated by averaging the values of the added resistance coefficients in each type of the four peripheral systems, and the results are shown in Table 4. Note the relative superiority of the all system type.

The Overstrength factor R_S was calculated and evaluated in the previous sections, and the reduction coefficient of shape deformation Rμ was calculated by dividing the linear base shear to the nonlinear base shear. In order to calculate the overall behavior coefficient of the frames, the average of RS and Rμ were calculated for each frame type. The values for the four peripheral systems can be seen in Table 5. The values for the middle system were calculated for 10-story and 13-story frames. According to the results, the All system has the highest overall behavior coefficient among the peripheral systems, indicating its superior performance in resisting lateral loads. Moreover, the behavior coefficient increased with the height of the structure, which is consistent with the findings of other researchers. The obtained results can be used as a reference in the design of high-rise structures with similar characteristics.

4. Conclusions

• The findings of this study suggest that the use of bone joints and knee braces in the lateral-resistant system of high-rise buildings can lead to significant improvements in their seismic performance. The all state, which combines both knee braces and distributed bone joints, has been shown to have the best performance in terms of both deformation and resistance coefficients. It also has the highest behavior coefficient, indicating its superior overall performance compared to other states.

• The results of this study also emphasize the importance of considering multiple factors and coefficients when evaluating the seismic performance of structures. The behavior factor, which consists of four coefficients, provides a comprehensive measure of a structure's ability to resist seismic forces. R_R and R_ζ, which were not used in this study, may also be important in certain situations, such as wind loads or the use of dampers.

• Finally, it should be noted that the behavior and performance of structures under seismic loads is a complex and multi-dimensional topic that requires careful consideration of various factors, including the design and construction of the structure, the characteristics of the site and soil, and the nature of the seismic hazard. The findings of this study contribute to our understanding of the behavior of high-rise buildings under seismic loads and provide useful insights for future research and design.

References

[1] Mario.P,1994, “Interational handbook of Earthquake Engineering codes programs and Examples” Chapman and Hall Inc.
[2] Engelhardt, M.D., Winneberger, T., Zekany, A.J., Potyraj, T.J. "Experimental Investigation of Dogbone Moment Connections," Engineering Journal, vol. 4, pp. 132-139, 1998.
[3] Huang, Z., and Liq Chen, L. "Elastoplastic Analysis of Knee Bracing Frame," Journal of Zhejiang University Science, ISSN:1009-3095, 2005.
[4] Asgarian.B, Shokrgozar.H.R.2009. “BRBF response modification factors”. Journal of Constructional Steel Research 65 . 290-298.
[5] Castiglioni.C.A, Zambrano.A.2012. “Determination of the behavior factor of steel moment-resisting (MR) frames by a damage accumulation approach”. Journal of Constructional Steel Research 66 . 723-735.
[6] Kang.C.K, Choi.B.J. September 2011. “New Approach to Evaluate the Response Modification Factors for Steel Moment Resisting Frames”. International Journal of Steel Structures. Vol 11, No 3, 275-286.
[7] Mahmoudi.M, Abdi.M.G.2012. “Evaluation response modification factors of TADAS frames”. Journal of Constructional Steel Research 71. 162-170.
[8] Izadinia.M, Rahgozar.M.A, Mohammadrezaei.O.2012. “Response modification factor for steel moment-resisting frames by different pushover analysis methods”. Journal of Constructional Steel Research 79 . 83-90.
[9] Attia.W.A, Irheem.M.M.M.2016. “Boundary condition effect on response modification factor of X-braced steel frames”. Housing and Building National Research Center (HBRC) Journal.
[10] Yavarian.S, Ahmad.R.2016. “Evaluation of Seismic Performance Factors in High Rise Steel Building with Dual Lateral Systems Consisting of Buckling Restrained Braced Frames and Intermediate Moment Frames”. World Multidisciplinary Civil Engineering. Procedia Engineering 161 . 680-686.
[11] Branci.T, Yahmi.D, Bouchair.A, Fourneley.E. 2016.“Evaluation of Behavior Factor for Steel Moment-Resisting Frames”. World Acamedy of Science, Engineering

and Technology. International Journal of Civil, Environmental, Structural, Construction and Architectural Engineering Vol:10, No:3.

[12] Structural response modification factor (Applied Technology Council NO. 19, 1995).

Journal of Civil Engineering Researchers

J-Researchers

JOURNAL OF CIVIL ENGINEERING RESEARCHERS

A Case Study of Mechanically Stabilized Earth (MSE) Retaining Wall Failure in the State of Tennessee; Recommendations for Future Design and Constructions

Hossein Alimohammadi[a,*], Ashfaq A. Memon[a]

[a]*Terracon Consultants, Inc., Nashville, TN, USA 37217*

Article History: Received date: 2023.02.11; revised date: 2023.03.14; accepted date: 2023.03.28

Abstract

This study presents an investigation into the failure of a Mechanically Stabilized Earth (MSE) retaining wall in Tennessee, USA. The wall was constructed to support an embankment development, but it failed catastrophically, causing damage to the road and posing a significant safety risk to the public. The investigation involved a comprehensive site visit, field data collection, laboratory testing, and numerical modeling. Our investigation revealed that the failure of the retaining wall was caused by inadequate construction practices. Specifically, the wall was not constructed in accordance with design specifications, and the backfill material used was not properly compacted. The construction issues resulted in the differential settlement of the wall, which ultimately caused it to fail. Based on our findings, we propose a set of recommendations for the design and construction of future retaining walls in similar geotechnical conditions. The recommendations include the proper selection and use of backfill material, proper compaction of backfill, and adherence to design specifications. The results of this study are expected to contribute to the development of improved design standards and construction practices for MSE retaining walls in Tennessee and other regions with similar geotechnical conditions. (DOI:https//**doi.org/10.52547/JCER.5.1.52**)

Keywords: Type your keywords here, separated by semicolons ;

1. Introduction

Retaining walls are an essential component of civil engineering projects, providing support to the soil, rock, and other materials that are prone to collapse or erosion [1]. However, the failure of MSE retaining walls can be attributed to various factors such as poor design, improper construction, inadequate drainage, substandard materials, poor site preparation, overloading, and natural disasters. Inadequate design specifications, selection of materials, and calculation of loads and forces can impact the wall's strength and durability. Non-compliance with design specifications can also lead to the inability of the wall to withstand the forces it is subjected to, resulting in failure. The absence of proper drainage systems can cause water to accumulate behind the wall and exert pressure on it, leading to failure. The quality of materials such as soil, reinforcement, and geosynthetic fabrics can also

* Corresponding author. Tel.: +12254853307; e-mail: Hossein.Alimohammadi@terracon.com.

impact the wall's strength and durability [2]–[4]. Insufficient site preparation can lead to soil instability, causing the wall to shift or settle over time. Overloading due to changes in the use of the area adjacent to the wall or an increase in the weight of stored materials can also cause the wall to fail. Natural disasters such as earthquakes, landslides, or heavy rainfall can also contribute to the failure of MSE retaining walls. Regular inspections, proper design, construction, and maintenance procedures must be followed to prevent the failure of MSE retaining walls. Several studies have investigated the causes of retaining wall failures and proposed remediation plans. These plans include reconstruction with improved design, construction techniques, and installation of drainage systems or geosynthetic reinforcement.

Poor construction quality is the most common cause of retaining wall failures, which include issues such as inadequate compaction, poor drainage, and inadequate reinforcement. H. Binici, et al. (2010) [5] investigated the failure of a case study retaining wall and found that poor construction quality was the primary cause of the failure. The retaining wall was constructed using poor-quality materials, and the construction techniques used were not in accordance with the design specifications. In another study, Kong et al. (2021) [6] illustrated that inadequate design was the primary cause of retaining wall failure in their case study. The study proposed a remediation plan that involved reconstructing the retaining wall with improved design and construction techniques.

Other researchers, such as [7]–[12], investigated retaining wall failures and identified poor construction quality and inadequate drainage as the primary causes. They proposed various remediation plans, including the installation of a new retaining wall with improved construction techniques and materials or the installation of geosynthetic reinforcement, reconstruction of the foundation, and installation of additional reinforcement.

In other studies, researchers such as [13]–[17] investigated retaining wall failures and identified inadequate design and construction as the primary causes. The proposed remediation plans involved reconstructing the retaining wall with improved design and construction techniques, installation of drainage systems, and use of higher quality materials and additional reinforcement.

Further research conducted by [18]–[22] investigated retaining wall failures and identified poor drainage, inadequate reinforcement, poor compaction, inadequate soil reinforcement, and poor maintenance as the primary causes. The proposed remediation measures included reconstruction of the retaining wall, installation of a new drainage system, or installation of a new retaining wall with improved construction techniques and materials.

This case study aimed to investigate the causes of the retaining wall failure that occurred in the state of Tennessee, USA, where a retaining wall constructed using Mechanically Stabilized Earth (MSE) blocks failed, resulting in significant damage to an embankment road and posing a threat to public safety and propose appropriate remediation measures. This paper discusses the factors that led to the retaining wall failure, the assessment methods used to determine the cause of failures, and the remediation measures taken to repair the retaining wall. The study also highlights the importance of proper design and construction, regular inspection and maintenance, and the use of appropriate assessment methods to prevent retaining wall failures. The results of this study are expected to contribute to the development of improved design standards and construction practices for MSE retaining walls in Tennessee and other regions with similar geotechnical conditions.

2. Methodology and Background

The case study involved a comprehensive investigation that combined field data collection, laboratory testing, and numerical modeling. A site visit was conducted to assess the damage caused by the retaining wall failure, and the wall's design and construction were analyzed to identify potential weaknesses. Field data collection involved conducting geotechnical investigations to assess the engineering properties of the soil and rock strata in the area [23]–[27]. The laboratory testing program

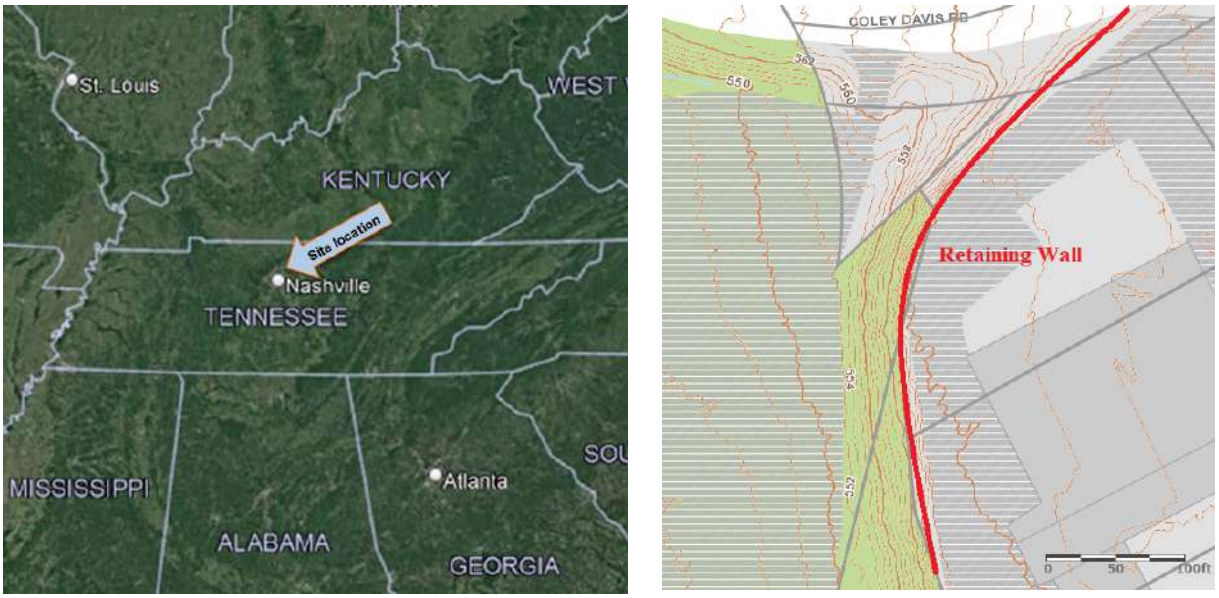

a) b)

Figure 1 a) site location map b) topographic layout of the site and the retaining wall's position from Metro GIS

a) b)

Figures 2a and 2b) The current state of the failed retaining wall

included assessing the properties of the soil and rock strata and examining soil samples in accordance with the Unified Soil Classification System (USCS) [28]. The USCS classification system is widely used in geotechnical engineering and provides a framework for describing the physical and mechanical properties of soils. Numerical modeling was conducted to simulate the behavior of the retaining wall under different loading conditions. The numerical models were validated using field data, and the results were used to identify potential causes of the retaining wall failure. Finite element analysis was used to model the retaining wall and simulate the behavior of the wall under various loads and conditions. The finite element analysis revealed that the retaining wall was well-designed to resist the lateral earth pressure and

vertical loads from the roadway above and utilized low-quality materials or construction were the factors that led to the retaining wall failure.

The location of this case study project is situated in Davidson County, TN, to the southeast of Nashville, and encompasses an existing development, infrastructure, and a retaining wall. The project area, as mapped by metro GIS [29] topography, is characterized by a general slope from east to west, with the retaining wall situated at an elevation of approximately 578 to 580 feet, MSL, near the top, and around 582 feet at/near the existing building. The ground in front of the wall sharply descends to the west, with an elevation range from approximately 572 feet at the top to 551 feet MSL at the bottom of the slope, creating a slope height of up to 21 feet along the wall and 26 feet in areas where no wall exists. The site location map and topographic layout of the site and the retaining wall's position are depicted in figures 1a and 1b respectively.

The retaining wall at the site has experienced partial failure along a section of its length, resulting in a loss of retained materials and consolidation of adjacent pavements. This mechanically stabilized earth (MSE) retaining wall was constructed using precast concrete panels interlocked with an anchorage system comprising concrete stretchers in the upper part of the wall and tandem epoxy-coated rebars with concrete deadman anchors in the lower portions. The approximate exposed height of the wall is estimated to be up to 10 feet tall. The wall was constructed to support new fill associated with the original grading of the existing development. However, a large portion of the wall has either failed or had its stability compromised. In some locations, the wall has completely collapsed, with the obvious failure of the wall anchorage system at its connection to the precast concrete facing panels. Figures 2a and 2b illustrate the current state of the failed retaining wall.

In order to support the recommendations outlined in this study and to gain insight into the construction of the current retaining wall, we conducted both geotechnical borings and excavated test pits to collect subsurface information regarding material stratification and strength. The field exploration program involved six borings, each extending to a depth of 30 ft or until auger refusal, and three pits, each excavated to a depth of 10 ft or until refusal, located in the backfill zone of the retaining wall. The subsurface exploration plan is presented in Figure 3, while Figure 4 a and b illustrate the excavated test pits and subsurface conditions found in the backfill of the retaining wall.

A truck-mounted rotary drill rig equipped with continuous flight augers was utilized to advance the borings, while the test pits were excavated using an excavator. The final logs for both borings and test pits were prepared by the Geotechnical Engineer, based on the field logs, and included modifications based on observations made during the exploration program. Soil samples collected were described and classified in accordance with the Unified Soil Classification System (USCS), and laboratory tests were performed to determine the backfill soil water content and Atterberg limits.

The investigation conducted in the backfill of the retaining wall revealed the presence of fill material up to a depth of 22 feet. The composition of the fill was highly variable, ranging from predominantly rock fill (with a majority of rock size <6”) containing a small amount of clay to mostly clay with some limestone fragments. Additionally, occasional large-size rocks were observed during test pit excavations. Out of six borings, four were obstructed by large-size rocks before reaching the natural ground. At one of the boring locations, asphalt debris/pieces were encountered within the fill at a depth of approximately 13½ feet below the existing grade. The Standard Penetration Tests (SPT) conducted within the existing fill indicated erratic N-values, ranging as low as 4 to 5 bpf, indicating the presence of poorly compacted (compressible) material in some layers. Below the existing fill, the soil was found to consist of stiff to very stiff natural residual clay (lean clay) extending to a depth of about 30 feet without encountering bedrock.

3. Geotechnical Overview

Based on our subsurface exploration and observations, the MSE retaining wall comprises precast concrete panels that are interconnected using some form of interlocking mechanism. Additionally,

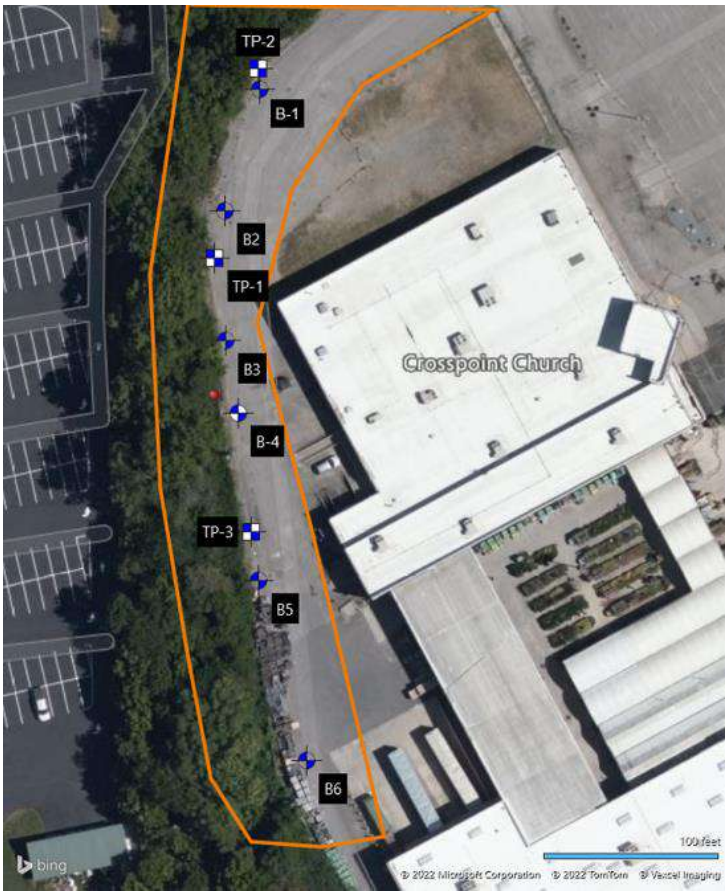

Figure 3 subsurface exploration plan

a) b)

Figures 4a and 4b) Excavated test pits and subsurface conditions found in the backfill of the retaining wall

an anchorage system consisting of concrete stretchers in the upper part of the wall and tandem epoxy-coated rebars with concrete deadmen anchors in the lower portions of the wall is used. The height of the exposed wall varied along its length and was observed to be as tall as 10 feet. However, our findings indicate that a significant portion of the wall has either failed or is compromised in terms of stability. At several points, we also observed a complete collapse of the wall, indicating an obvious failure of the wall anchorage system at its connection to the precast concrete facing panels.

The assessment of the retaining wall failure revealed additional concerns beyond just wall movement. Both vertical settlement and lateral movement of the asphalt pavement and concrete curbs were observed over the reinforced backfill zone of the retaining wall. Our investigation suggests that the accumulation of surface water runoff from the parking lot, illustrated in figure 2a, has been directed towards the wall over time, instead of flowing into the designated site stormwater drainage system. The failure of the retaining wall seems to have occurred due to a connection failure at the facing panels, where the anchorage system pulled out of or sheared off the panels as illustrated in figure 2b. This failure may have been caused by backfill settlement and the added hydrostatic pressure imposed on the wall from the migration of surface water runoff into the backfill. Our examination also revealed anchor system failures both at the wall panel connection locations as well as within the concrete deadmen anchors, where rebars appeared to have pulled out from the concrete anchor block.

The intrusion of water into the soil rock mixture has resulted in the loss of strength in the backfill material, which has settled over time. It is noteworthy that most MSE wall systems of this type are designed using a free-draining granular backfill material. However, at several locations, the wall backfills contained significant amounts of clay that hindered the drainage of water entering the reinforced zone. As a consequence, lateral earth pressures acting on the wall system may increase, not only due to the added weight of the backfill material but also due to the likelihood of hydrostatic pressures imposed on the wall. Additionally, we observed the absence of any drainage system in the retaining wall such as weep holes, perforated drainage pipes, or other similar features. It is possible that a chimney drain system is located at the back of the reinforced zone, which was unable to be detected during our exploration, or a drainage system may run underneath the wall and empty onto the slope below, which was obscured by vegetation.

4. Numerical Modelling

One method of analyzing the behavior of retaining walls is numerical modeling, which involves simulating the behavior of the wall using computer software. In this research, we use the SLOPE/W software to model the behavior of an MSE (Mechanically Stabilized Earth) retaining wall under different conditions and loads. The numerical models were validated using field data, and the results were used to identify potential causes of the retaining wall failure. Finite element analysis was used to model the retaining wall and simulate the behavior of the wall under various loads and conditions.

The numerical modeling in this research was performed using the SLOPE/W software, which is a powerful tool for analyzing the stability of slopes and retaining structures. The software uses finite element analysis to model the behavior of the retaining wall, taking into account the properties of the soil, the wall geometry, and the loads it will be subjected to. The numerical models were validated using field data, which were collected from the site of a retaining wall failure.

The MSE retaining wall that was analyzed in this research was constructed using low-quality materials, and it failed due to a combination of factors, including inadequate drainage, poor compaction, and overloading. The numerical models were used to simulate the behavior of the wall under different loads and conditions, including different angles of internal friction, different wall heights, and different surcharge loads.

The finite element analysis revealed that the retaining wall was well-designed to resist the lateral earth pressure and vertical loads from the roadway above. However, the use of low-quality materials and

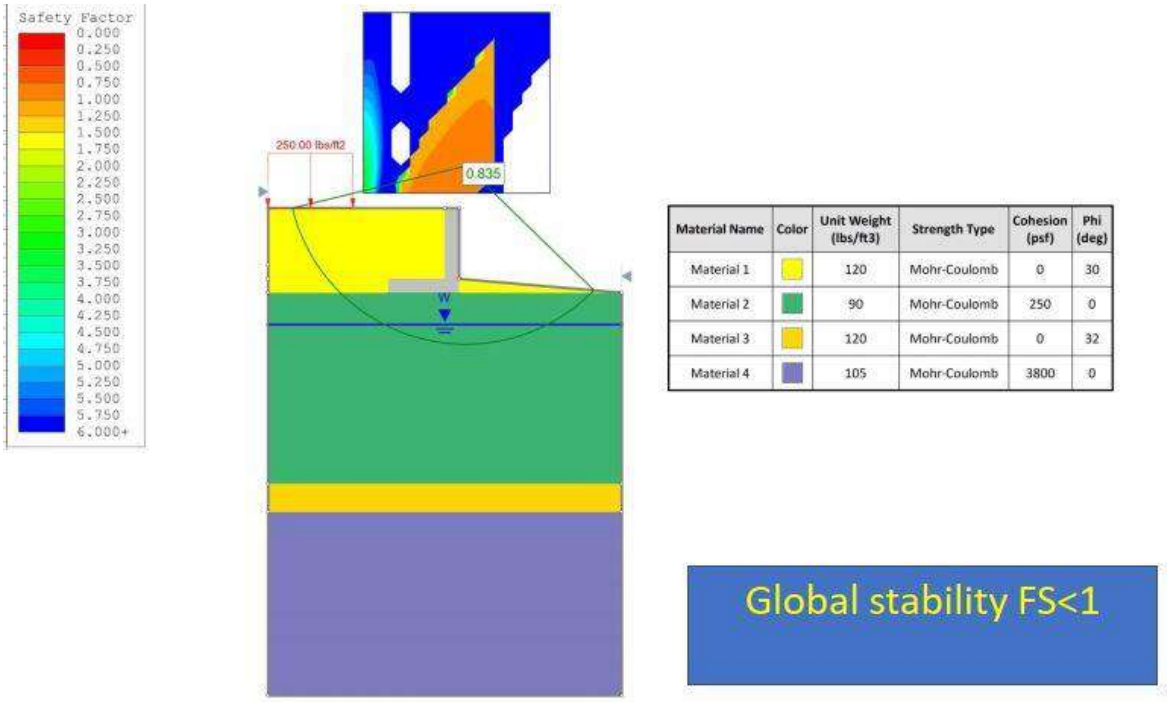

Figure 5 simulated MSE retaining wall using SLOPE/W software

poor construction practices led to the retaining wall failure. The numerical models showed that the wall was most susceptible to failure under high surcharge loads, which caused the wall to tilt and lose stability. The models also showed that the use of geogrid reinforcement and proper compaction of the soil could significantly improve the stability of the wall.

The finite element analysis revealed that the retaining wall was well-designed to resist the lateral earth pressure and vertical loads from the roadway above and utilized low-quality materials or construction were the factors that led to the retaining wall failure.

5. Recommendations

When dealing with retaining wall failure, several factors must be considered in order to make informed decisions and provide effective recommendations. Firstly, the type and cause of the failure must be determined in order to choose the appropriate solution. Common causes of retaining wall failure include poor construction, soil erosion, inadequate drainage, and seismic activity. Secondly, the severity of the failure will dictate the course of action, as minor damage may only require minor repairs, while a complete reconstruction may be necessary for significant collapses. Site conditions, such as soil type, slope, and groundwater level, must also be taken into account when developing a repair or replacement plan. Environmental factors like rainfall, temperature, and seasonal changes can also impact the performance of the retaining wall and must be considered when developing a solution. Additionally, the available budget and resources will determine the feasibility and scope of any repair or replacement work. Compliance with local regulations and requirements is also critical to ensure the safety and structural integrity of the retaining wall. Finally, the planned future use of the area may influence the design and construction of any repair or replacement work.

There are several methods used to assess the causes of retaining wall failures, including visual inspections, soil testing, and structural analysis. Visual inspections involve examining the wall for signs of damage or distress, such as cracks, bulges, or leaning. Soil testing can help determine the soil's properties, including its shear strength, compaction, and moisture content. Structural analysis involves using mathematical models to analyze the wall's behavior under various loads and conditions. All these assessment methods are important and necessary to identify the root cause of the failure [30]–[39]. Once the cause of the retaining wall failure is identified, remediation measures can be taken to repair the wall and prevent future failures. These measures may include reinforcing the wall with additional materials or support structures, repairing any damage, improving drainage, and implementing regular inspection and maintenance programs. The remediation measures taken should be based on the specific cause of the failure and should be designed to address the underlying problem. Proper design and construction, regular inspection and maintenance, and appropriate assessment methods are all critical to preventing retaining wall failures [40]–[46]. A well-designed and constructed wall that is regularly inspected and maintained is less likely to fail. If a failure does occur, appropriate assessment methods can help determine the cause of the failure, and remediation measures can be taken to prevent future failures. It is important to recognize that retaining walls are complex structures that require expertise in design, construction, and maintenance. Therefore, it is essential to hire qualified professionals who have experience in these areas to ensure the safety and stability of the retaining wall.

Retaining walls can fail if not constructed correctly, leading to property damage, personal injury, and legal disputes. One critical factor that can prevent retaining wall failure is the proper selection and use of backfill material. Backfill is the material placed behind the retaining wall to provide support and counteract the force of the retained soil. The choice of backfill material depends on several factors such as soil type, groundwater level, and wall height. The backfill material should be free of debris, large rocks, and organic matter that can create voids and affect the wall's stability. Moreover, the backfill material should be compacted correctly to minimize settlement and lateral movement. The backfill material should be placed in layers and compacted using appropriate equipment and techniques to achieve the required density and moisture content. The use of geotextiles and drainage systems can also improve the backfill's performance and prevent water build-up and hydrostatic pressure.

The Backfill material required to achieve design grade should be classified as structural fill. Structural fill is material used below, or within 10 feet of the retaining wall, pavements or constructed slopes. Compacted structural fill should meet the material property requirements mentioned in table 1.

Another critical factor in preventing retaining wall failure is adherence to design specifications and proper compaction of the backfill material. The retaining wall's design should be based on the site's soil conditions, slope angle, and anticipated loads. The design should include details on wall height, thickness, reinforcement, drainage, and backfill material. The contractor should follow the design specifications and use the appropriate construction methods and materials. Proper compaction of the backfill material is crucial to prevent settlement and lateral movement, which can affect the wall's stability. The compaction should be done in layers, using the appropriate equipment, and testing the density and moisture content. The contractor should also monitor the wall's performance during and after construction to detect any signs of movement, cracking, or distress. Regular maintenance and inspection can also prevent retaining wall failure by identifying and addressing any issues before they become critical. Backfill Compaction Requirements should meet the requirements in table 2.

In this case study, the retaining wall on the north side has failed and requires complete removal and reconstruction to support the pavement and backfill. Various retaining wall systems are available for construction, a gravity wall concept was recommended for this site, such as Redi-Rock or gabion basket wall systems, or an MSE retaining wall system over traditional cast-in-place concrete retaining walls, soldier pile or secant pile walls for their cost-effectiveness. To ensure suitable bearing

Table 1 Structural fill material requirements

Soil Type [1]	USCS Classification	Acceptable Parameters (for Structural Fill)
Low Plasticity Cohesive	CL	Liquid Limit ≤ 45 Plasticity index ≤ 25 Not recommended for reuse below and behind wall
High Plasticity "Fat" Cohesive [2]	CH	Liquid Limit ≥ 50, Plasticity index ≥30 not recommended for reuse
Granular	GW [3]	Less than 5% Passing #200 sieve, can be used at all locations and elevations. Terracon recommends any fill material used within the geogrid reinforced wall backfill should be granular fill with rock size less than 3 inches. The actual wall backfill material should be as specified by the designer of the retaining wall.
Existing Fill	CL	A large portion of the existing fill may not be suitable for reuse due to the presence of clay in the rock fill. However, if the fill contains predominantly clean well-graded rock (particle size ≤6") this material can be reused as engineered fill below the wall bearing or beneath the pavement area in the retained zone of the wall if approved by the geotechnical engineer
Clean well graded processed rock, surge stone (max. rock size 6 inches) [4]	--	Can be used at all locations and elevations except in the reinforced backfill zone of the retaining wall

1. Structural fill should consist of approved materials free of organic matter and debris. Frozen material should not be used, and fill should not be placed on a frozen subgrade. A sample of each material type should be submitted to the Geotechnical Engineer for evaluation prior to use on this site.
2. CH soils should not be used.
3. Similar to TDOT Section 903.05 Type A, Grading D crushed limestone aggregate, limestone screenings, or granular material such as well-graded gravel or crushed stone.
4. Approval of surge stone should be made prior to placement. Any rock fill containing clay fines should not be used as engineered fill.

and limit settlement to tolerable limits, the new retaining wall should be supported on engineered fill, and the existing fill must be undercut and replaced with approved engineered fill. However, a portion of deeper fill (below 15') may not require replacement if it can be recompacted to a non-yielding state and reinforced with a layer of geogrid prior to the placement of newly engineered fill and any wall construction. It is crucial to compact each lift of new fill, not exceeding 9 inches, according to our recommendations.

Additionally, a proper drainage system is imperative for the long-term performance of the retaining wall. Incorporating relief drains at the bottom of the rock fill is recommended, which may be daylighted on the face of the slope to bleed off any trapped water within the backfill. Furthermore, pavement near and around the retaining wall should slope away from the wall and collect into the site stormwater drainage system. All grades must provide effective drainage away from the wall during and after construction and should be maintained throughout the life of the wall.

The results of borings and test pits conducted in the wall backfill area revealed that the fill was placed up to a depth of 22 feet against and below the retaining wall. During drilling, Standard Penetration Tests (SPT) conducted within the existing fill indicated the presence of poorly compacted and compressible material layers. Consequently, in this case study it is recommended to excavate the existing fill to a depth of 15 feet below the existing grade or

Table 2 Backfill compaction requirements

Item	Structural Fill
Maximum Lift Thickness	9 inches or less in loose thickness when heavy, self-propelled compaction equipment is used 4 to 6 inches in loose thickness when hand guided equipment (i.e. jumping jack or plate compactor) is used
Minimum Compaction Requirements [1, 2]	98% of the material's standard Proctor maximum for granular fill material The surge should be placed in max. 9-inch thick lifts. and compacted with a heavy-duty vibratory smooth drum roller or D-6 class dozer Each lift of shot rock or surge fill should be compacted using a minimum of ten passes, five in one direction and five that are at a right angle to the initial passes. A complete pass consists of complete coverage of the surface with the tracks (roller).
Water Content Range [1]	Cohesive: -1% to +3% of optimum Granular: -2% to +2% of optimum

1. Maximum density and optimum water content as determined by the standard Proctor test (ASTM D 698 [47]).
2. If the granular material is coarse sand or gravel, or of a uniform size, or has a low fines content, compaction comparison to relative density may be more appropriate. In this case, granular materials should be compacted to at least 70% relative density (ASTM D 4253 and D 4254 [48]).

until stiff natural clay is reached, whichever comes first. The recommended undercutting should extend laterally at least 5 feet beyond the wall-bearing footprint on both sides. The exposed existing fill should be scarified or over-excavated and recompacted to a minimum of 95 percent of the material's standard Proctor maximum dry density. Next, a single layer of geogrid should be placed directly on top of the recompacted fill subgrade, followed by at least 12 inches of crushed rock-engineered fill. Any subsequent fill above this layer should consist of either crushed rock engineered fill, well-graded clean surge stone (rock size <6 inches), or material specified by the designer of the new retaining wall.

It is essential to ensure that retaining walls are constructed with high-quality materials, appropriate foundations, and proper drainage systems. Regular inspections and maintenance can help identify any signs of deterioration or structural weaknesses, allowing for timely repairs or replacements to prevent failure [49]–[56]. The use of appropriate assessment methods, such as geotechnical evaluations and structural analysis, can provide valuable insights into the integrity of the retaining wall, identifying potential problems before they become major issues. Proper design, construction, inspection, maintenance, and assessment are all critical components in preventing retaining wall failures and ensuring the safety and longevity of the structure and the people who rely on it. By prioritizing these factors, we can create a safer and more sustainable built environment.

6. Construction of New MSE Retaining Wall

In this journal paper, we provide recommendations and parameters for the construction of a new MSE wall. Our proposed design assumes that the wall will be supported on an engineered fill that meets the outlined recommendations. When designing the retaining wall foundations, a maximum net allowable bearing pressure of 2,000 psf can be used in this case study, while the recommended net allowable bearing pressure should provide a factor of safety of 3 (2 for MSE Wall) with respect to anticipated shear strength.

MSE retaining walls are typically composed of modular concrete block face units, geogrids for reinforcement, and compacted soil or select granular material that creates a reinforced soil mass acting as a gravity-type retaining wall. Design considerations for

Table 3 Recommended MSE wall soil strength parameters – foundation soils

Material Type	Moist Unit Weight (pcf)	Total Stress (Undrained) Parameters		Effective Stress (Drained) Parameters	
		c_u, psf	ϕ, degrees	c', psf	ϕ', degrees
New engineered granular fill	110	0	32	0	32

Table 4 Recommended MSE wall soil strength parameters – backfill materials

Material Type	Moist Unit Weight (pcf)	Total Stress (Undrained) Parameters		Effective Stress (Drained) Parameters	
		C_u, psf	ϕ, degrees	c', psf	ϕ', degrees
No. 57 Stone or Surge Stone	105	0	34	0	34
Crushed rock engineered fill [1]	135	0	32	0	32

1. Fill should be compacted to at least 95% of standard Proctor maximum dry density.

the MSE wall should include geotechnical parameters such as the unit weight and strength of in-place native materials, compacted soil for the reinforced zone, and foundation subgrade. The parameters used in the design and global stability analyses of the MSE retaining wall should not exceed those outlined in provided tables 3 and 4. It is also important to consider any surcharge loading that will be placed on the completed wall. It is crucial to exercise caution in the design and construction stages to establish and sustain swift and positive drainage away from the retaining wall area. Also, an effective surface drainage is necessary to prevent water from flowing over the wall face and saturating the fill behind the wall or subgrade soils at the base of the wall.

Before commencing construction of the MSE wall, it is essential to collect and analyze samples of the fill material proposed to be used in constructing the reinforced zone for the wall. This laboratory testing is critical to confirm that the engineering properties of the backfill align with the assumed properties utilized in the design. Additionally, it is recommended that qualified geotechnical personnel conduct field testing and observations during the MSE wall's construction. Table 3 illustrates recommended MSE wall soil strength parameters for foundation soils and table 4 shows recommended MSE wall soil strength parameters for backfill materials.

The retaining wall failure under investigation was found to be caused by construction practices. The wall was not built to withstand the lateral forces exerted by the embankment and soil retention. Other factors, such as unsuitable backfill materials, inadequate compaction, and poor drainage, were also found to have contributed to the failure. A remediation plan was proposed based on our findings, which involved reconstructing the retaining wall using improved design and construction techniques. The proposed design included additional reinforcement and drainage systems to prevent the accumulation of water and soil pressure. This study's results are expected to contribute to the development of better design standards and construction practices for retaining walls in Tennessee and other regions with similar geotechnical conditions. The study emphasizes the importance of proper design, construction, and maintenance practices in ensuring the long-term stability and safety of retaining walls. The value of a comprehensive investigation that combines field data collection, laboratory testing, and numerical modeling to identify the causes of retaining wall failure and propose appropriate remediation measures is also demonstrated by this study.

7. Conclusions

In conclusion, the case study involved a comprehensive investigation that combined field data collection, laboratory testing, and numerical modeling to identify potential causes of a retaining wall failure in Davidson County, TN. The investigation revealed that the retaining wall was well-designed to resist the lateral earth pressure and vertical loads from the roadway above; however, utilizing low-quality materials or construction was the factor that led to the retaining wall failure. Based on the subsurface exploration and observations, it was evident that the retaining wall in question was compromised in terms of stability. The assessment of the retaining wall failure revealed additional concerns beyond just wall movement, such as the presence of poorly compacted (compressible) material in some layers and the occurrence of occasional large-size rocks. The findings from this investigation highlight the importance of proper design and construction of retaining walls. The study provides insights into the need for careful consideration of soil properties and design loads, as well as the use of appropriate materials and construction techniques. The investigation also underscores the importance of regular monitoring and maintenance of retaining walls to identify and address potential issues before they result in catastrophic failure. Overall, this case study provides insights into the investigation of retaining wall failures and highlights the importance of proper design, construction, monitoring, and maintenance of retaining walls. The study findings can be useful for geotechnical engineers, contractors, and developers involved in the design and construction of retaining walls.

Acknowledgments

The authors would like to acknowledge the engineers in the soil mechanic laboratory facility, the field group members, and the drilling crews who performed SPT in the Terracon company in Nashville, TN, and thank them for their help in providing the data for this research. The opinions, findings, and conclusions presented herein are those of the authors and do not necessarily reflect any sponsors.

Conflict of Interest

The authors declare that there is no conflict of interest.

References

[1] S. Satvati, H. Alimohammadi, M. Rowshanzamir, and S. M. Hejazi, “Bearing Capacity of Shallow Footings Reinforced with Braid and Geogrid Adjacent to Soil Slope,” Int. J. Geosynth. Gr. Eng., vol. 6, no. 41, p. https://doi.org/10.1007/s40891-020-00226-x, 2020.

[2] H. Alimohammadi, J. Zheng, A. Buss, V. R. Schaefer, and G. Zheng, “Evaluating the Rutting Performance of Hot Mix Asphalt and Warm Mix Asphalt Mixtures by Using Viscoelastic Finite Element Simulations,” Int. Conf. Transp. Dev. 2020, p. https://doi.org/10.1061/9780784483183.009, 2020.

[3] H. Alimohammadi and B. Izadi Babokani, “Finite element electrodynamics modeling of a layered piezoelectric composite shell with different materials by using numerical software,” ISSS J. Micro Smart Syst., 2020.

[4] H. Alimohammadi, J. Zheng, V. Schaefer, J. Siekmeier, and R. Velasqueze, “Evaluation of Geogrid Reinforcement of Flexible Pavement Performance: A Review of Large-Scale Laboratory Studies,” Transp. Geotech., p. https://doi.org/10.1016/j.trgeo.2020.100471, 2020.

[5] H. Binici, “Retaining Wall Failure due to Poor Construction and Design Aspects A Case Study:” .

[6] S. M. Kong, D. W. Oh, S. Y. Lee, H. S. Jung, and Y. J. Lee, “Analysis of reinforced retaining wall failure based on reinforcement length,” Int. J. Geo-Engineering, vol. 12, no. 1, pp. 1–14, Dec. 2021.

[7] Nasar Ali.R, “Measures to prevent retaining wall distress and failures, a review in light with previous available work,” IJCRT, 2022.

[8] C. Yoo, A. M. Asce, and H.-Y. Jung, “Case History of Geosynthetic Reinforced Segmental Retaining Wall Failure.”

[9] D. Kazmi, S. Qasim, • I S H Harahap, and • Syed Baharom, “Landslide of Highland Towers 1993: a case study of Malaysia.”

[10] M. Abu-Farsakh, H. Alimohammadi, and L. N. Mohammad, “Finite Element Analysis to Evaluate the Benefits of Geosynthetic Reinforcement in Flexible Pavements Over Weak Subgrade for Low-Volume Traffic Roads,” Transp. Res. Board Conf. 99th Annu. Meet., 2020.

[11] A. Sesha, S. Raghuram, and · S M Dasaka, “Forensic Analysis of a Distressed RE Wall and Rigid Pavement in a Newly Constructed Highway Approach,” Int. J. Geosynth. Gr. Eng., vol. 8, no. 3, p. 38, 2022.

[12] H. Alimohammadi, “A framework for evaluation of existing pavement conditions and selection of feasible maintenance/rehabilitation alternatives; a case study in some routes of Livingston Parish in the state of Louisiana,” SN Appl. Sci., vol. 2, no. 2, p. 289, Feb. 2020.

[13] E. J. Nelson et al., “Lessons Learned from Foundation and Slab Failures on Expansive Soils,” 2016.
[14] Y. Tan, M. Asce, and Y.-Y. Long, “Review of Cave-In Failures of Urban Roadways in China: A Database,” 2021.
[15] T. Mulugeta, · Workineh, and T. Ayele, “Assessment of Irrigation Scheme Failure Factors: a Case Study on Marza Irrigation Scheme Fogera, Amhara, Ethiopia,” vol. 1, p. 3.
[16] J. L. M. Clemente, K. A. Lamote, J. R. Davie, and M. R. Lewis, “Risk Evaluation and Mitigation for Mechanically-Stabilized Earth (MSE) Walls—Perspectives from an EPC/EPCM Contractor,” Geotech. Struct. Eng. Congr. 2016 - Proc. Jt. Geotech. Struct. Eng. Congr. 2016, pp. 314–328, 2016.
[17] G. Zheng, H. Alimohammadi, J. Zheng, and V. R. Schaefer, “Effectiveness of Geosynthetics in the Construction of Roadways: A Full-Scale Field Studies Review,” in IFCEE 2021, 2021, pp. 223–232.
[18] R. M. Koerner and G. R. Koerner, “A data base, statistics and recommendations regarding 171 failed geosynthetic reinforced mechanically stabilized earth (MSE) walls,” Geotext. Geomembranes, vol. 40, pp. 20–27, Oct. 2013.
[19] R. M. Koerner and G. R. Koerner, “An extended data base and recommendations regarding 320 failed geosynthetic reinforced mechanically stabilized earth (MSE) walls,” Geotext. Geomembranes, vol. 46, no. 6, pp. 904–912, Dec. 2018.
[20] J. Y. Wu, M. Asce, N. N. Chou, and F. Asce, “Forensic Studies of Geosynthetic Reinforced Structure Failures,” 2013.
[21] W. Sun, C. Yan, W. Xu, Y. Shi, Z. Zhang, and Y. Xie, “Deformation of Geogrid-Reinforced Segmental Retaining Wall due to Insufficient Compaction of Loess Backfill: Case Study in Shaanxi Province, China,” J. Perform. Constr. Facil., vol. 33, no. 6, Dec. 2019.
[22] M. S. Hossain, G. Kibria, M. S. Khan, J. Hossain, and T. Taufiq, “Effects of Backfill Soil on Excessive Movement of MSE Wall,” J. Perform. Constr. Facil., vol. 26, no. 6, pp. 793–802, Dec. 2012.
[23] H. Alimohammadi and J. N. Tahat, “A Case Study Pile Load Testing (PLT) to Evaluate Driven Pile Behaviors,” Indian Geotech. J. 2022, pp. 1–10, Apr. 2022.
[24] H. Alimohammadi, V. R. Schaefer, J. Zheng, and H. Li, “Performance evaluation of geosynthetic reinforced flexible pavement: a review of full-scale field studies,” Int. J. Pavement Res. Technol., 2020.
[25] H. Alimohammadi, V. Schaefer, J. Ashlock, A. Buss, C. Rutherford, and B. Li, “Effectiveness of geogrids in roadway construction; determine a granular equivalent (G.E.) factor.”
[26] M. Y. Abu-Farsakh, Alimohammadi, Hossein, and Mohammad, Louay N., “Finite Element Analysis to Evaluate the Benefits of Geosynthetic Reinforcement in Flexible Pavements over Weak Subgrade for Low Volume Traffic Roads,” Geosynth. Int., 2020.
[27] H. Alimohammadi, J. Zheng, A. Buss, V. R. Schaefer, C. Williams, and G. Zheng, “Field and simulated rutting behavior of hot mix and warm mix asphalt overlays,” Constr. Build. Mater., vol. 265, p. 120366, Dec. 2020.
[28] “ASTM D2487 Unified Soil Classification System - ANSI Blog.” [Online]. Available: https://blog.ansi.org/2018/03/unified-soil-classification-astm-d2487-17/#gref. [Accessed: 24-Feb-2023].
[29] “Parcel Viewer.” [Online]. Available: https://maps.nashville.gov/ParcelViewer/. [Accessed: 24-Feb-2023].
[30] H. Alimohammadi, V. Schaefer, J. Zheng, and D. White, “A full-scale field approach for evaluating the geogrid reinforcement effectiveness in flexible pavement,” 22nd Int. Conf. Soil Mech. Geotech. Eng., 2022.
[31] H. Alimohammadi and · Jamal Tahat, “A case study experimental pile load testing (PLT) for evaluation of driven pile behaviors,” Arab. J. Geosci. 2022 159, vol. 15, no. 9, pp. 1–11, Apr. 2022.
[32] H. Alimohammadi, M. Amirmojahedi, and J. N. Tahat, “A Case History of Application of Deep Compaction Method with Comparison to Different Ground Improvement Techniques,” Transp. Infrastruct. Geotechnol., pp. 1–26, Mar. 2022.
[33] S. Satvati, H. Alimohammadi, M. A. Rowshanzamir, and S. M. Hejazi, “Evaluation the Effects of Geosynthetic Reinforcement on Bearing Capacity of Shallow Foundations in Soil Slopes,” 101st Transp. Res. Board Annu. Meet., 2022.
[34] H. Alimohammadi and J. Tahat, “A State-of-The-Art Evaluation of Driven Pile Behaviors Using Pile Load Testing (PLT),” 101st Transp. Res. Board Annu. Meet., 2022.
[35] H. Alimohammdi, V. R. Schaefer, J. Zheng, C. T. Jahren, G. Zheng, and D. White, “Effectiveness of Geotextiles/Geogrids in Roadway Construction; Determine a Granular Equivalent (GE) Factor,” Minnesota Dep. Transp., 2021.
[36] T. Mahmood, “FAILURE ANALYSIS OF A MECHANICALLY STABILIZED EARTH (MSE) WALL USING FINITE ELEMENT PROGRAM PLAXIS,” 2009.
[37] A. R. Kashani, C. V Camp, K. Azizi, and M. Rostamian, “Multi-objective optimization of mechanically stabilized earth retaining wall using evolutionary algorithms,” 2022.
[38] B. J. Khan, M. Ahmad, M. M. S. Sabri, I. Ahmad, B. Zamin, and M. Niekurzak, “Experimental and Numerical Evaluation of Mechanically Stabilized Earth Wall with Deformed Steel Bars Embedded in Tire Shred-Sand Mixture,” Buildings, vol. 12, no. 5, 2022.
[39] F. K. Nagy-Göde and Á. Török, The probabilistic analysis of steep lakeside slopes; geotechnical-geological-hydrogeological constraints and numerical analysis, an example from Hungary. 2022.
[40] H. Alimohammadi, V. Schaefer, J. Zheng, D. J. White, and G. Zheng, “A State-of-the-art Large-scale Laboratory Approach to Evaluating the Effectiveness of Geogrid Reinforcement in Flexible Pavements,” Geosynth. Conf. 2021, 2021.
[41] H. Alimohammadi, A. Buss, V. R. Schaefer, J. Zheng, and G. Z. Christopher Williams, “Finite element viscoelastic simulations of rutting behavior of hot mix and warm mix asphalt overlay on flexible pavements,” Int. J. Pavement Res. Technol., 2020.

[42] H. Alimohammadi, A. Buss, V. Schaefer, C. Williams, and M. Mina, "Rutting behavior of laboratory, field, and finite element simulated hot mix and warm mix asphalt overlays."
[43] H. Alimohammadi, J. Zheng, A. Buss, V. R. Schaefer, and G. Zheng, "Rutting Performance Evaluation of Hot Mix Asphalt and Warm Mix Asphalt Mixtures by Using Dynamic Modulus, Hamburg Wheel Tracking Tests, and Viscoelastic Finite Element Simulations," 2020, pp. 83–94.
[44] J. Zheng, H. He, and H. Alimohammadi, "Three-dimensional Wadell roundness for particle angularity characterization of granular soils," Acta Geotech., vol. 9, p. https://doi.org/10.1007/s11440-020-01004-9, 2020.
[45] B. Leshchinsky, "Limit Analysis Optimization of Design Factors for Mechanically Stabilized Earth Wall-Supported Footings," Transp. Infrastruct. Geotechnol., vol. 1, no. 2, pp. 111–128, 2014.
[46] V. S. Dantal, "Material Characterization and Design Recommendations for Mechanically Stabilized Earth Retaining Walls. (Doctoral Dissertation). Texas A&M University, USA.," no. December, 2013.
[47] "Standard Test Methods for Laboratory Compaction Characteristics of Soil Using Standard Effort (12,400 ft-lbf/ft3 (600 kN-m/m3))." [Online]. Available: https://www.astm.org/d0698-12r21.html. [Accessed: 24-Feb-2023].
[48] "ASTM D4253 - 00 Standard Test Methods for Maximum Index Density and Unit Weight of Soils Using a Vibratory Table." [Online]. Available: https://www.astm.org/DATABASE.CART/HISTORICAL/D4253-00.htm. [Accessed: 28-May-2020].
[49] H. Alimohammadi, K. Yashmi Dastjerdi, and M. Lotfollahi Yaghin, "The study of progressive collapse in dual systems," Civ. Environ. Eng., vol. 16, 2020.
[50] H. Alimohammadi, J. Zheng, A. Buss, V. Schaefer, C. Williams, and Guangfan Zheng, "Performance Evaluation of Hot Mix and Warm Mix Asphalt Overlay Layers Based on Field Measurements and Finite Element Viscoelastic Simulations," Transp. Res. Board Conf. 99th Annu. Meet., 2020.
[51] H. Alimohammadi, A. Hesaminejad, and M. Lotfollahi Yaghin, "Effects of different parameters on inelastic buckling behavior of composite concrete-filled steel tubes," Int. Res. J. Eng. Technol., vol. 6, no. 12, 2019.
[52] H. Alimohammadi, M. D. Esfahani, and M. L. Yaghin, "Effects of openings on the seismic behavior and performance level of concrete shear walls," Int. J. Eng. Appl. Sci., 2019.
[53] H. Alimohammadi, "Finite element analysis of a Piezoelectric layered plate with different materials," Int. J. Eng. Appl. Sci., vol. 6, no. 7, 2019.
[54] H. Alimohammadi and M. Lotfollahi Yaghin, "Study on the Effect of the Concentric Brace and Lightweight Shear Steel Wall on Seismic Behavior of Lightweight Steel Structures," Int. Res. J. Eng. Technol., vol. 6, no. 8, pp. 1358–1362, 2019.
[55] H. Alimohammadi and M. Abu-Farsakh, "Finite Element Parametric Study on Rutting Performance of Geosynthetic Reinforced Flexible Pavements," Transp. Res. Board, vol. 98th, 2019.
[56] H. H. Muteb and M. W. Falah, "IOP Conference Series: Earth and Environmental Science Mechanically Stabilized Earth MSE Walls Applications: Review Mechanically Stabilized Earth MSE Walls Applications: Review."

Author Guidelines EditEdit Author Guidelines

GENERAL GUIDELINES FOR AUTHORS

Journal of civil engineering researches invites unsolicited contributions of several forms: articles, reviews and discussion articles, translations, and fora. Contributions should fall within the broad scope of the journal, as outlined in the statement of scope and focus. Contributors should present their material in a form that is accessible to a general anthropological readership. We especially invite contributions that engage with debates from previously published articles in the journal.

Submissions are double-blind peer-reviewed in accordance with our policy. Submissions will be immediately acknowledged but due to the review process, acceptance may take up to three months. Submissions should be submitted via our website submission form (see links above for registration and login). Once you login, make sure your user profile has "author" selected, then click "new submission" and follow the instructions carefully to submit your article. If problems arise, first check the FAQ and Troubleshooting guide posted below. If you are still experiencing difficulty, articles can be submitted to the editors as email attachments.

Each article should be accompanied by a title page that includes: all authors' names, institutional affiliations, address, telephone numbers and e-mail address. Papers should be no longer than 10,000 words (inclusive of abstract 100-150 words, footnotes, bibliography and notes on contributors), unless permission for a longer submission has been granted in advance by the Editors. Each article must include a 100 words "note on contributor(s)" together will full institutional address details, including email address. We request that you submit this material (title page and notes on the contributors) as "supplementary files" rather than in the article itself, which will need to be blinded for peer-review.

We are unable to pay for permissions to publish pieces whose copyright is not held by the author. Authors should secure rights before submitting translations, illustrations or long quotes. The views expressed in all articles are those of the authors and not necessarily those of the journal or its editors. After acceptance, authors and Special Issue guest editors whose institutions have an Open Access library fund must commit to apply to assist in article production costs. Proof of application will be requested. Though publication is not usually contingent on the availability of funding, the Journal is generally under no obligation to publish a work if funding which can be destined to support open access is not made available.

Word template and guidelines

Our tailored Word template and guidelines will help you format and structure your article, with useful general advice and Word tips.

(La)TeX template and guidelines

We welcome submissions of (La)TeX files. If you have used any .bib files when creating your article, please include these with your submission so that we can generate the reference list and citations in the journal-specific style

Artwork guidelines

Illustrations, pictures and graphs, should be supplied with the highest quality and in an electronic format that helps us to publish your article in the best way possible. Please follow the guidelines below to enable us to prepare your artwork for the printed issue as well as the online version.

Format: TIFF, JPEG: Common format for pictures (containing no text or graphs).

EPS: Preferred format for graphs and line art (retains quality when enlarging/zooming in).

Placement: Figures/charts and tables created in MS Word should be included in the main text rather than at the end of the document.

Figures and other files created outside Word (i.e. Excel, PowerPoint, JPG, TIFF, EPS, and PDF) should be submitted separately. Please add a placeholder note in the running text (i.e. "[insert Figure 1.]")

Resolution: Rasterized based files (i.e. with .tiff or .jpeg extension) require a resolution of at least 300 dpi (dots per inch). Line art should be supplied with a minimum resolution of 800 dpi.

Colour: Please note that images supplied in colour will be published in colour online and black and white in print (unless otherwise arranged). Therefore, it is important that you supply images that are comprehensible in black and white as well (i.e. by using colour with a distinctive pattern or dotted lines). The captions should reflect this by not using words indicating colour.

Dimension: Check that the artworks supplied match or exceed the dimensions of the journal. Images cannot be scaled up after origination

Fonts: The lettering used in the artwork should not vary too much in size and type (usually sans serif font as a default).

Authors services:

For reformatting your manuscript to fit the requirement of the Journal of Civil Engineering Researchers and/or English language editing please send an email to the following address:

researchers.services@gmail.com

Noted: There is a fixed charge for these mentioned services that is a function of the manuscript length. The amount of this charge will be notified through a reply email.

FAQ AND TROUBLESHOOTING FOR AUTHORS

I cannot log in to the system. How do I acquire a new user name and password?

If you cannot remember your username, please write an email to (journals.researchers@gmail.com), who will locate your username and notify you. If you know your username, but cannot remember your password, please click the "Login" link on the left-hand menu at homepage. Below the fields for entering your username and password, you will notice a link that asks "Forgot your password?"; click that link and then enter your email adddress to reset your password. You will be sent an automated message with a temporary password and instructions for how to create a new password. TIP: If you do not receive the automated email in your inbox, please check your SPAM or Junk Mail folder. For any other issues, please contact our Managing Editor,Kamyar Bagherinejad (admin@journals-researchers.com).

How do I locate the online submission form and fill it out?

First you need to register or login (see above). Once you are logged in, make sure the "roles" section of your profile has "Author" selected. Once you assign yourself the role of "Author," save your profile and then click the "New Submission" link on your user home page.

Once you arrive at the submission form page, please read the instructions carefully filling out all necessary information. Unless specified otherwise by the editors, the journal section to be selected for your submission should be "Artlcles." Proceed to the remaining sections, checking all boxes of the submission preparation checklist, and checking the box in the copyright notice section (thus agreeing to journals-researchers's copyright terms). Once the first page is completed, click "Save and Continue." The next page allows you to upload your submission. Use the form to choose your file from your computer. Make sure you click "Upload." The page will refresh and you may then click "Save and Continue." You will then proceed to a page for entering the metadata for your article. Please fill out all required fields and any further information you can provide. Click "Save and Continue." The next page allows you to upload supplementary files (images, audiovisual materials, etc.). These are not required, but if you wish to provide supplementary materials, please upload them here (do no forget to click "Upload." Then click "Save and Continue." This brings you to the final page of the submission form. Please click "Finish Submission" in order to close the

submission process. You wil then be notified by email that your article has been successfully submitted. TIP: If you do not receive the automated email in your inbox, please check your SPAM or Junk Mail folder. For any other issues, please contact our Managing Editor, Kamyar Bagherinejad (admin@journals-researchers.com).

Why am I not receiving any email notifications from HAU?

Unfortunately, some automated messages from Open Journal Systems arrive in users' Spam (or Junk Mail) folders. First, check those folders to see if the message was filtered into there. You may also change the settings of your email by editing your preferences to accept all mail from [jcer] and related journals-researchers.com email accounts.

I am trying to upload a revised article following an initial round of peer-review, but I cannot locate where to upload the article. Where do I submit a revised article?

Follow the login process outlined above and when you successfully login you will see on your user home page a link next to "Author" for "active" articles in our system (usually it is only one article, but if you have mulitple submissions currently in our system, the number could be higher. Click the "Active" link and you will be led to a page that lists your authored articles currently in our system. Click the link under the column labeled "Status" and this will take you to a page showing the current review status of your article. At the very bottom of the screen, you will see an upload form under the heading "Editor decision." Here you may upload your revised article. An automated email will be sent to the editors and you may also notify them directly via email. You may then logout.

I successfully submitted an article; how long will it take for the editors to respond to me with a decision.

For all articles that are recommended for peer-review, the editors of JCER strive to notify authors of a decision within 4-6 weeks. You may contact JCER's Managing Editor, Kamyar Bagherinejad (admin@journals-researchers.com). if you have any questions relating to the review process and its duration.

For all other inquiries, please contact: Kamyar Bagherinejad (Managing Editor)

Privacy Statement

The names and email addresses entered in this journal site will be used exclusively for the stated purposes of this journal and will not be made available for any other purpose or to any other party.

Articles

Section default policy

Make a new submission to the Articles section.

Copyright Notice EditEdit Copyright Notice

Journal of Civil Engineering Researchers follows the regulations of the International Committee on Publication Ethics (COPE) and the ethical principles of publishing articles in this journal are set based on the rules of this committee, and in case of problems, it will be treated according to these rules.

Privacy Statement EditEdit Privacy Statement

The names and email addresses entered in this journal site will be used exclusively for the stated purposes of this journal and will not be made available for any other purpose or to any other party.

Scholars Pavilion

Scholars Pavilion or **Scholars Chartagi** is a monument donated by the Islamic Republic of Iran to the United Nations Office at Vienna. The monument architecture is claimed by the Islamic Republic News Agency of Iran to be a combination of Islamic and Achaemenid architecture, although the latter clearly predominates in the decorative features, with Persian columns and other features from Persepolis and other remains from the Achaemenid dynasty. The Chahartaq pavilion form runs through the architecture of Persia from pre-Islamic times to the present.

Statues of four famous Persian medieval scholars, Omar Khayyam, Al-Biruni, Muhammad ibn Zakariya al-Razi and Ibn-Sina are inside the pavilion. This monument donated in June 2009 in occasion of Iran's peaceful developments in science.

J-Researchers